CHAPTER THREE

GEOLOGICAL SETTINGS OF RARE-EARTH-ELEMENT DEPOSITS IN AUSTRALIA

3.1. INTRODUCTION

In Australia, REE are associated with igneous, sedimentary, and metamorphic rocks from a wide range of geological settings. Elevated concentrations of REE have been documented in various heavy-mineral sand deposits, carbonatite intrusions, alkaline igneous complexes, iron-oxide breccia complexes, calc-silicate skarns, fluorapatite veins, pegmatites, phosphorites, lignites, cemented fluviatile sandstones, and unconformity-related uranium deposits. The age of the REE-bearing host rocks range from ~2890 million years (Archean) for pegmatites in Western Australia to late Cenozoic for residual lateritic deposits and heavy-mineral sand deposits widespread throughout eastern Australia. The geological settings of Australia's REE deposits and prospects are shown in Figure 3.1, and their operational status in Figure 3.2. Appendix 8 provides further details of individual deposits and prospects. The presence of REE in mineral occurrences and deposits have not been recorded in older sample analyses when there was a much lower demand for resources of REE, and such occurrences of REE are not shown on Figures 3.1 and 3.2 due to incomplete databases.

Australia's historic REE production has been dominated by monazite by-products from heavy-mineral sand mining largely in southwest and eastern Australia. Significant resources of REE are contained in the monazite component of the heavy-mineral sand deposits, which are mined for their ilmenite, rutile, leucoxene, and zircon contents. In current heavy-mineral mining operations, monazite is no longer recovered for extraction of REE. During the last decade there has been increasing industry interest in hard-rock REE deposits. A number of significant deposits (e.g., Mount Weld, WA; Nolans Bore, NT; Toongi, NSW) with different geological settings (i.e., age and style of mineralisation, rock types, tectonic environment, etc) have provided the catalyst for this exploration interest. These deposits have well advanced mining development programs and their impending production contributions (e.g., 2011 for Mount Weld) are likely to have an impact on the global supply of REE.

Primary hard-rock REE deposits are widely distributed throughout the continent, being particularly prominent in Proterozoic and Phanerozoic provinces (Fig. 3.1). The oldest REE deposits that have been dated in Australia are hosted by Archean pegmatites in the eastern Pilbara Craton (Pinga Creek, Cooglegong, WA). The pegmatites are interpreted to have been emplaced during two periods: an early phase at 2890 Ma to 2880 Ma and a later phase at between 2840 Ma to 2830 Ma (Sweetapple and Collins, 2002). Carbonatite complexes comprising stocks and dykes are prominent in Western Australia, with important examples in the Yilgarn Craton (Mount Weld, Ponton Creek), Capricorn Orogen (Yangibana), and Halls Creek Orogen (Cummins Range). Interestingly, no carbonatites of Archean age have been confirmed in Australia, with the oldest dated examples being the mineralised Mount Weld and nearby Ponton Creek, both emplaced at ~2025 million years in the eastern Yilgarn Craton. The mineralised regolith associated with the Mount Weld Carbonatite is much younger than the host rock and is interpreted to have developed during the Late Mesozoic to Early Cenozoic (Bunting et al., 1974; Duncan and Willett, 1990). Mineralised Proterozoic fluorapatite veins at Nolans Bore in the Arunta Region of the Northern Territory could have been derived from a carbonatite or alkaline magmatic source at depth that has so far not been recognised in geophysical surveys. Alkaline rock complexes with REE resources feature in the Halls Creek Orogen (Brockman) and in the Tasman Orogen (Toongi, Narraburra) of New South Wales. The type example of the iron-oxide breccia complex association is the world-class Mesoproterozoic Olympic Dam deposit in the Gawler Craton, where the REE are associated (but not extracted) with the copper-gold-uranium mineralisation. REE also occur in the similar iron-oxide-hosted Carrapateena deposit. In the Mount Painter–Olary regions of the Curnamona Province east

Australian Rare-Earth-Element (REE) Deposits and Prospects

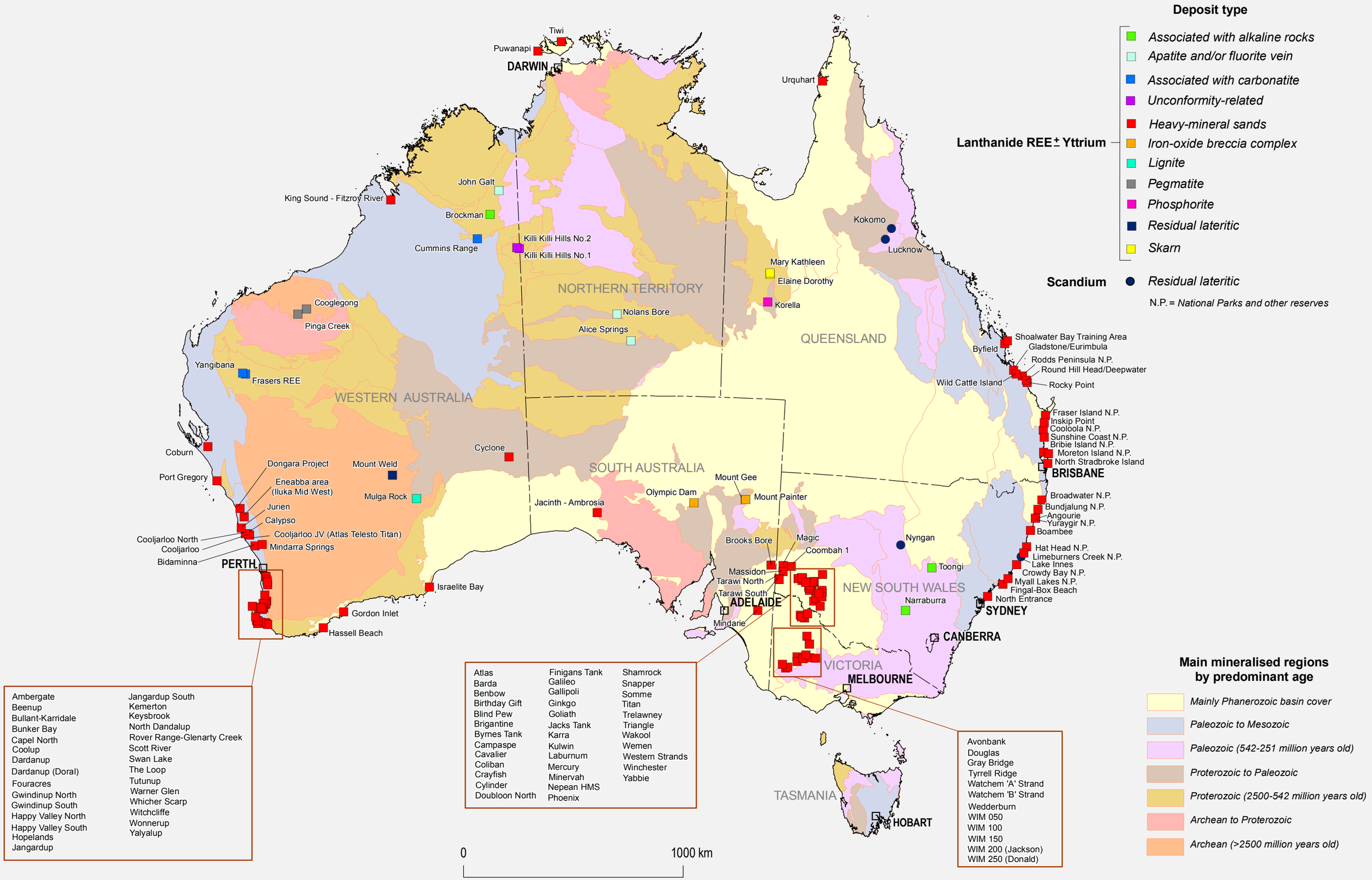

Figure 3.1. Distribution of Australian rare-earth-element deposits and prospects: Deposit type.

Australian Rare-Earth-Element (REE) Deposits and Prospects

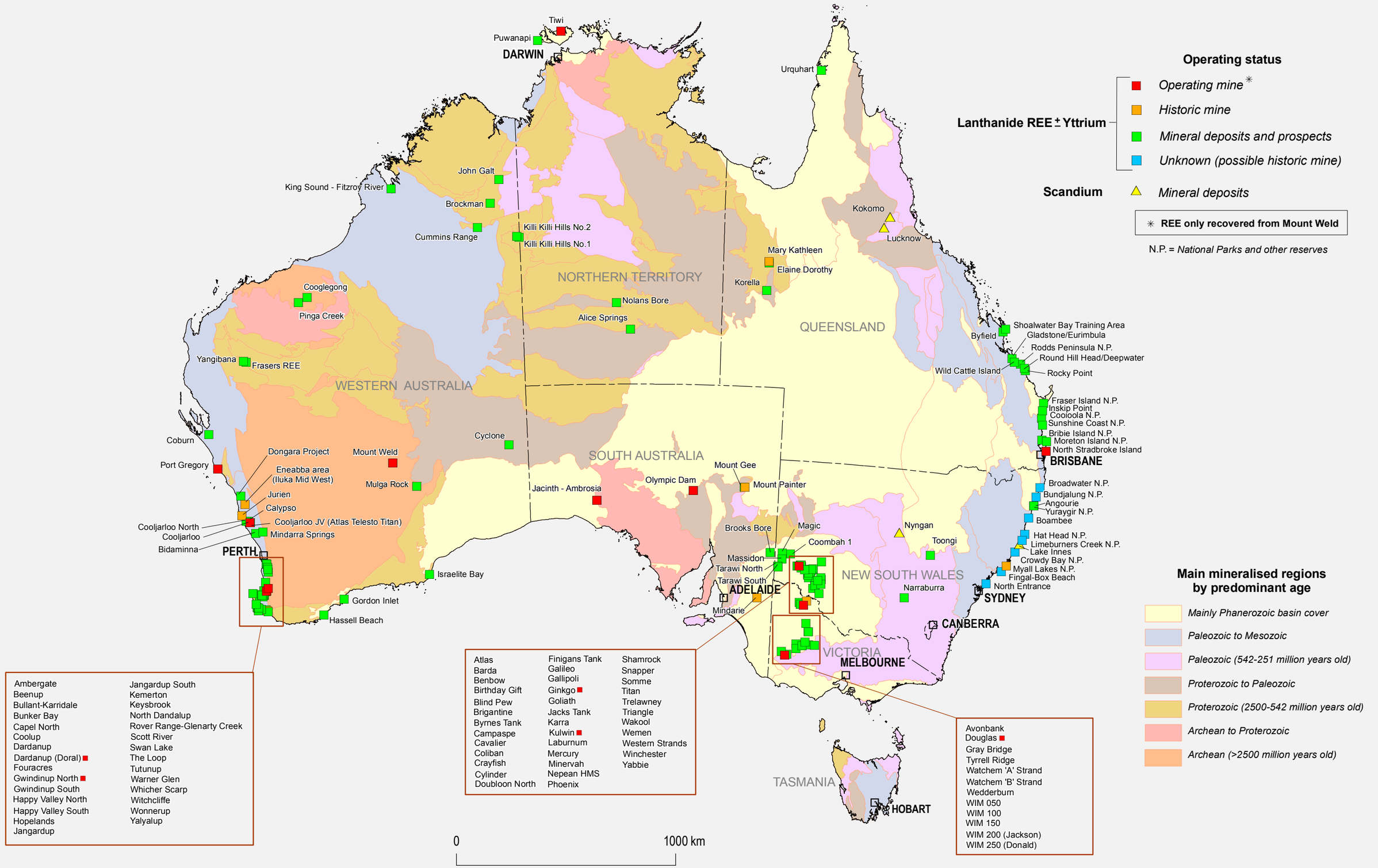

Figure 3.2. Distribution of Australian rare-earth-element deposits and prospects: Operating status.

of Olympic Dam are several Proterozoic REE-bearing iron-oxide uranium breccia deposits. One of the type examples of a metamorphic/metasomatic or skarn-bearing deposit containing REE is the Mary Kathleen uranium deposit in the Mount Isa Inlier, northwestern Queensland. Scandium-bearing nickel-cobalt laterites of Cenozoic age are associated with tectonically emplaced Phanerozoic ultramafic and mafic complexes in the Tasman Orogen of eastern Australia.

The heavy-mineral sand and placer deposits are concentrated along the coastlines of southern Western Australia, northern New South Wales, and southern Queensland. Major deposits occur along fossil shorelines inland in the Murray Basin centred near the junction of Victoria, New South Wales, and South Australia, and in the Eucla Basin in South Australia and Western Australia. Heavy-mineral deposits in beach, high dune, and offshore shallow marine environments are generally Cenozoic in age, whereas channel heavy-mineral deposits extend further back to the Mesozoic.

Currently, there are twelve REE-bearing deposits in Australia that are of operating status (Fig. 3.2; Appendix 8). Mount Weld (WA) is the only current REE mine in Australia from which REE are going to be produced once construction of a concentrator at the mine site and a processing plant in Malaysia are completed. REE are not recovered at the only other hard-rock REE-bearing deposit being mined at Olympic Dam (SA). The remaining ten active mines are heavy mineral sand deposits located at Cooljarloo, Dardanup (Doral), Gwindinup North and Port Gregory (all in WA); Douglas and Kulwin (Vic); Ginkgo (NSW); Jacinth-Ambrosia (SA); North Stradbroke Island (Qld); and Tiwi (NT). The REE in the heavy-mineral deposits are held in monazite, which occurs in minor amounts, usually 0.1 to 1.5%, in the heavy-mineral concentrate dominated by ilmenite, rutile, and zircon. As the monazite has a thorium content of around 5 to 7%, the REE are not recovered because of the cost of thorium disposal.

3.2. CLASSIFICATION OF RARE-EARTH-ELEMENT DEPOSITS

The distribution and concentration of REE into mineral deposits is influenced by various rock-forming processes including enrichment in magmatic or hydrothermal fluids, separation into mineral species and precipitation, and subsequent redistribution and concentration through weathering and other surface processes. Using this evolutionary framework, Walters et al. (2010) proposed that REE deposits can be broadly divided into: (1) primary deposits associated with igneous and hydrothermal processes; and (2) secondary deposits concentrated by sedimentary processes and weathering. Further sub-division of these general categories can be applied using such criteria as lithological association, mineralogy, and morphology of occurrence.

Traditional classification schemes of REE deposits are based on either descriptive-, or genetically (i.e., geological process)-derived criteria, or a combination of these. For example, the descriptive classification of REE deposits in China by Wu et al. (1996) is simply based on the type of host rocks, since they considered genetic-based classifications too controversial for many deposits (e.g., Bayan Obo). The major sub-groups in their 10-fold classification includes: carbonatitic rocks; quartz syenite; alkali granite; alkali complexes; alkali pegmatites; metamorphic rocks; phosphorites; bauxite; lateritic weathering crusts; and placers. Neary and Highley (1984) used a simple five-class structure for the major REE deposits of the world: alkaline rocks and carbonatites; vein; placer; apatite; and other deposits. The United States Geological Survey (Long et al., 2010) employed a rock-association scheme for their highest level categories, namely: peralkaline igneous rocks; carbonatite; iron-oxide copper-gold; pegmatite; porphyry molybdenum; metamorphic; stratiform phosphate residual; paleoplacer; and placer. The next hierarchical level, titled 'Type' with 34 sub-groups, has a much more 'process'-based emphasis, with such type examples as carbonate-rock replacement, metasomatic-fenite, and Climax-type. The classification scheme proposed by the British Geological Survey (Walters et al., 2010) is based on two criteria at the highest level, namely 'Primary deposit' or 'Secondary deposit', with carbonatite; alkaline igneous rocks; iron-REE; and hydrothermal (unrelated to alkaline igneous rocks) representing the sub-groups under the former criteria; and marine placer, alluvial placer, paleoplacer; lateritic; and ion-adsorption clays categorised under the latter criteria.

The classification of REE deposits in the world by Cassidy et al. (1997) is based on the relative 'abundance status' of the REE component in the deposit, i.e., where the REE are (1) a co-product or primary product, or (2) a by-product of the deposit.

1. A number of REE occurrences can be classified as a co-product or, in some cases, primary product deposits. The major deposit types in this class are those associated with carbonatites (sub-groups of primary, hydrothermal, supergene), alkaline igneous rocks and, to a lesser extent, hydrothermal iron-

oxide copper-gold-uranium (iron-rich, copper-uranium-gold-rich), and uranium-bearing skarns.

2. By-product deposits are dominated by heavy-mineral sands and placer deposits. However, discoveries of non-traditional REE resources in combination with new mining and processing techniques are now responsible for a significant proportion of TREE production. Such 'new' deposits include ionic adsorption clays (China), marine phosphorites (in several continents, including Australia), and anatase (Brazil) deposits.

Cassidy et al. (1997) have provided one of the few examples of classifying REE deposits in Australia. They divided the REE occurrences into six major groups, namely: shoreline placer; carbonatite; REE-enriched uranium; alkaline igneous rock; phosphorite; and unclassified (see their Fig. 2).

This report uses a mineral-systems approach to classify REE deposits in Australia and outside Australia (Table 3.1; Fig. 3.3). This approach focuses on mineral-forming process (see Chapter 4 for a definition of a mineral system) and has the advantage over more traditional descriptive classifications in that it attempts to identify those geological processes considered critical to the formation of a 'clan of deposit types' that share common parameters. This information can then be applied in a predictive sense to assist mineral exploration in the identification of potential new areas and types of REE mineralisation.

The mineral-systems classification is hierarchical in structure, with the most general grouping of deposits called 'Mineral-system association' (Table 3.1). This high-level category is divided into Regolith, Basinal, Metamorphic, and Magmatic associations, which are further subdivided into 'Deposit types'. An essential element of the magmatic association is the emplacement of REE-enriched melt. Various deposit types result either directly from the crystallisation of the melt and/or fluids predominantly derived from the melt. Deposit types of the basinal association can be formed from mechanical (e.g., placer) and chemical sedimentary (e.g., phosphorite) processes and from diagenetic fluids generated in sedimentary basins. Deposit types of the regolith association require a REE-bearing source rock to form economic-grade concentrations of REE. The REE deposits are formed either due to enrichment of REE in the residual material and/or from local remobilisation of REE. Deposit types of the metamorphic association are generated during regional and/or contact metamorphism and can involve metamorphic-derived fluids.

The mineral-system association concept used in this report can help relate mineral deposits to a general geochemical cycle (mantle-crustal-surface) of REE (Fig. 3.3). The data compiled for Figure 3.3 shows (see Chapter 2 for a detailed discussion) that REE are derived from the mantle and are enriched in the crust. Partial melting in the mantle generates (per)alkaline and carbonatitic melts enriched in REE. It has been generally recognised that highly alkaline melts can not readily be derived from 'normal' mantle melting of anhydrous chromium-diopside peridotite, which is poor in incompatible elements. This source material needs to be metasomatically enriched in incompatible elements to be a viable source of alkaline melts (e.g., Bailey, 1970; Roden and Murthy, 1985; Chesley et al., 2004). One possible source of fluids for the metasomatism of the mantle is the dehydration of the subducted slab, which can metasomatise asthenospheric mantle and subcontinental lithospheric mantle.

Partial melting of metasomatised mantle can generate (per)alkaline and carbonatitic melts, which can result in the enrichment of REE by about two orders of magnitude (Fig. 3.3). The partial melting of crustal material also produces felsic melts that are enriched in REE, but the enrichment factors are relatively smaller (by an order of magnitude). In general, sövitic carbonatitic melts show the highest levels of REE enrichment. They also show significant enrichment in LREE (LREE/HREE ratio of ~40, compared to ~7 for alkaline and felsic melts).

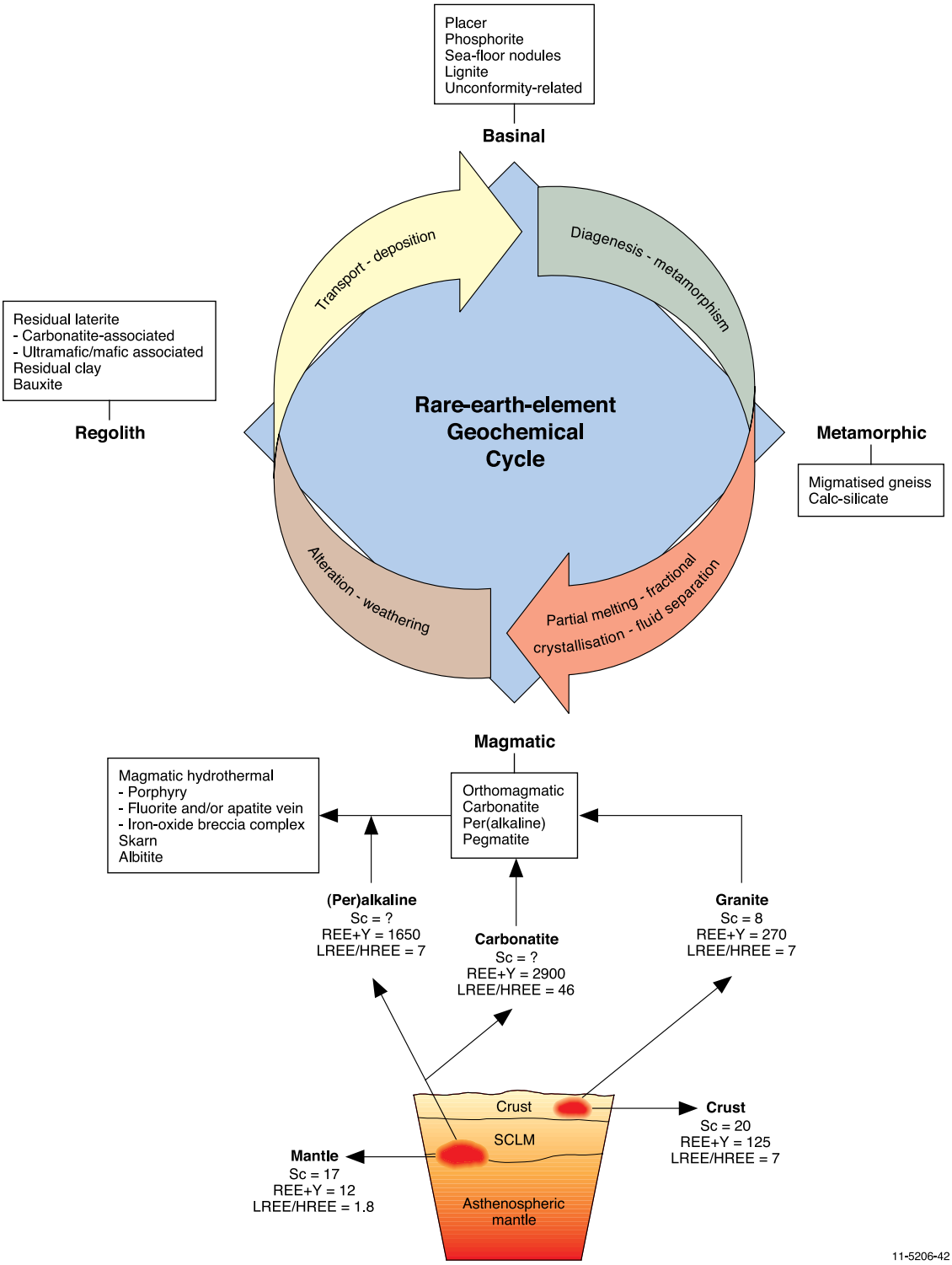

Figure 3.3. Mantle–crust–surface geochemical cycle for rare-earth elements (REE concentrations in parts per million). Alkaline and carbonatitic melts that are produced by the partial melting of metasomatised subcontinental lithospheric mantle (SCLM) transport the rare-earth elements from the mantle into the crust. Granites that are produced from the partial melting of crustal material are also enriched in rare-earth elements (less enriched than alkaline and carbonatitic melts). A more detailed classification of the rare-earth-element deposits is in Table 3.1. The rare-earth-element data for sövitic carbonatites are from Hornig-Kjarsgaard (1998), and the (per)alkaline rock data are from Gerasimovsky (1974). See Tables 2.2 and 2.3 for the other rare-earth-element data and LREE/HREE ratios shown in this figure.

Table 3.1. Mineral-system classification of rare-earth-element deposits. Australian deposit types and type examples are shown in **blue** font.

Mineral-system association	Deposit type	Example of Australian deposit/prospect
Regolith	Residual lateritic	
	• Carbonatite-associated	• Mount Weld, WA
	• Ultramafic/mafic rock-associated	• Lucknow, Qld
	Residual clay	
	Bauxite	
Basinal	Sedimentary	
	• Placer ◦ Quartz-pebble conglomerate ◦ Alluvial ◦ Heavy-mineral sands · Beach · High dune · Offshore shallow marine · Channel	 • Eneabba, WA • North Stradbroke Island, Qld • WIM 150, Vic • Calypso, WA
	• Phosphorite	• Korella, Qld
	• Sea-floor manganese nodule	
	• Lignite	• Mulga Rock, WA
	Diagenetic-hydrothermal	
	• Unconformity-related	• Killi Killi Hills, NT
Metamorphic	• Migmatised gneiss	
	• Calc-silicate	• Mary Kathleen, Qld[1]
Magmatic	Orthomagmatic	
	• Alkaline igneous rock	• Brockman, WA
	• Carbonatite	• Yangibana, WA
	• Pegmatite	• Cooglegong–Pinga Creek, WA
	Magmatic-hydrothermal	
	• Albitite	
	• Porphyry	
	• Skarn	• Mary Kathleen, Qld[1]
	• Apatite and/or fluorite vein	• Nolans Bore, NT
	• Iron-oxide breccia complex	• Olympic Dam, SA

[1] The Mary Kathleen example(s) shown was initially a skarn deposit that was subsequently modified to a calc-silicate-type deposit during regional metamorphism.

3.3. GEOLOGICAL SETTINGS OF RARE-EARTH-ELEMENT DEPOSITS IN AUSTRALIA

This section (3.3.1) describes the geological characteristics of the major REE deposits and occurrences in Australia. The first part (3.3.1) of the section summarises the geological features of fourteen deposits considered the type example of that deposit style in a pro forma containing the following attributes:

General description
Australian deposits/prospects
Deposits outside Australia
Type example in Australia
Location
Geological province
Resources
Current status
Economic significance
Geological setting
Host rocks
REE mineralisation
Source of REE
Age of mineralisation
Petrogenesis
Key references

The fourteen deposit types and their type example (see Table 3.1) are:

Deposit Type 3.1: Laterite associated with carbonatite complexes; Mount Weld, WA

Deposit Type 3.2: Scandium in laterite associated with ultramafic-mafic rocks; Lucknow, Qld

Deposit Type 3.3: Heavy-mineral sand—beach; Eneabba, WA

Deposit Type 3.4: Heavy-mineral sand—high dune; North Stradbroke Island, Qld

Deposit Type 3.5: Heavy-mineral sand—offshore shallow marine; WIM 150, Vic

Deposit Type 3.6: Heavy-mineral sand—channel; Calypso, WA

Deposit Type 3.7: Phosphorite; Korella, Qld

Deposit Type 3.8: Lignite; Mulga Rocks, WA

Deposit Type 3.9: Alkaline igneous rocks; Brockman, WA

Deposit Type 3.10: Carbonatite; Yangibana, WA

Deposit Type 3.11: Pegmatite; Cooglegong–Pinga Creek, WA

Deposit Type 3.12: Skarn; Mary Kathleen, Qld

Deposit Type 3.13: Apatite and/or fluorite veins; Nolans Bore, NT

Deposit Type 3.14: Iron-oxide breccia complex; Olympic Dam, SA

The second part (3.3.2) of the section describes the geological features of other REE occurrences (most without JORC-compliant resources: Appendix 7) not mentioned in the Deposit Types of Section 3.3.1.

3.3.1. Type examples of major rare-earth-element deposits in Australia

Deposit Type 3.1: Rare-earth-element-bearing laterite associated with carbonatite complexes

General description: Carbonatites are igneous rocks composed of more than 50% carbonate minerals, often spatially and temporally associated with alkaline felsic magmas, and have somewhat contentious origins. Primary carbonatites consist mainly of calcitic (sövite) and/or dolomitic (rauhaugite) rock types. Carbonate-rich melts can extract incompatible elements (e.g., REE, zirconium, niobium, phosphorus) from coexisting silicate melts or solids, concentrating them for subsequent deposition of rare-element cumulates from the carbonate magma (Mungall, 2007). Carbonatite complexes have generated considerable exploration interest in Australia because of their potential to host significant resources of REE, copper, niobium, tantalum, phosphorus, and uranium. Such intrusions occur near major structural features throughout the cratonic blocks and they range in age from Paleoproterozoic to Jurassic (Jaques, 2008). The largest deposits in Australia (Mount Weld, Cummins Range) formed from the supergene enrichment of REE in the laterite profile above large composite carbonatite bodies that are generally of Proterozoic age. Deeply weathered carbonatites also occur in Brazil, Canada, Finland, Guyana, Kenya, Tanzania, Uganda, and Zaire (see references in Lottermoser and England, 1988). In contrast to such world-class REE deposits as Mountain Pass in California, few Australian occurrences contain significant abundances of REE in the primary zones of carbonatite. Possible exceptions to this include two mineralised examples in Western Australia, namely Ponton Creek (see Appendix 7) and Yangibana (see Deposit Type 3.10 template).

Australian deposits/prospects: Mount Weld (Yilgarn Craton, WA); Cummins Range (near junction of Halls Creek and King Leopold orogens, Western Australia).

Deposits outside Australia: Araxá, Catalão, Goias, Minas Gerais, and Tapira (all Brazil); Mabounié (Gabon); Mrima (Kenya); Lueshe (Zaire); Dorowa and Shawa (Zimbabwe): Christie et al. (1998) and Lottermoser (1994).

Table 3.2. Resources for the Central lanthanide and Duncan deposits at Mount Weld (using cut-off grade of 2.5% REO).

	000 tonnes	REO%[1]	Total LnREO%[2]	Y_2O_3 ppm
Central lanthanide deposit				
Measured[3]	3550	14.4	14.3	820
Indicated	1440	8.2	8.1	960
Inferred	4884	8.6	8.5	1120
Total	9880	10.7	10.6	990
Duncan deposit				
Measured	3640	5.5	5.2	2700
Indicated	3560	4.1	3.9	2460
Inferred	410	4.3	4.1	2360
Total	7620	4.8	4.5	2570
Total REO resource				
Measured	7200	9.8	9.7	1770
Indicated	5000	5.3	5.1	2020
Inferred	5290	8.3	8.2	1210
Total	17 490	8.1	7.9	1680

Source: Lynas Corporation Limited www site: http://www.lynascorp.com/page.asp?category_id=2&page_id=4

[1] REO includes the oxides of the lanthanide group of REE and yttrium.

[2] Total LnREO includes the oxides of the lanthanide group of REE, but excluding yttrium.

[3] Category of resources.

Type example in Australia: Mount Weld, Western Australia (Figs 3.4 and 3.5).

Location: Longitude: 122.5475; Latitude: -28.8626
~35 km south-southeast of Laverton, Western Australia
1:250 000 map sheet: Laverton (SH 51–02)
1:100 000 map sheet: Burtville (3440)

The Mount Weld Carbonatite complex also hosts significant resources of niobium, tantalum, and phosphate. The Crown deposit in the northern part of the complex has an indicated and inferred resource of 37.7 Mt @ 1.07% Nb_2O_5, 1.16% total lanthanide oxides, 0.09% Y_2O_3, 0.3% ZrO, 0.024% Ta_2O_5, and 7.99% P_2O_5 (as of January, 2010), while phosphorous mineralisation in the Swan deposit in the northern half of the complex has an indicated and inferred resource of 77 Mt @ 13.5% phosphorous oxide (MiningNewsPremium.net, 16th March 2011). The Anchor deposit in the southwest of the Mount Weld complex contains niobium-tantalum mineralisation.

Geological province: Eastern Goldfields Province, Yilgarn Craton, Western Australia.

Resources: TREO resources (Table 3.2) at Mount Weld (as of 16th March 2011) to JORC Code standards are 17.49 Mt @ 8.1% REO for 1.416 million tonnes of contained metal (http://www.lynascorp.com/page.asp?category_id=2&page_id=4 and http://www.lynascorp.com/content/upload/files/Presentations/Investor_Presentation_March_2011_950850.pdf).

Current status: Advanced economic deposit with stockpiling of different grade ores and production planned to commence in 2011. Expected mine life is estimated to be at least twenty years.

Economic significance: 'World-class' economic deposit containing some of the highest REE grades (8.1% REO).

Geological setting: The ~2025 Ma Mount Weld Carbonatite complex (Figs 3.4 and 3.5) intrudes Archean sedimentary-volcanic sequences in the Eastern Goldfields Province of the Yilgarn Craton, Western Australia. The carbonatite intrudes the central part of the fault-bounded Laverton tectonic zone (linear graben-like zone) and it has been overprinted by greenschist facies metamorphism (Duncan and Willett, 1990). The Mount Weld Carbonatite belongs to a regional alkaline province represented by coeval low- to high-MgO alkaline ultramafic-mafic igneous rocks, kimberlites, and carbonatites that were emplaced into

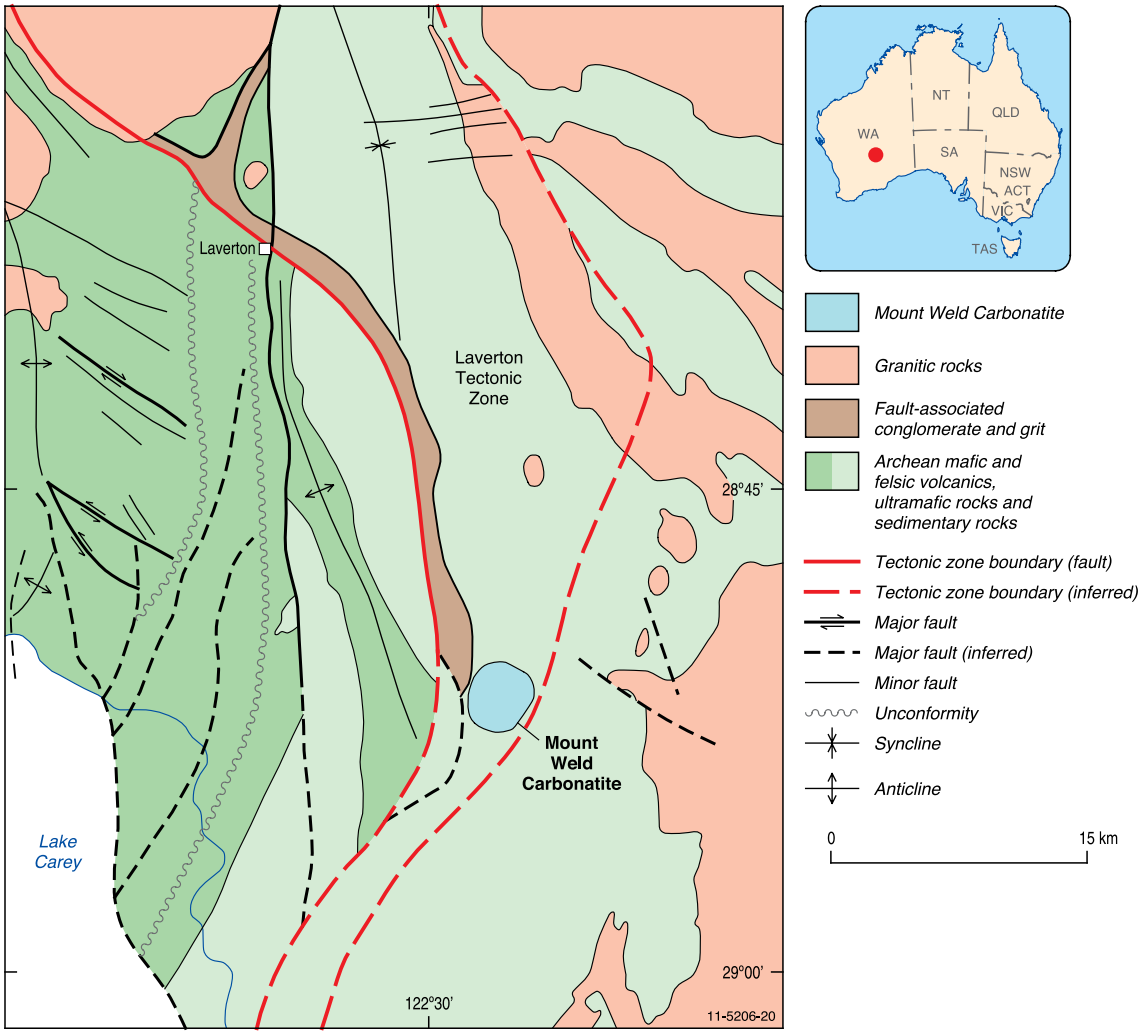

Figure 3.4. Regional geological setting of the Mount Weld Carbonatite, Yilgarn Craton, Western Australia. Modified from Duncan and Willett (1990).

the crust during the middle Paleoproterozoic (Graham et al., 2003; 2004). Incompatible element geochemistry, stable isotope, and Sm-Nd isotope data indicate that all these rocks are strongly enriched in incompatible elements and are comagmatic. The genetic and spatial relationships between the alkaline ultramafic and carbonatitic melts appear to be controlled by the depth and composition of the continental lithospheric mantle (Graham, et al., 2004).

The Mount Weld Carbonatite complex is a steeply plunging cylindrical body, 3 to 4 km in diameter, surrounded by a 500 m-wide fenitic (glimmerite) alteration zone (Fig. 3.5). Carbonatite dykes persist for up to 5 km from the main body. A thick (10 to 70 m) laterite overlying the unweathered carbonatite contains high-grade REO deposits and concentrations of niobium, tantalum, zirconium, and other 'rare' metals. The laterite regolith is covered by lacustrine and alluvial sedimentary rocks. The primary carbonatite consists mainly of calcitic (sövite) and dolomitic (rauhaugite) igneous rock types that contain more than 50% carbonate (Duncan and Willett, 1990). Relict cumulus textures involving carbonate minerals are locally preserved, with minor apatite, biotite, carbonate, and magnetite forming the intercumulus phases. The altered annulus surrounding the complex shows a gradational alteration transition from dominantly potassium-rich micaceous rock (glimmerite) to mafic volcanic country rocks. The altered zone contains phlogopite-rich rocks, brecciated wall-rocks, and is characterised by alkali

Figure 3.5 (see opposite). Geological map (Cenozoic units above carbonatite have been removed) and cross-section of the Mount Weld Carbonatite rare-earth-element deposit, Yilgarn Craton, Western Australia. Geological map and cross-section are modified from Fetherston and Searston (2004), and outlines of Central lanthanide and Duncan deposits are from Lynas Corporation Limited (2011). The minerals in the laterite profile (Inset A) are from Lottermoser and England (1988).

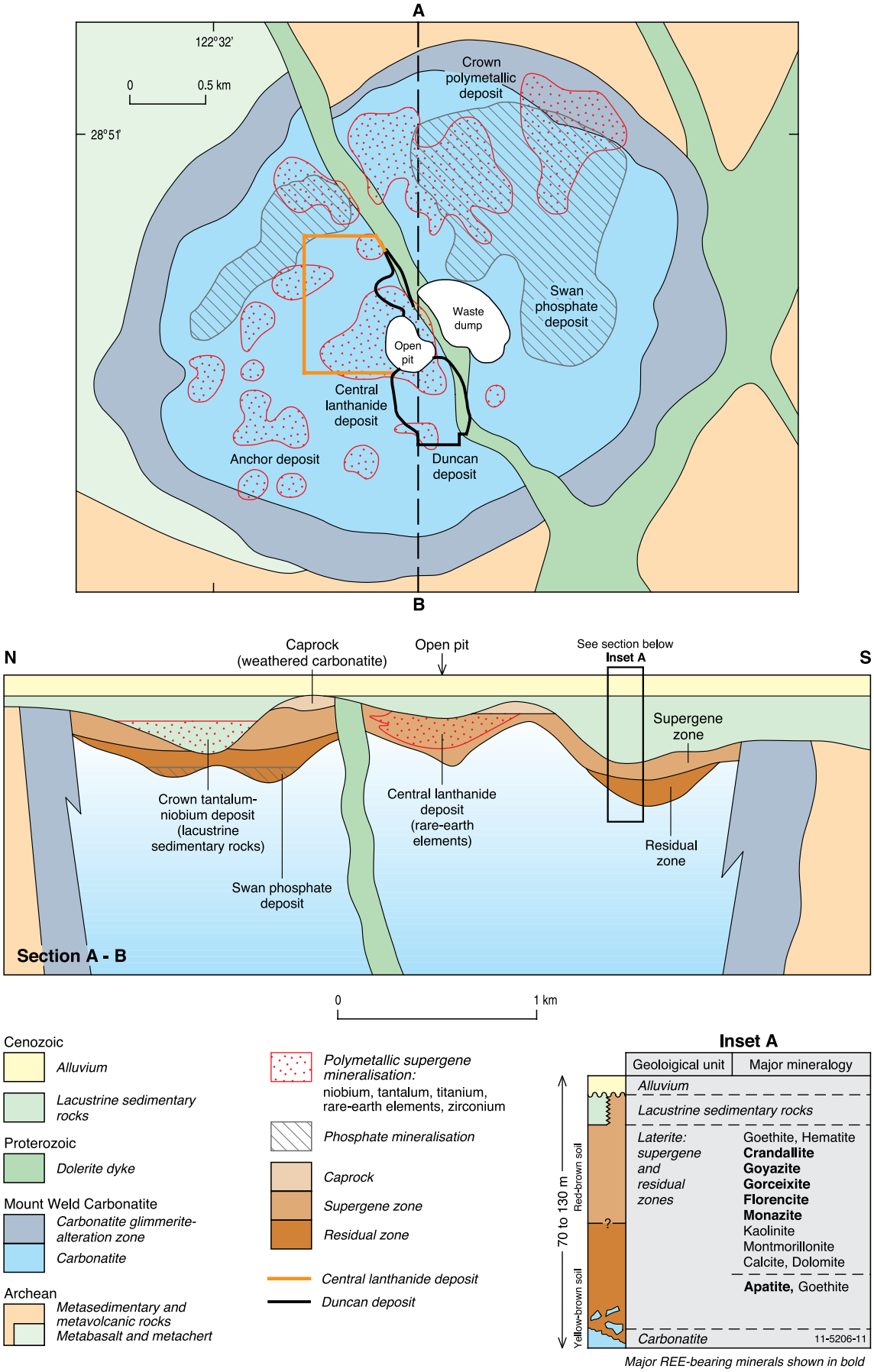
A
122°32'
0
0.5 km
28°51'
Crown polymetallic deposit
Swan phosphate deposit
Waste dump
Open pit
Central lanthanide deposit
Anchor deposit
Duncan deposit
B
N
Caprock (weathered carbonatite)
Open pit
See section below
Inset A
S
Supergene zone
Crown tantalum-niobium deposit (lacustrine sedimentary rocks)
Central lanthanide deposit (rare-earth elements)
Residual zone
Swan phosphate deposit
Section A - B
0
1 km
Cenozoic
Alluvium
Lacustrine sedimentary rocks
Proterozoic
Dolerite dyke
Mount Weld Carbonatite
Carbonatite glimmerite-alteration zone
Carbonatite
Archean
Metasedimentary and metavolcanic rocks
Metabasalt and metachert
Polymetallic supergene mineralisation:
niobium, tantalum, titanium, rare-earth elements, zirconium
Phosphate mineralisation
Caprock
Supergene zone
Residual zone
Central lanthanide deposit
Duncan deposit
Inset A
Geoloigical unit
Major mineralogy
Alluvium
Lacustrine sedimentary rocks
Laterite: supergene and residual zones
Goethite, Hematite
Crandallite
Goyazite
Gorceixite
Florencite
Monazite
Kaolinite
Montmorillonite
Calcite, Dolomite
Apatite, Goethite
Carbonatite
70 to 130 m
Red-brown soil
Yellow-brown soil
?
11-5206-11
Major REE-bearing minerals shown in bold

metasomatism under strongly oxidising conditions (i.e., fenitisation). As indicated by minor, but widely disseminated sulphides, periods of carbonate invasion that introduced calcite, dolomite, and ankerite, occurred under mildly reducing conditions.

Duncan (1990) estimated that during its evolutionary history about four vertical kilometres of the carbonatite intrusion and surrounding greenstone country rocks were removed by erosion. An important aspect of the economic status of the Mount Weld deposit is the geological preservation of the regolith profile. In contrast, the mineralised Ponton Creek carbonatite ~190 km south-southeast of Mount Weld, has no preserved paleo-regolith due to the scouring of the complex by Permian glaciation.

Host rocks: The lateritic regolith above the intrusive carbonatite contains all the currently known economic resources of REE in the Mount Weld deposit (Figs 3.5 and 3.6A). The following summary of the mineralogy and supergene enrichment processes that operated in the host lateritic rocks is from Duncan and Willett (1990) and Lottermoser (1990). Leaching and removal of carbonate by groundwater activity led to the progressive accumulation of primary igneous apatite and minor oxides, sulphides, and silicates. This was accompanied by the replacement, decomposition, and oxidation of primary igneous minerals, crystallisation of secondary minerals, and the formation of ferruginous cap rocks. These complex weathering-hydrological processes resulted in the formation of a mineralogically and chemically zoned laterite profile. The base of this profile is defined by a relatively sharp, karst-like interface with the underlying carbonatite. A residual zone containing relict igneous minerals (apatite, magnetite, ilmenite, pyrochlore, monazite, silicates) concentrated by the removal of carbonate directly overlies the unweathered carbonatite. The residual zone is overlain by a supergene-enriched zone containing abundant insoluble phosphates, aluminophosphates, clays, crandallite-group minerals, iron and manganese-bearing oxides that contain elevated concentrations of REE, Y, U, Th, Nb, Ta, Zr, Ti, V, Cr, Ba, and Sr. Of major exploration interest are the REE, niobium-tantalum, and phosphatic minerals concentrated in the laterite. The highest grades of niobium-tantalum occur in 6 to 15 m-thick horizontal units composed of unconsolidated, highly phosphatic lacustrine sedimentary rocks that grade upwards into smectite clays. Extreme conditions of lateritic weathering that prevailed in the supergene zone over a protracted period of time ensured the degradation of the residual magmatic REE-bearing minerals.

REE mineralisation: The Central lanthanide (9.88 Mt @ 10.7% REO) and the Duncan (7.62 Mt @ 4.8% REO) deposits contain the largest resources of REE in the carbonatite complex. The Crown and Coors polymetallic deposits in the northern part of the carbonatite body contain Nb, P, REO, Ta, Zr, Y, and Ti resources, and in addition, extensive phosphate-rich resources of the Swan phosphate deposit occur in the lower regolith. The Central lanthanide deposit (CLD) contains an indicative mix of predominantly LREE from CeO_2 (46.7%), La_2O_3 (25.5%), Nd_2O_3 (18.5%), Pr_6O_{11} (5.32%), Sm_2O_3 (2.27%), to Eu_2O_3 (0.443%), together with minor components of HREE: Dy_2O_3 (0.124%) and Tb_4O_7 (0.068%: Lawrence, 2006). The lower-grade Duncan REE deposit located southeast of the CLD contains about 25% of the TREO resource, but it has a higher component of the more valuable HREE relative to the CLD.

Very high-grade lanthanide concentrations (up to 45% combined lanthanide oxides) in the regolith are attributed to secondary monazite in polycrystalline aggregates that often pseudomorph apatite. This monazite is particularly rich in LREE and low in thorium. The weathered monazite (Fig. 3.6C) is 50 times less radioactive than monazite from beach sands, having only 0.07% thorium and 0.003% uranium (Lottermoser, 1990). Other REE-bearing minerals include crandallite, rhabdophane, cerianite, and churchite (Fig. 3.6B). Churchite contains considerable amounts of high-grade yttrium (up to 2.5% Y_2O_3) and is an important host to the HREE. Niobium and tantalum-bearing pyrochlore, ilmenite, and niobian rutile in the primary carbonatite are concentrated in the apatite and magnetite-rich residual zone. Grades are typically variable and locally high (up to 1.5% Nb_2O_5 and 0.05% Ta_2O_5: Duncan and Willett, 1990). Higher grades of niobium (up to 6% Nb_2O_5) characterise the supergene zone where crandallite and goethite have been partly derived from the lacustrine-fluviatile sedimentary rocks. Richardson and Birkett (1995a) note that the LREE-bearing minerals monazite and rhabdophane occur in the upper part of the residuum, whereas the HREE and Y are preferentially concentrated at depth as xenotime and churchite. The mineralogy and spatial distribution of the REE-bearing minerals in the laterite profile are discussed in detail by Lottermoser and England (1988) and Lottermoser (1990). A schematic section of the mineralised laterite is shown in the inset diagram of Figure 3.5.

Source of REE: The lanthanide group of REE and yttrium are widely dispersed throughout the laterite regolith. These metals are derived from the major REE-bearing minerals (apatite, monazite, synchysite)

of the primary igneous carbonatite, and to a lesser degree, from other silicate and carbonate minerals (feldspar, calcite, dolomite) that contain trace amounts of REE. Primary apatite has an average lanthanide oxide content of ~0.5%. REE-bearing phosphatic lacustrine sedimentary rocks appear to be derived from the weathering of fine-grained detrital apatite and pyrochlore deposited in the deeper parts of broad paleodrainage channels (Fetherston, 2004).

Age of mineralisation: The age of the mineralised laterite (Fig. 3.6A) above the Mount Weld Carbonatite is not known, however, an overlying sequence of bioturbated lacustrine clay and sand, up to 70-m thick, is by analogy with other similar sequences in the Eastern Goldfields Province, considered to be Late Cretaceous to Early Cenozoic in age (Bunting et al., 1974; Duncan and Willett, 1990). A further relative age constraint on the development of the carbonatite weathering profile is provided by a Permian glaciation event, which would have removed any previous weathering products. Thus the surface exposure of the carbonatite intrusion and subsequent weathering are interpreted to have taken place during the Late Mesozoic to Early Cenozoic.

A maximum age for the supergene REE mineralisation is constrained by the age of the carbonatite intrusive host, which has been dated by several isotopic methods with various levels of precision. K.D. Collerson (1982: unpublished data) obtained a Rb-Sr isotopic age from fresh rock of 2021 ± 13 Ma with an initial $^{87}Sr/^{86}Sr$ ratio of 0.70200 ± 0.00006. This ratio is similar to that of the upper mantle approximately 2025 million years ago, indicating the carbonatite was directly derived from the mantle without significant crustal contamination. A biotite-rich calcite and apatite-bearing fragment has a K-Ar age of 2064 ± 40 Ma (A.W. Webb, 1973, unpublished data), and two Pb analyses yield a Pb-Pb age of 2090 ± 10 Ma, within error of the K-Ar age (Nelson et al., 1988). Mineral and whole-rock Re-Os isotopic data indicate that the Mount Weld Carbonatite is part of a larger coeval suite of low- to high-MgO alkaline ultramafic rocks (Turkey, Melrose, Granny Smith) and carbonatites (Ponton Creek) that were emplaced into the crust in the middle Paleoproterozoic. Isotopic data for oxide minerals, and carbonatite, kimberlite, and melonite rock types yield a precise Re-Os isochron of 2025 ± 10 Ma (Graham et al., 2003; 2004).

The age constraints discussed above indicate that the Mount Weld Carbonatite intrusive was part of a regional alkaline magmatic event that occurred about 2025 million years ago in the eastern Yilgarn Craton.

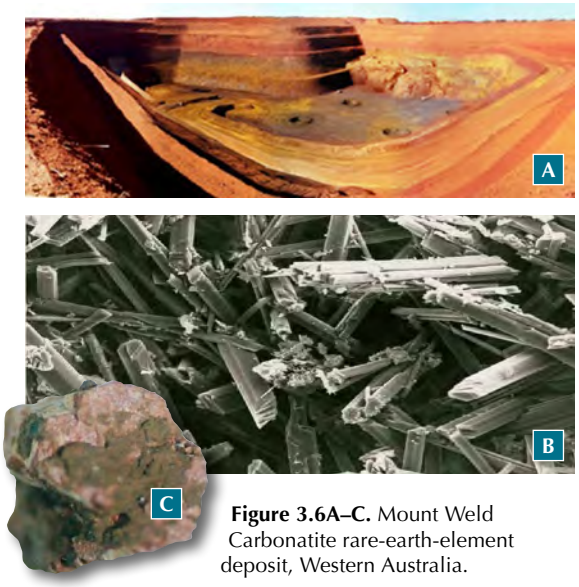

Figure 3.6A–C. Mount Weld Carbonatite rare-earth-element deposit, Western Australia.

A. Main open pit in the Mount Weld deposit. The REE-enriched laterite zone (yellow and orange colours) near the base of the pit is overlain by alluvium (red).

B–C. Two of the major REE-bearing minerals from Mount Weld are: B. churchite ($YPO_4 \cdot 2H_2O$: scanning-electron microscope image), and C. monazite $(Ce,La,Nd,Th)PO_4$.

Georgia Bunn (Lynas Corporation Limited: http://www.lynascorp.com/) provided the photographs.

Genetic model: The Mount Weld REE deposit formed from supergene enrichment processes that operated in the deep weathering profile of a large carbonatite body. Long-term leaching and redeposition by groundwater movement is the preferred model for REE enrichment (Cassidy et al., 1997). Lottermoser (1990) showed that the REE underwent pronounced lateral and vertical mobility during weathering, which was favoured by high-fluid/rock ratios, long fluid residence times, abundant REE complexing agents, and the decomposed condition of the primary igneous carbonatite minerals. Lottermoser (1990) also determined that the wide range of pH and alkaline conditions, and the carbonate anion concentrations in the groundwater variably influenced the different stabilities of LREE and HREE complexes which caused fractionation, separation, and deposition of LREE and HREE. The formation of a highly REE-enriched central laterite zone was facilitated by the lateral movement of groundwater flow towards a central topographic low of the laterite, and also the associated decreasing pH of the solutions favoured the mobilisation of large amounts of REE.

Key references: Duncan and Willett (1990): exploration history, regional and local geological setting, geochronology, mineral resources;
Lottermoser (1990), Lottermoser and England (1988): mineralogy, geochemistry; and
Graham et al. (2004): geochronology, petrogenesis.

Deposit Type 3.2: Scandium-bearing laterite associated with ultramafic-mafic rocks

General description: In contrast to the lanthanide group of REE (lanthanum to lutetium) and yttrium, which show a close genetical and spatial association with alkaline felsic igneous rocks, scandium has a closer affinity with high-magnesian ultramafic-mafic igneous rocks. In particular, the recent economic significance of scandium has been highlighted by its association with nickel and cobalt in deeply weathered laterite profiles superimposed above Phanerozoic mafic-ultramafic intrusions in New South Wales and ?older correlatives in Queensland. These intrusions have been variously described in the literature to having 'alpine'-, 'ophiolite'-, and 'Alaskan'-type affinities. Most of the Paleozoic intrusions are fault-bounded linear bodies that occur in anastomosing north-trending serpentinite belts associated with crustal-scale fault systems in the Lachlan Orogen of eastern Australia. The enrichment of scandium in the laterites appears to be a feature of the younger Phanerozoic bodies of eastern Australia, whereas the Ni-Co ± PGE laterites superimposed over Archean ultramafic (e.g., komatiitic) rocks in the Yilgarn and Pilbara cratons of Western Australia appear to have much lower concentrations of scandium. The most advanced projects with JORC-determined resources of nickel, cobalt, and scandium are the Lucknow and Greenvale deposits in Queensland and the Nyngan and Syerston deposits in New South Wales.

Australian deposits/prospects: Lucknow, Greenvale, and Kokomo (all Greenvale Province, Qld); Gilgai–Nyngan (Lachlan Orogen, NSW); Owendale-Tout–Fifield (Lachlan Orogen, NSW); Thuddungra (Lachlan Orogen, NSW), and Lake Innes near Port Macquarie (?New England Orogen, NSW).

Deposits outside Australia: Significant deposits of scandium associated with nickel-cobalt laterites appear to be rare, with few occurrences documented outside Australia. The Sipilou South nickel-cobalt-scandium laterite deposit is located in western Côte d'Ivoire, Africa (http://www.marketwire.com/press-release/Sama-Resources-Intersects-137-Metres-Up-25-Nickel-Its-Nickel-Cobalt-Scandium-Laterite-TSX-VENTURE-SME-1419535.htm). Drill intersections include 13.7 m @ 2.5% Ni, and scandium and cobalt concentrations in the limonitic section of the deposit attain 110 ppm and 0.34%, respectively. Similar scandium-bearing laterite deposits (Lola Project) also occur in the Republic of Guinea, West Africa.

Type example in Australia: Lucknow (part of NORNICO Project, Greenvale region), Queensland (Figs 3.7 and 3.8).

Location: Longitude: 144.9555; Latitude: -19.0284
~10 km southwest of Greenvale township, Queensland
1:250 000 map sheet: Clarke River (SE 55–13)
1:100 000 map sheet: Burges (7859)

Geological province: Greenvale Province (near boundary with Broken River Province), Lachlan Orogen, Queensland.

Resources: The Measured, Indicated and Inferred scandium resource (as of 19th January 2011; Table 3.3) for the Lucknow deposit that conforms to JORC guidelines is 6.24 Mt @ 169 g/t Sc (using 70 g/t Sc cut-off grade) including a higher-grade zone of 4.15 Mt @ 205 g/t Sc (using 120 g/t Sc cut-off grade).

Current status: Advanced projects with JORC-compliant resources.

Economic significance: The economic impacts of the scandium-bearing laterites in the Greenvale (Queensland) and Nyngan–Fifield (New South Wales) regions are generally not well understood at their early stages of development.

Geological setting: The southeastern part of the Georgetown Inlier in northern Queensland contains a number of mafic-ultramafic igneous complexes that have been the focus of exploration since nickeliferous laterites were first discovered in the Greenvale area in 1957 (see Appendix 7). The Boiler Gully, Sandalwood, Gray Creek and a number of smaller complexes occur in a structurally deformed region (Greenvale Province) located between the Precambrian rocks of the Georgetown Inlier and the Paleozoic rocks of the Broken River Province (Fergusson et al., 2007; Henderson et al., 2011). The complexes are spatially associated with the regional northeast–trending Gray Creek Fault Zone and Burdekin Fault Zone (Henderson et al., 2011). They show a common geological history of layered peridotite and gabbro intruded by gabbro and mafic dykes regionally metamorphosed and deformed (Arnold and Rubenach, 1976). Laterite cappings are developed on all types of basement rocks in the Greenvale region. For those associated with ultramafic rocks, the laterite profile is deep and mature, and nickel-cobalt concentrations attain ore grades in some deposits. The most significant scandium-enriched Ni-Co laterites are associated with the Gray Creek Complex (Lucknow deposit) and Boiler Gully Complex (Greenvale deposit).

The Gray Creek Complex is a ~25 km-long, northeast-trending lenticular body near Greenvale. This fault-bounded complex is surrounded by Paleozoic sedimentary and volcanic rocks of the Broken River

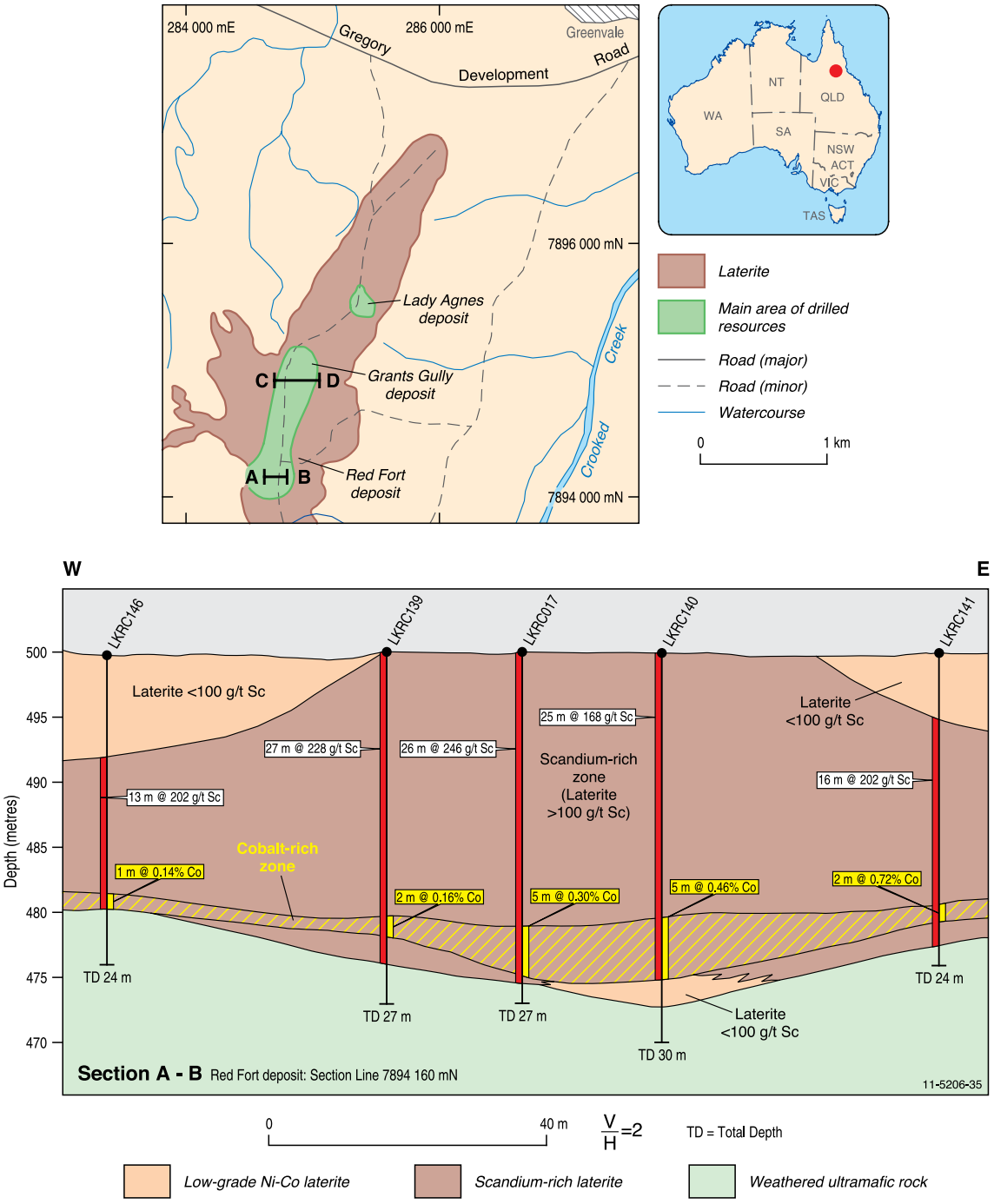

Figure 3.7. Distribution of scandium-bearing laterite (Lucknow Ni-Co-Sc Project) in the Greenvale region of northern Queensland. The Red Fort, Grants Gully, and Lady Agnes deposits have been the focus of drilling. The cross-section A–B for the Red Fort deposit highlights the wide thickness of scandium mineralisation (>100 g/t Sc) and the enrichment of cobalt in the lower part of the laterite profile. Modified from Metallica Minerals Limited (2010).

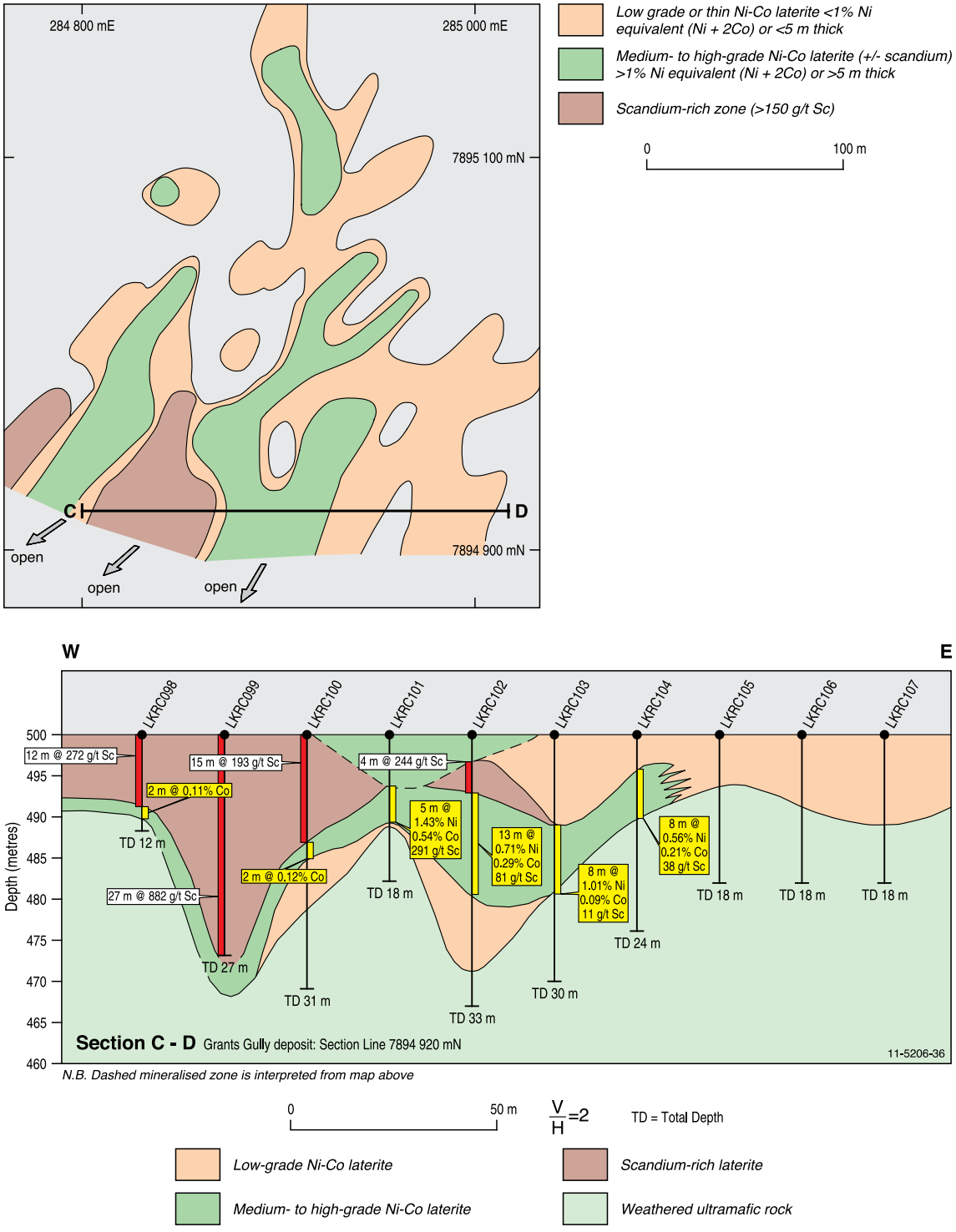

Figure 3.8. Metal distribution plan and cross-section C–D for the Grants Gully Sc-Ni-Co laterite deposit. The spatial distribution of metals has been generalised in the cross-section. The dashed mineralised zone in the cross-section is centred about drill hole LKRC101. The locations of the Grants Gully deposit and cross-section are shown in Figure 3.7. Modified from Metallica Minerals Limited (2010).

Province and is situated within the Gray Creek Fault Zone bounded by the Halls Reward Fault in the west and the Grey Creek Fault in the east (Henderson et al., 2011). Ultramafic and amphibolite rocks similar to those in the nearby Boiler Gully and Sandalwood complexes compose most of the northern and central parts of the complex. Dominant rocks include lateritised serpentinite, clinopyroxenite with interlayered wehrlite and gabbro, and amphibolite. The lateritised serpentinite is probably derived from dunite and peridotite. It contains relict olivine and enstatite, serpentine, chrysotile, chlorite, spinel, chromite, and magnetite. Cumulus textures are locally preserved in the pyroxenites. The northern end of the complex is characterised by a 500 m-wide core-zone of serpentinite flanked by clinopyroxenite that is interlayered with wehrlite and metagabbro. The southern part of the complex is represented by a younger phase of mafic magmatism that has produced a variety of rock types including extensive dykes, gabbro, tonalite, and trondhjemite. The complex has been intensely faulted both along the margins and internally, and it has been metamorphosed to amphibolite facies (Arnold and Rubenach, 1976). Fault zones have provided permeable zones for the advancement of alteration, and as major conduits for flushing away the soluble products of lateritisation. Rubenach (1982) notes that the mafic rocks of the Gray Creek and Boiler Gully complexes have geochemical characteristics of island-arc and ocean-floor tholeiites. Interpreted tectonic settings for the complexes range from Precambrian layered mafic-ultramafic intrusions, sills, and dykes emplaced along the southeastern margin of the Georgetown Inlier (Green, 1958; Arnold and Rubenach, 1976), to tectonically emplaced Precambrian ophiolites along the faulted margin of a Proterozoic craton (Rubenach, 1982), to fault-bounded Cambro-Ordovician bodies representing oceanic crustal components in an island-arc environment (Henderson et al., 2011).

Host rocks: Metallica Minerals Limited has defined high-grade nickel-cobalt and nickel-cobalt-scandium zones, as well as broad and thick scandium zones in the Lucknow deposit (Figs 3.7 and 3.8). The high-grade scandium mineralisation is contained within highly oxidised and weathered red-brown lateritic material and in many areas the mineralisation starts at surface and persists to a maximum depth of 40 m. Where the scandium is associated with high-grade nickel-cobalt grades, it usually occurs above these metals in the laterite profile. However, the scandium mineralisation is predominantly associated with low-grade nickel and cobalt abundances which possibly reflects the ultramafic rock protolith on which the laterite formed (Metallica Minerals Limited, 2010). The distribution of scandium in the laterite profile at Lucknow is summarised in Figures 3.7 and 3.8.

Table 3.3. Resource data for the Lucknow and Greenvale Sc-Ni-Co lateritic deposits.

Lucknow Sc-Ni-Co resource using a 70 g/t Sc cut-off grade (subject to Straits Resources Exploration Limited Joint Venture)						
Classification	Mt	Sc g/t	Ni%	Co%	NiEq%	Fe%
Measured	0.72	197	0.26	0.05	0.34	30.8
Indicated	2.67	171	0.19	0.04	0.27	35.4
Inferred	2.85	159	0.20	0.04	0.27	35.1
Total	6.24	169	0.20	0.04	0.28	34.7
Greenvale Ni-Co-Sc resource using a 0.70% nickel equivalent cut-off grade						
Classification	Mt	Sc g/t	Ni%	Co%	NiEq%	Fe%
Measured	2.63	33	1.08	0.09	1.26	22
Indicated	4.47	33	1.03	0.08	1.19	21
Inferred	0.90	30	0.99	0.07	1.12	19
Total	8.00	33	1.04	0.08	1.20	21

Source: Metallica Minerals Limited (2011).

The laterites at Greenvale are enriched in nickel (up to 2.5%), chromium (up to 3%), and to a lesser degree cobalt (up to 0.5%). Details of the behaviour and distribution of scandium in the Greenvale laterite are not available. The ore blanket extends over about 3.3 km^2 and averages about 8-m thickness with only minor lateral and vertical grade variation (Fletcher and Couper, 1975; Burger, 1982). Nickel in the ore horizon is fixed in goethite and népouite ($Ni_3Si_2O_5(OH)_4$), whereas cobalt is absorbed on smectite and manganese oxides (Burger, 1982). Fletcher and Couper (1975) divided the laterite profile at Greenvale into four zones; from the base they are:

1. weathered serpentinite laterite zone (average thickness ~10 m)—transition from fresh to weathered serpentinite corresponds to a specific gravity decrease from 2.7 to 1.4 and the development of saprolitic clays with parent-rock textures still preserved. Magnesite and goethite veinlets are developed along fractures, and chalcedonic and chrysoprase veins are abundant. Nickel is concentrated about 10 times the parent rock value and reaches a maximum near the upper boundary of this zone, whereas cobalt shows only minor enrichment. Almost 50% of the resources for the deposit are from this zone. The upper part of the zone is characterised by MnO_2 coatings and films on joints;
2. limonitic laterite zone (~5 m)—characterised by the lack of parent rock textures, with the mineralogy dominated by goethite and massive bands and irregular pods of secondary silica. Nickel concentrations are lower than the underlying zone, but cobalt attains maximum concentrations of 0.5% (25 times concentration) sympathetic with increased abundances of Cr_2O_3 and MnO_2;
3. pisolitic laterite zone (~7 m)—composed of ferruginous concretions, either partly cemented or unconsolidated, as pisolites, oolites, or irregular plates, which increase in abundance and diameter (to 5 cm) up the zone. A marked increase in density accompanies the mineralogical changes in this zone. Nickel and cobalt are depleted to background concentrations towards the top of the zone, with a marked increase in Al_2O_3; and
4. surface soils (~3 m)—red-brown unconsolidated residual soil with clayey layers, up to 10-m thick, but averaging 3 m, overlie pisolitic laterite or limonite.

REE mineralisation: Scandium is the only 'REE' documented in the laterite profile of the Lucknow deposit (Metallica Minerals Limited: http://www.metallicaminerals.com.au/). Serpentinised ultramafic rocks at the northern end of the Gray Creek Complex are mantled by a 500 to 1000 m-wide laterite layer containing several areas of Ni-Co-Sc mineralisation (Grants Gully, Red Fort, Lady Agnes). The Lucknow scandium-rich laterite deposit has significant bulk mineable drill intercepts of >200 g/t Sc that occur close to the Ni-Co ore zones. Extremely rich intersections of scandium (e.g., 27 m @ 882 g/t Sc) have been reported within these zones.

Source of REE: As with nickel, chromium, and cobalt, scandium is derived from the weathering of high MgO-bearing igneous rocks such as serpentinised dunite, peridotite, pyroxenite, and from more primitive basalts. Fresh serpentinite at Greenvale has a composition of about 37.1% SiO_2, 39.2% MgO, 0.63% Al_2O_3, 6.7% Fe_2O_3, 0.47% FeO, 0.28% Ni, and 0.01% Co. There are no known published references describing the scandium-bearing minerals concentrated in the Lucknow laterite deposit. In general, scandium is found in common rock-forming minerals, such as pyroxene, hornblende, and biotite, and in trace amounts (5 to 100 ppm) in basalt and gabbro. These three rock-forming minerals and mafic rock types are integral components of the igneous rock stratigraphy at Lucknow, and potentially could be a source(s) for the scandium. Scandium can also reside in the rare minerals thortveitite [$(Sc,Y)_2Si_2O_7$], which contains 44–48% scandium oxide Sc_2O_3, bazzite ($Be_3(Sc,Al)_2Si_6O_{18}$), wiikite (ill-defined mixture of REE), euxenite, and gadolinite.

Age of mineralisation: The precise age of the Ni-Co ± Sc laterites in the Greenvale region is not known. Fletcher and Couper (1975) proposed that erosion of cover rocks at Greenvale resulted in 5.5 km^2 of fractured hydrated serpentinite containing an evenly distributed 0.2% nickel being exposed to a Cenozoic land surface and climate. Burger (1982) suggested a possible mid-Cenozoic age for the main period of weathering and Ni-Co-Sc mineralisation, but there has been subsequent reworking and erosion of parts of the original laterite profile.

Similarly, the age(s) of the associated mafic-ultramafic protolith rocks are not well constrained with ages in the literature ranging from Late Proterozoic to early Paleozoic. Arnold and Rubenach (1976) showed that the Gray Creek Complex is structurally identical and chemically similar to the nearby Boiler Gully Complex suggesting a coeval/comagmatic association. Black et al. (1979) determined Mesoproterozoic Ar–Ar isotopic ages for S_1 hornblende from the Gray Creek Complex of 1111 ± 30 Ma and 1316 ± 40 Ma; the latter

providing a minimum age for the complex. However, Rubenach (1982) considers these ages equivocal due to possible complications of excess argon during isotopic analysis. Henderson et al. (2011) proposed that if a temporal relationship to other mafic-ultramafic belts in eastern Australia is used, then a Cambrian age is possible for the Greenvale complexes (Spaggiari et al., 2003). Recently, Huston (GA: pers. comm., 2011) determined a preliminary whole-rock Sm-Nd age of 466 ± 37 Ma for the Gray Creek Complex.

Similar laterites associated with 'Alaskan'-type mafic-ultramafic intrusions in the Fifield district of New South Wales are enriched in scandium (see Appendix 7). During the late Paleozoic, deep erosion exposed these intrusive complexes whilst continued weathering during the Mesozoic saw the development of up to 50-m thick laterite profiles and the scouring of paleo-alluvial channels in the underlying intrusions (http://www.platinaresources.com.au/files/projects/PC00736_Platina_Factsheet_Owendale_v1.pdf).

Genetic model: The following summary describing the genesis of the Ni-Co ± Sc laterite profiles in the Greenvale region is in part from Solomon and Groves (1994), and the references cited within. The prolonged weathering of serpentinised ultramafic rocks in a well drained, well aerated, and hence highly oxidised environment resulted in the removal of elements such as magnesium, and retention of nickel, chromium, cobalt, and scandium. Fracturing of the source serpentinite rock may have preceded weathering and facilitated the formation of a permeable profile. The water table probably was near the top of the saprolite zone. At a predicted rate of formation of 10 to 20 metres per million years, the Greenvale profile would have required at least one million years to become established during the Cenozoic. Fletcher and Couper (1975) suggested the rainfall was cyclic (monsoonal?), with periods of downward leaching by acid waters alternating with periods of oxidation; acidity derives from CO_2 in the atmosphere and NO_3^{2-} from the decay of vegetation. Steep groundwater gradients and lateral water movement allowed removal of soluble elements. The enrichment in nickel (factor of 10 times), chromium, cobalt, and scandium results in part from retention of primary metals in secondary silicates (e.g., népouite), and also from a concentration at the base of the profile of metal dissolved from higher levels. Dissolved nickel species migrate further down the profile due to higher solubilities compared to aqueous species of scandium, chromium, and cobalt. The development of lateritic profiles superimposed on ultramafic rocks in the Greenvale region is a function of the rate of downward movement of oxidation and surface erosion (Fletcher and Couper, 1975).

Key references: Fletcher and Couper (1975): petrology of ultramafic rocks, mineralisation and genesis of mineralised laterite;

Arnold and Rubenach (1976): regional geological setting, geology, and structure of mafic-ultramafic complexes;

Solomon and Groves (1994): genesis of mineralised laterites;

Fergusson et al. (2007): lithostratigraphy, structural, and deformational history of Greenvale region;

Henderson et al. (2011): regional geological setting, petrology, and geochemistry of country rocks, tectonic synthesis;

Metallica Minerals Limited: ASX Release 19th January 2011 (http://www.metallicaminerals.com.au/sites/default/files/MLM_Greenvale_Resource_Update.pdf); and

Metallica Minerals Limited: Quarterly Report to 31 December 2010, ASX Release 31st January 2011 (http://www.metallicaminerals.com.au/sites/default/files/MLM%20Qtly%20Dec10.pdf): mineralisation and resources of Lucknow and Greenvale laterite deposits.

Deposit Type 3.3: Beach sand heavy-mineral deposits with rare-earth-element-bearing monazite

General description: Heavy-mineral beach sand deposits have maintained Australia's position as a major world producer of rutile, ilmenite, and zircon for over four decades. Mining of beach sands first started on a major scale on the Australian east coast in the late fifties, then shifted to the fossil beach sand deposits of the Capel, Yoganup, and Happy Valley strandlines in the southwest of Western Australia, south of Perth, and on the fossil beach sand deposits at Eneabba (Fig. 3.9) and Cooljarloo north of Perth. The fossil beach sand deposits of the Murray Basin emerged in the mid nineties and now support mining operations at Ginkgo and Snapper in central New South Wales and the Douglas and Kulwin operations in Victoria. The latest emerging heavy-mineral province is the Eucla Basin where zircon is the dominant commercial mineral rather than the titanium-rich minerals of rutile, ilmenite, and leucoxene. The accessible beach sand heavy-mineral resources of the east coast of Australia have been mined out and all beach sand operations have closed down. The heavy-mineral beach sand deposits as defined here include a suite of beach placers comprising 'lag' deposits, 'transgressive' deposits, 'regressive' deposits, and 'aeolian' deposits in associated coastal

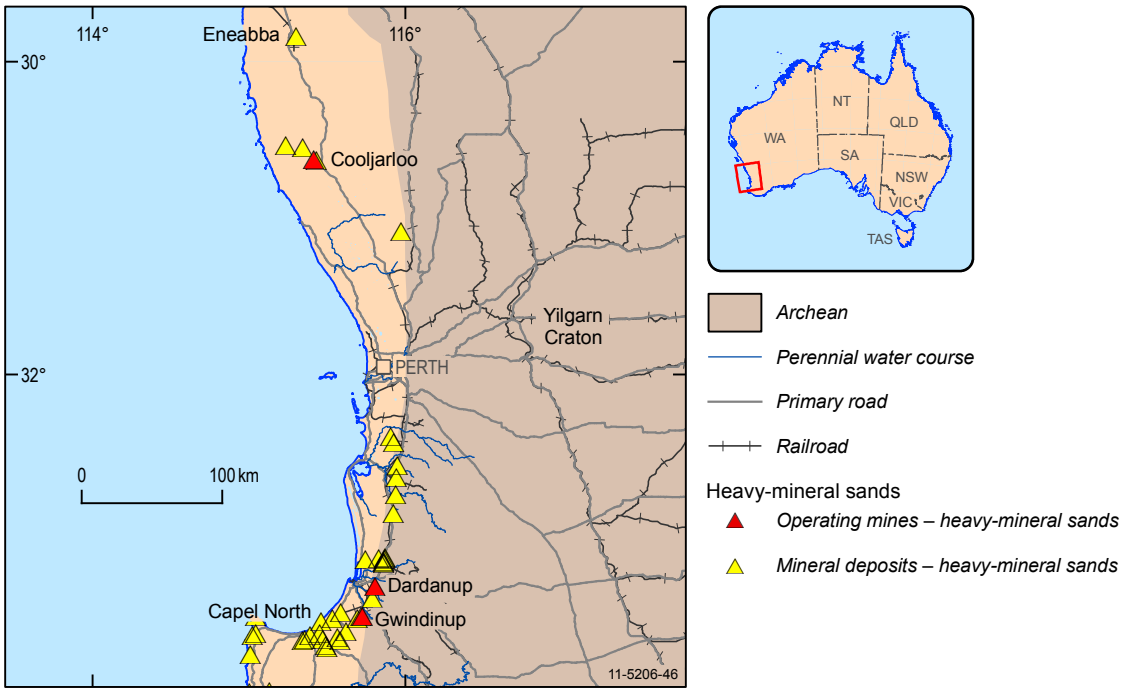

Figure 3.9. Beach sand heavy-mineral deposits along fossil beach strandlines in the Perth Basin, Western Australia.

dunes (Roy, 1999; Hou, 2005). The high dunes as described by McKellar (1975) are described separately under Deposit Type 3.4.

Australian deposits: Virtually all of the heavy-mineral resources in beach sand deposits in Australia are hosted in numerous deposits in inland fossil beach strandlines. The heavy-mineral sand deposits in fossil beach strandlines are located in the Murray Basin, of New South Wales, Victoria, and South Australia; in the southern Perth Basin along the Yoganup and Happy Valley strandlines and along the Eneabba and Cooljarloo fossil strandlines in the northern part of the Perth Basin in Western Australia. Some of the more important heavy-mineral sand developments in the Eucla Basin of South Australia include the recently commissioned heavy-mineral sand mine of Jacinth-Ambrosia, and the undeveloped deposit of Cyclone (Fig. 3.10).

Deposits outside Australia: Lake Malawi, Malawi; Srikurman, Andhra Pradesh, India; Chavara, Kerala, India; Alcobaca, Bahia, Brazil (Orris and Grauch, 2002).

Type example in Australia: Eneabba (Perth Basin, WA: Fig. 3.9); Jacinth-Ambrosia and Cyclone (both in Eucla Basin, SA: Fig. 3.10); Douglas and Ginkgo (both in Murray Basin: Vic and NSW, respectively).

Location: Eneabba: Longitude: 115.3003; Latitude: -29.8368
~240 km northwest of Perth, Western Australia
1:250 000 map sheet: Dongara (SH 50–05)
1:100 000 map sheet: Arrowsmith (1938)

Geological province: The Eneabba fossil beach strandlines are located on the Northern Swan Coastal Plain and overlie the Perth Basin, and there are also fossil beach strandlines on the Southern Swan Coastal Plain over the southern Perth Basin in southwest of Western Australia. The other provinces with fossil beach strandline heavy-mineral sand deposits are the Murray Basin in New South Wales, Victoria, and South Australia, and the Eucla Basin in South Australia and Western Australia (Fig. 3.10).

Resources: Beach sand placer deposits represent a major source of rutile, ilmenite, zircon, and in the past–of monazite. According to Lissiman and Oxenford (1975), the original resource at Eneabba was of the order of 25 to 30 million tonnes of recoverable heavy minerals with a monazite content of about 0.5%. Production of monazite at Eneabba, for extraction of REE and thorium, peaked between 1975 and 1985 (Shepherd, 1990).

Current status: Eneabba is a major heavy-mineral sand mine currently under care and maintenance, but REE have not been recovered from monazite since 1995.

Economic significance: Prior to 1995, Eneabba was a significant exporter of monazite for extraction of REE and thorium. Currently the REE are not extracted from the monazite which is returned back to the mine site.

Geological setting: Heavy-mineral deposits in coastal regions require a stable tectonic environment with efficient sorting and winnowing mechanism by wave action and wind which sort sediments derived from deeply weathered igneous–metamorphic terranes or from older sedimentary rocks derived from the original igneous–metamorphic terranes. Faulting during sedimentation has influenced the distribution of heavy-mineral deposits in the Murray Basin (Roy et al., 2000).

Host rocks: Pleistocene–Holocene dune sand, Middle Eocene to Miocene in Eucla Basin.

REE mineralisation: The REE are held within the monazite and xenotime contents of the heavy-mineral concentrate. The range of REO contents in monazite and xenotime in both minerals from concentrates from Western Australia is shown in Table 3.4. Table 3.5 shows REO and thorium oxide contents in monazite and xenotime concentrates from Eneabba, Capel, and Yoganup mines in Western Australia as produced prior to 1996. Figures from similar concentrates from the USA, India, and Malaysia are also included for comparison. Table 3.6 provides a comparison of the distribution of REO in monazite from three mines in Western Australia with mines in the USA, Taiwan, China, and India.

Table 3.4. Variation of the chemical composition (%) of individual monazite and xenotime grains from concentrates, Western Australia (Elsner, 2010).

	Monazite			Xenotime		
	Range	Mean	Standard deviation	Range	Mean	Standard deviation
La_2O_3	8.9–21.0	14.53	2.13	-	-	-
Ce_2O_3	21.7–35.0	28.52	2.17	-	-	-
Pr_2O_3	1.8–3.2	2.53	0.26	-	-	-
Nd_2O_3	4.8–12.7	8.85	0.26	-	-	-
Sm_2O_3	0.36–2.89	1.53	0.45	<0.16–1.82	0.47	0.22
Gd_2O_3	<0.16–2.71	0.88	0.51	<0.16–4.56	1.91	0.59
Dy_2O_3	<0.16–1.28	0.26	0.30	2.4–7.5	5.11	0.72
Ho_2O_3	-	-	-	<0.16–1.59	1.17	0.16
Er_2O_3	<0.16–0.45	0.02	0.08	2.5–6.6	4.63	0.49
Tm_2O_3	-	-	-	<0.16–0.70	0.70	0.14
Yb_2O_3	-	-	-	1.4–11.4	4.56	1.22
Lu_2O_3	-	-	-	<0.16–1.95	0.54	0.24
Y_2O_3	<0.06–6.25	1.19	0.66	40.2–53.2	46.82	1.91
ThO_2	1.2–21.9	8.79	0.08	<0.17–8.44	0.46	0.68
UO_2	<0.17[1]–0.75	0.08	0.23	<0.17[1]–5.82	0.57	0.86
CaO	0.12–2.50	0.98	1.10	<0.02[1]–0.54	0.06	0.06
SiO_2	0.12–4.01	1.09	0.66	<0.02[1]–1.98	0.38	0.26
P_2O_5	25.1–32.6	30.33	1.24	29.7–36.4	34.55	0.73
Total	92.5–103.1	99.58	2.10	96.0–105.2	101.93	1.17

[1] Below detection limit.

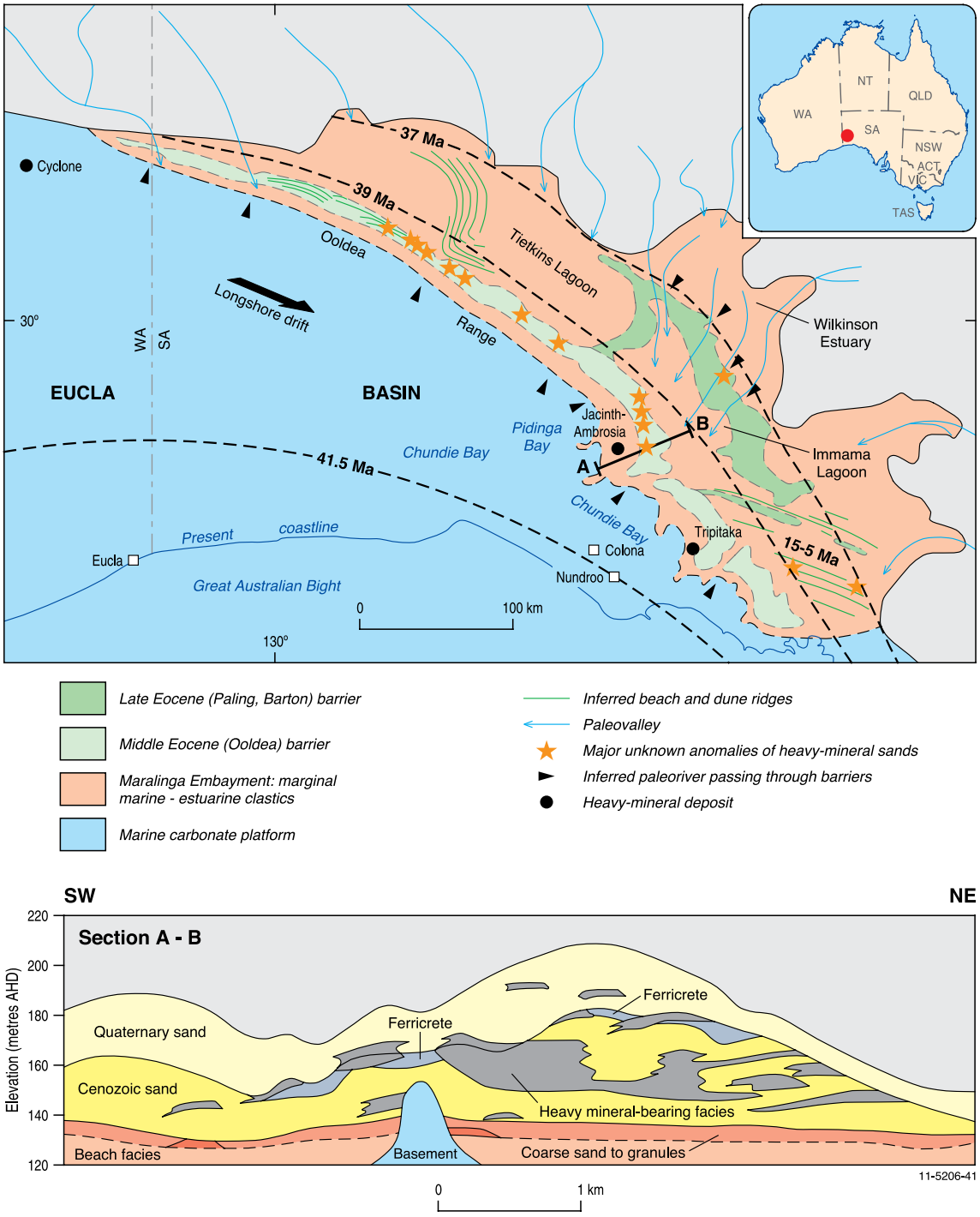

Figure 3.10. Fossil beach strandlines and heavy-mineral deposits in the Eucla Basin and cross-section, South Australia. Four generations of shorelines are shown by dashed lines at 41.5 Ma, 39 Ma, 37 Ma, and 15–5 Ma. Modified from Hou (2005).

Table 3.5. Chemical composition (%) of monazite and xenotime concentrates (Elsner, 2010).

Area of deposit or producer	REO	ThO_2	H_2SO_4-insoluble	TiO_2	P_2O_5
WA–Eneabba	58	6.4			
WA–Capel	57	7			
WA–Yoganup (guaranteed)	>55	>6	<10		
WA–Yoganup (typical)	56–58	6.5–7.0	7.0–8.5	0.3–0.6	
USA–Green Cove Springs	57	7			
India–KMML	57.5	7.96	5.05		28.2
Malaysia–monazite average		6			27
Malaysia–xenotime average		0.7			29

Source of REE: At Eneabba the immediate source for the REE-bearing monazite in the dune and beach sands is considered to be the underlying Mesozoic sedimentary rocks, but the Archean crystalline basement provided the original source rocks (Shepherd, 1990).

Age of mineralisation: The age range varies from late Neogene to early Pleistocene for the Eneabba region on the Northern Swan Plain. Elsewhere the age varies from Holocene along present day beaches to as old as Eocene in the Eucla Basin.

Genetic model: Heavy-mineral concentrations in beach sands form by high energy wave action and are built up along coastal regions of stable crustal margins with tectonic stability important for preservation of deposits. Environmental conditions for fractionating mechanisms to operate include: low rates of clastic sediment supply and long periods of weathering and abrasion to create a mature heavy-mineral suite, an energetic swell wave climate driving large sand fluxes onshore and alongshore, and changing sea levels (especially marine transgressions) that have the effect of moving heavy minerals from the shelf onto the present coast (Roy, 1999). The sorting action is most effective under conditions of surf wave action during storms and long-shore drift along 'J' curved shorelines preceding a headland (McKellar, 1975; Baxter, 1977). The heavier minerals are obstructed by the headlands to form deposits while the lighter grains are carried around the headlands by wave action. At Eneabba, monazite contents can be up to 7% near the southern end of the strandlines, i.e., in the direction of the longshore drift approaching a headland (Shepherd, 1999; page 1593). The Eneabba heavy-mineral deposits are located in a series of fossilised shorelines between 29 and 115 m above sea level. The highest heavy-mineral concentrations occur over a length of 20 km and a width of 9 km (Shepherd, 1990).

Key references: Baxter (1977) and Roy (1999): origin and resources of heavy-mineral deposits; and Elsner (2010): chemical analyses of monazite and xenotime from heavy-mineral deposits.

Deposit Type 3.4: High dune sand heavy-mineral deposits with rare-earth-element-bearing monazite

General description: McKellar (1975) noted that remnants of a system of old dunes exceeding 180 m in height occur at intervals along the east coast from the Hawkesbury River in New South Wales to Fraser Island in Queensland. The very large low-grade heavy-mineral resources in these high dune sand deposits are described here as a separate class from the usual transverse aeolian and beach foredunes associated with the suite of beach sand heavy-mineral deposits. The most significant high dune sand heavy-mineral deposits are along the east coast of Queensland between the North and South Stradbroke Islands near Brisbane in south and Fraser Island in the north. The Byfield deposit, 380 km northwest of Fraser Island, is also hosted in high dune sands. Generally the heavy-mineral content in dune sands is less than 0.05 %, but in places it attains ore grades of 1 to 2% heavy minerals with sand tonnages ranging from a few hundred million tonnes to large mineralised zones in dune sands in excess of a billion tonnes. The Byfield deposit, for example, has 2.4 billion tonnes of sand at 1.14% heavy minerals, or 0.09% ilmenite, 0.06% rutile, and 0.16% zircon (Strategic Minerals Corporation, 2004). Unpublished data indicate that the heavy minerals contain about 0.2% monazite. The high dune sand heavy-mineral deposits are often fringed by heavy-mineral beach sand deposits.

Table 3.6. Chemical composition of monazite concentrates from selected deposits world wide (Elsner, 2010).

	Manavalakurichi MK-Grade Indian Rare Earths Ltd. Tamil Nadu, India	**Beihai Processing Plant** Guangxi Province China	**Folkston (I)** Humphreys Gold Corp. Georgia, USA	**Folkston (II)** Humphreys Gold Corp. Georgia, USA	**Green Cove Springs (I)** Iluka Resources Ltd. Florida, USA	**Green Cove Springs (II)** Iluka Resources Ltd. Florida, USA	**Capel** Western Titanium N.L. Western Australia	**Eneabba** RGC Mineral Sands Ltd. Western Australia	**Yoganup** Westralian Sands Ltd. Western Australia	**Indonesia**	**Black Monazite** Taiwan	**Brazil**
REO total		**61.86**	**av. 58.9**	**60.53**	**58.57**	**55.04**			**56.0-58.0**			**59.2**
La_2O_3	15.7			11.99	11.98	10.03	16.20	14.82	13.5	14.29	25.41	8.64
CeO_2	30.6		av. 25.4	26.45	26.49	27.12	26.70	27.60	26.0	30.25	23.18	26.94
Pr_6O_{11}	2.9			3.07	2.99	2.55	2.60	2.93	2.85	3.35	1.27	3.55
Nd_2O_3	10.5			10.6	9.99	8.72	11.00	9.44	9.82	10.77	7.95	14.50
Sm_2O_3				2.09	2.09	1.72	1.30	1.45	1.43	2.01		3.26
Eu_2O_3				0.16	0.14	0.12	0.02		0.03			
Gd_2O_3				1.38	1.40	1.41	0.30		0.84			
Tb_4O_7				0.16	0.15	0.14			<0.02			
Dy_2O_3				0.77	0.63	0.53	0.20		0.39			
Ho_2O_3				0.14	0.107	0.087	+		<0.03			
Er_2O_3				0.312	0.168	0.139			0.12			
Tm_2O_3				0.038	0.018	0.014			<0.01			
Yb_2O_3				0.178	0.066	0.058			0.07			
Lu_2O_3				0.0200	0.0090	0.0068			<0.02			
Y_2O_3	0.04	2.22		3.16	2.35	2.39	0.60	1.42	1.36	2.51	1.07	
H_2SO_4-insol.[1]			av. 8.2			8.25	8.50		7.0-8.5		22.94	
TiO_2	0.4		av. 0.42			0.09		0.81	0.3-0.6	0.09		1.75
SiO_2	2.4	1.23	av. 2.6					2.55		2.17	18.08	2.2
ZrO_2	1.3	0.13	av. 3.8					2.05		0.20		
$Al2O_3$	0.1	0.14	av. 1.7					0.81		0.37		
Fe_2O_3	0.9	0.62	av. 0.63					0.33		n.d.		0.51
P_2O_5	29.2	30.00					27.00	26.55		27.46	20.55	26.0
ThO_2	9.0	6.31	av. 4.2			4.24	6.80	6.40	6.5-7.0	4.67		6.5
U_3O_8								0.31		0.32		0.17
CaO		0.16	av. 1.1					0.95		0.18	+	
LOI	0.1							0.52		0.60		

[1] Proportion of REO insoluble (insol.) in H_2SO_4.

Australian deposits: Byfield, Fraser Island, Cooloola, Moreton Island, and North Stradbroke Island (all Qld).

Deposits outside Australia: Richards Bay South Africa, Trail Ridge USA (Orris and Grauch, 2002; Jackson and Christiansen, 1993).

Type example in Australia: North Stradbroke Island, Queensland (Fig. 3.11).

Location: Longitude: 153.4425; Latitude: -27.4784
~30 km east-southeast of Brisbane, Queensland
1:250 000 map sheet: Brisbane Special (SG 56–15)
1:100 000 map sheet: Brisbane (9543)

Geological province: The high dune sands occur at intervals over a distance of about 1400 km along the east coast of Australia from the Hawkesbury River in New South Wales to Byfield in Queensland (Fig. 3.11).

Resources: The latest published resources for North Stradbroke Island, as in December 2008, amounted to Measured, Indicated, and Inferred Resources of 1195 million tonnes of sand at 0.9% heavy minerals, or 10.36 million tonnes of heavy minerals at 47% ilmenite, 11% zircon, and 14% rutile (Iluka Resources Limited, 2008). Gardner (1955) reported the monazite content in the heavy-minerals concentrate as 0.3%. Cassidy et al. (1997) reported a total resource for the North Stradbroke Island deposit in the order of 3000 million tonnes at about 1% heavy minerals with the proportion of monazite recovered from the heavy-minerals concentrate of about 0.2% of the heavy-mineral concentrate.

Current status: A major operating heavy-mineral sand mine but REE are not recovered from monazite.

Economic significance: The North Stradbroke Island dune sand deposit is the only heavy-mineral-mining operation remaining on the east coast of Australia. Fraser Island, Cooloola, and Moreton Island deposits are within various types of conservation reserves and these resources are not available for mining. The North Stradbroke Island deposit is mined for its rutile, zircon, and ilmenite content. The REE are not extracted from the monazite which is returned back to the mine site.

Geological setting: Heavy-mineral concentrations in dune sands form by the winnowing action of wind. Dune sands built up along coastal regions of stable crustal margins with tectonic stability important for preservation of deposits. North Stradbroke Island is a complex coastal sedimentary system comprising beach sand, parallel dune sand and high transverse dune sand deposits. Most of the heavy-mineral sand resource occurs as low-grade heavy-mineral zones in the large transverse dune sand. North Stradbroke Island forms part of the Pleistocene–Holocene heavy-mineral-bearing sand mass of the east Australia coastal zone between the Hawkesbury River in the south in New South Wales to Byfield in Queensland in the north.

Host rocks: Pleistocene–Holocene dune sand, some possibly as old as Miocene.

REE mineralisation: The REE is held within the monazite content of the heavy-mineral concentrate with the REO content in monazite at around 55% to 60%. The distribution of the REO in monazite from North Stradbroke Island is shown in Table 3.7 and a world-wide distribution of REO in monazite from undifferentiated types of heavy-mineral sand deposits is shown in Table 3.8.

Table 3.7. Distribution of types of rare-earth elements in monazite from North Stradbroke Island, Queensland (Hedrick, 2000).

REO	REO in monazite from North Stradbroke Island, Queensland (weight%)
La_2O_3	21.50
CeO_2	45.80
Pr_6O_{11}	5.30
Nd_2O_3	18.60
Sm_2O_3	3.10
Eu_2O_3	0.80
Gd_2O_3	1.80
Tb_4O_7	0.30
Dy_2O_3	0.60
Ho_2O_3	0.10
Er_2O_3	0.20
Tm_2O_3	-
Yb_2O_3	0.10
Lu_2O_3	0.01
Y_2O_3	2.10
Total	100.71

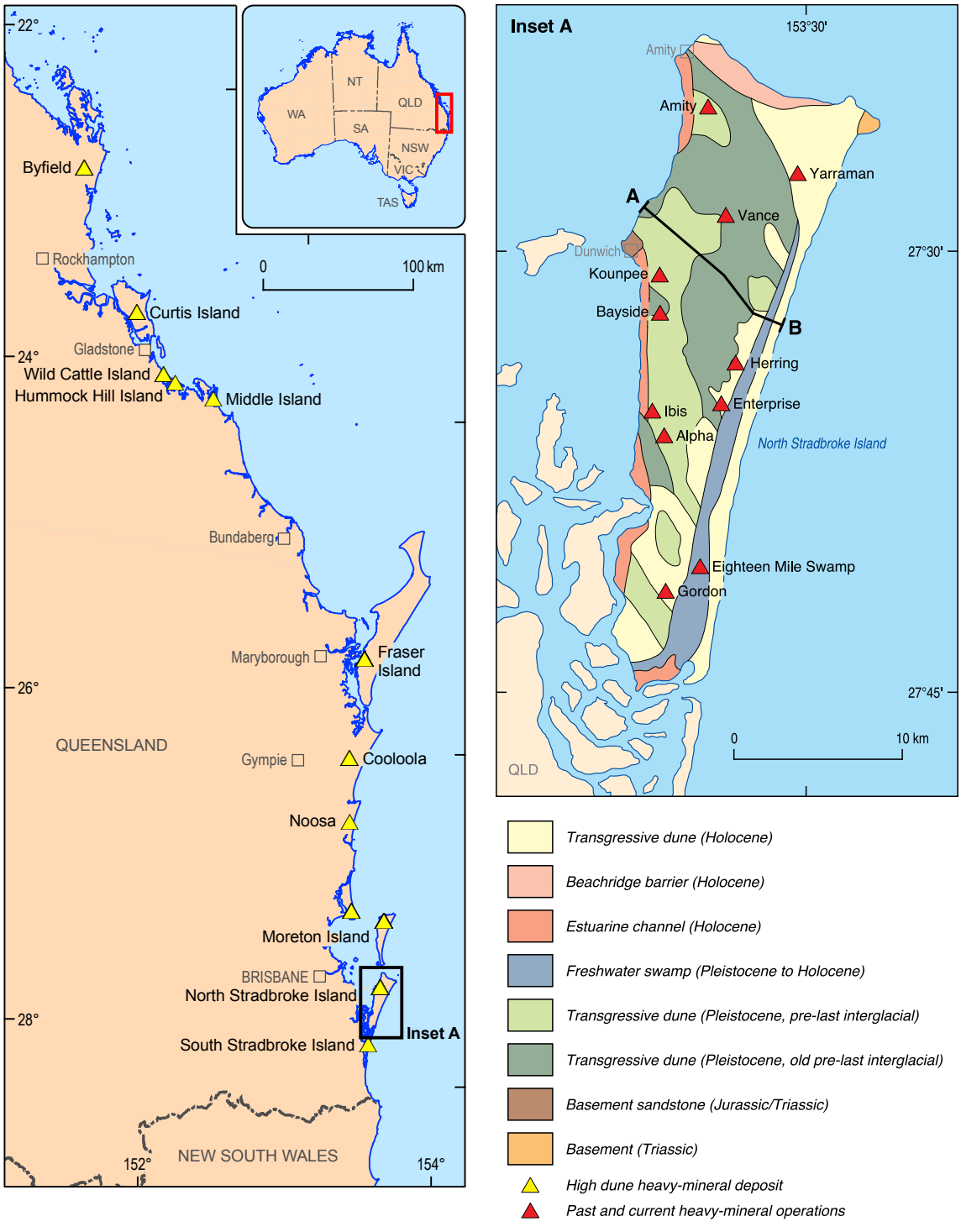
22°
24°
26°
28°
152°
154°
NEW SOUTH WALES
QUEENSLAND
Byfield
Rockhampton
Curtis Island
Gladstone
Wild Cattle Island
Hummock Hill Island
Middle Island
Bundaberg
Maryborough
Fraser Island
Gympie
Cooloola
Noosa
Moreton Island
BRISBANE
North Stradbroke Island
South Stradbroke Island
Inset A
0
100 km
NT
WA
SA
QLD
NSW
VIC
TAS
Inset A
153°30'
27°30'
27°45'
Amity
Yarraman
Vance
Dunwich
Kounpee
Bayside
Herring
Enterprise
Ibis
Alpha
North Stradbroke Island
Eighteen Mile Swamp
Gordon
A
B
0
10 km
QLD
Transgressive dune (Holocene)
Beachridge barrier (Holocene)
Estuarine channel (Holocene)
Freshwater swamp (Pleistocene to Holocene)
Transgressive dune (Pleistocene, pre-last interglacial)
Transgressive dune (Pleistocene, old pre-last interglacial)
Basement sandstone (Jurassic/Triassic)
Basement (Triassic)
High dune heavy-mineral deposit
Past and current heavy-mineral operations

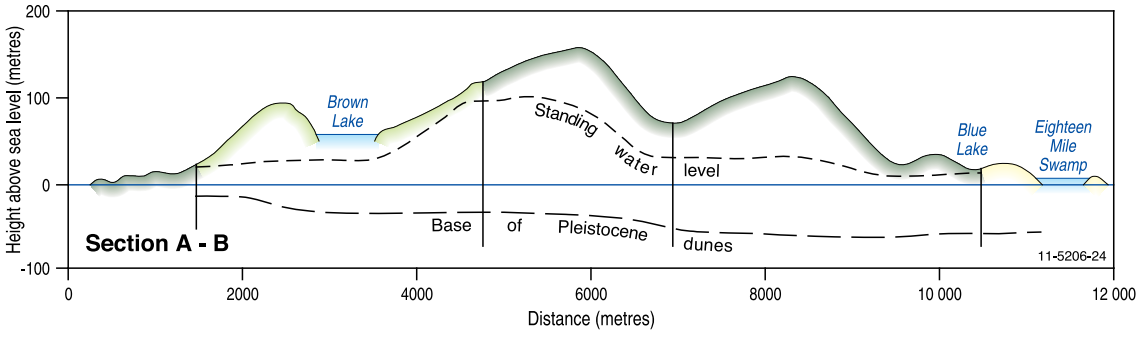
Height above sea level (metres)
200
100
0
-100
Brown Lake
Standing water level
Blue Lake
Eighteen Mile Swamp
Base of Pleistocene dunes
Section A - B
11-5206-24
0
2000
4000
6000
8000
10 000
12 000
Distance (metres)

Table 3.8. Distribution of types of rare-earth elements in monazite from different parts of the world (modified from Mukherjee, 2007).

Rare-earth oxide	Guangdong, China (wt %)	Taiwan (wt %)	Florida, USA (wt %)	India (wt %)	Australia (wt %)
La_2O_3	23	21	17.4	22	23.2
CeO_2	42.7	47.9	43.7	46	46.3
Pr_6O_{11}	4.1	5.4	4.9	5.5	4.9
Nd_2O_3	17	18.7	17.1	20	18.3
Sm_2O_3	3	3.3	4.9	2.5	2.5
Eu_2O_3	<0.1	0.54	0.16	0.016	0.04
Gd_2O_3	2	1.6	6.5	1.2	1.7
Tb_4O_7	0.7	0.19	0.26	0.06	0.22
Dy_2O_3	0.8	0.35	0.59	0.18	0.56
Ho_2O_3	0.12	0.03	0.11	0.02	0.08
Er_2O_3	<0.03	0.03	0.04	0.01	0.06
Tm_2O_3	Tr	-	0.03	Tr	-
Yb_2O_3	0.24	0.07	0.21	Tr	0.04
Lu_2O_3	<0.14	-	0.03	Tr	-
REO	55	48–62	-	58	58.5
Y_2O_3	2.4	0.19	3.18	0.45	1.57

Source of REE: The ultimate source for the REE-bearing monazite in the dune and beach sands is considered to be igneous–high-grade metamorphic rocks, but generally monazite was captured with zircon, rutile, and ilmenite in earlier depositional cycles and subsequently eroded.

Age of mineralisation: The age range of dune and beach sands is considered to be Miocene to Holocene, but generally Pleistocene to Holocene. Limited data summarised by Lees (2006) indicate that at least eight dune sand emplacements can be recognised in the sand masses of the Great Sandy region of southern Queensland that includes Fraser Island, Cooloola, the Peregian sandhills, Moreton, and the Stradbroke islands. Available optically stimulated luminescence (OSL) dating has identified episodes of dune emplacements at Cooloola at about 730 000 years ago (years before present (YBP)), at about 460 000 YBP, 395–280 000 YBP, 215–195 000 YBP, 170–130 000 YBP at between 9500–7500 YBP, 3100 YBP and 500 YBP. Lees (2006) noted that there were very few dates available for the other dune sand masses in the area.

New South Wales data summarised by Lees (2006) show a complex sequence of six dune forming events for Newcastle Bight–Myall Lakes area in New South Wales. Age estimates for these events range from 36–30 000 YBP (^{14}C), 18–17 000 YBP, 9–7000 YBP (7280 ± 220 ^{14}C YBP and 8850 ± ^{14}C YBP), one at about 3500 YBP, another at about 2500 YBP, and one between 800 and 400 YBP. Older dune-forming events (170–130 000 YBP) have been identified at other locations including Red Point and Port Stephens in New South Wales, but error ranges for these older events are considered to be too broad for meaningful analysis (Lees, 2006).

Genetic model: Heavy-mineral deposits in coastal regions require a stable tectonic environment with efficient sorting and winnowing mechanism by wave action and wind which sort sediments from a deeply weathered igneous–metamorphic terranes or from older sedimentary rocks derived from the original igneous–metamorphic terranes. The low-grade heavy-mineral concentrations in the dune sands are usually derived by wind action from higher-grade heavy-mineral concentrations on the beach previously formed by wave action. McKellar (1975) postulated that the

Figure 3.11 (see opposite). High dune sand heavy-mineral deposits along the southern Queensland coast, including geology of North Stradbroke Island (Inset A) and cross-section. Modified from Wallis and Oakes (1990).

high dune system on the east coast of Australia was formed during periods of maximum sea level depression under climatic extremes of the ice ages. According to Chappell and Shackleton (1986), sea level oscillations over the last 150 000 years are marked by a large marine recession 150 000 years ago when the sea level dropped to a maximum of 150 m below the present sea level followed by a similar drop of 150 m about 10 000 years ago. At times of maximum low sea levels, broad expanses of unconsolidated sand would have been exposed and swept inland by wind to form high dune systems which reach heights in excess 180 m and above the current sea level. According to Lees (2006), while the bulk of the dunes on the north and northeast Australian coast were emplaced during glacial maxima, this does not appear to be the case for the east coast where the high dunes on the North Stradbroke Island are located and more dates are required to determine the formation of the dunes in the eastern region.

Key references: McKellar (1975): distribution and origin of the high dune sands; and
Lees (2006): age estimates of dune formation.

Deposit Type 3.5: Offshore-shallow-marine heavy-mineral deposits with rare-earth-element-bearing monazite–(WIM 150 type)

General description: The resources of the five fine-grained (less than 80 micron) WIM deposits (WIM 50, 100, 150, 200 (now renamed as Jackson deposit) and 250 (Donald deposit)) have not been fully assessed and are currently under investigation for their zircon, rutile, and ilmenite content (Fig. 3.12). The presence of thorium and uranium in monazite discourages commercial interest in processing monazite for its rare earth content. Mining companies generally do not publish detailed resource assessments of monazite in heavy-mineral deposits, including those of the WIM deposits. Detailed assessments of the REO content in the monazite also are not generally available in the public domain. According to historic resource estimates, the five WIM heavy-mineral sand deposits could contain of the order of 3 million tonnes of REO in over 200 million tonnes of heavy-mineral (HM) concentrates and could represent a major proportion of the REO resources in monazite in Australian beach sands (Cassidy et al., 1997). Description of the model derived from descriptions by Williams (1990), Stitt (1999), Mason (1999), and Roy and Whitehouse (1999).

Australian deposits: WIM 150, Donald (WIM 250), Jackson (WIM 200), WIM 100, and WIM 50 (all in the Murray Basin, Vic). Beenup? (WA).

Deposits outside Australia: Not known.

Type example in Australia: WIM 150, Victoria (Fig. 3.13).

Location: Longitude 142.3400; Latitude -36.8062 ~18 km southeast of Horsham, Victoria

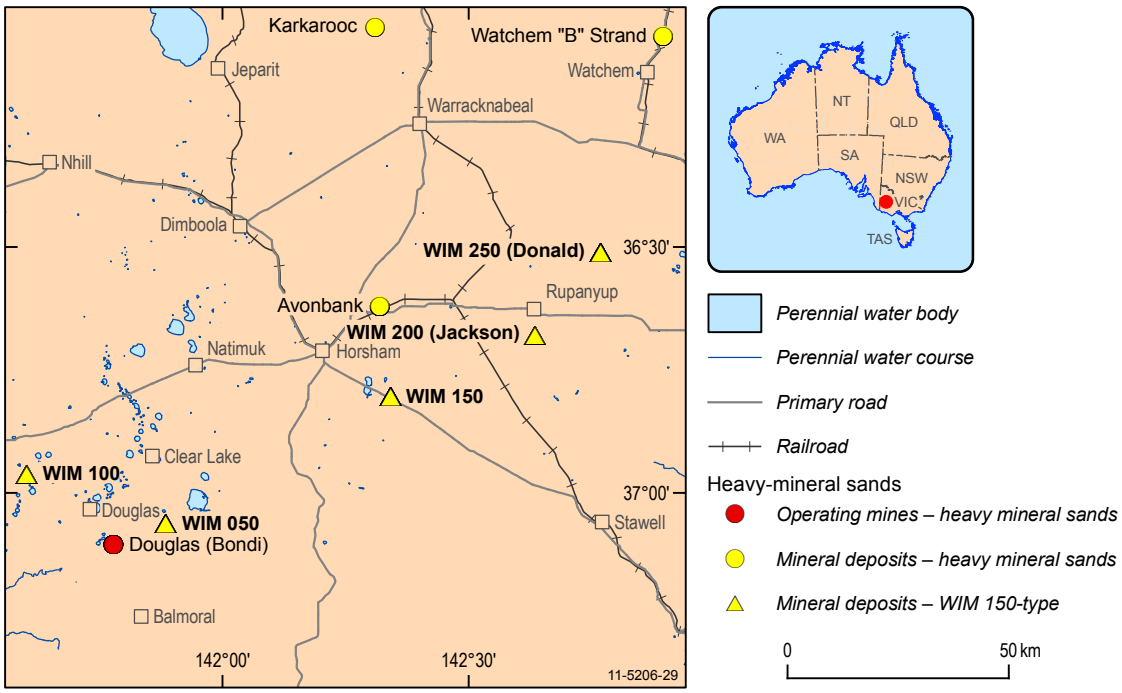

Figure 3.12. Regional map of WIM 150-type heavy-mineral deposits near Horsham, Victoria.

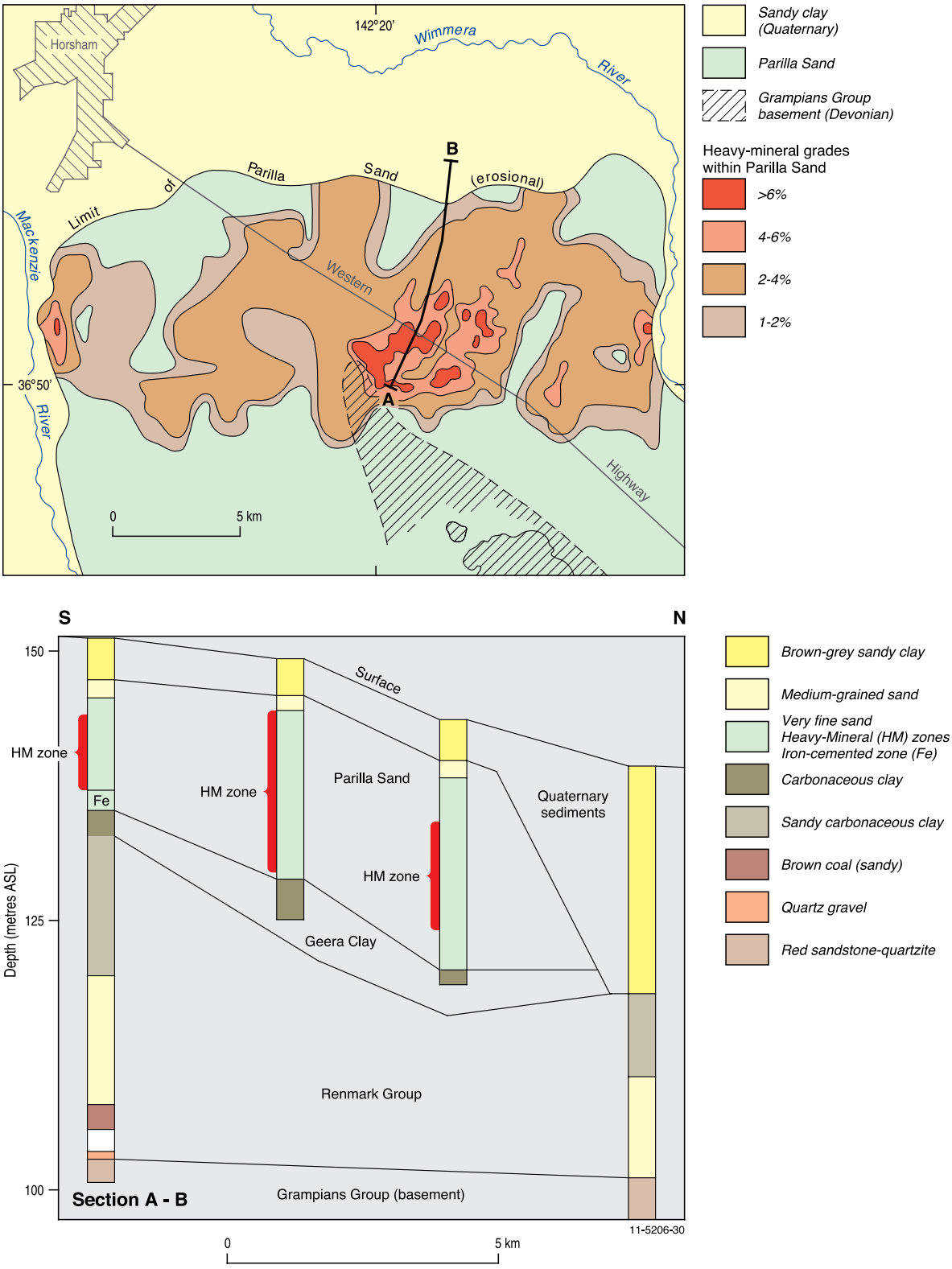

Figure 3.13. Geological map and cross-section of the WIM 150 heavy-mineral deposit (see Fig. 3.12), Victoria. Modified from Williams (1990).

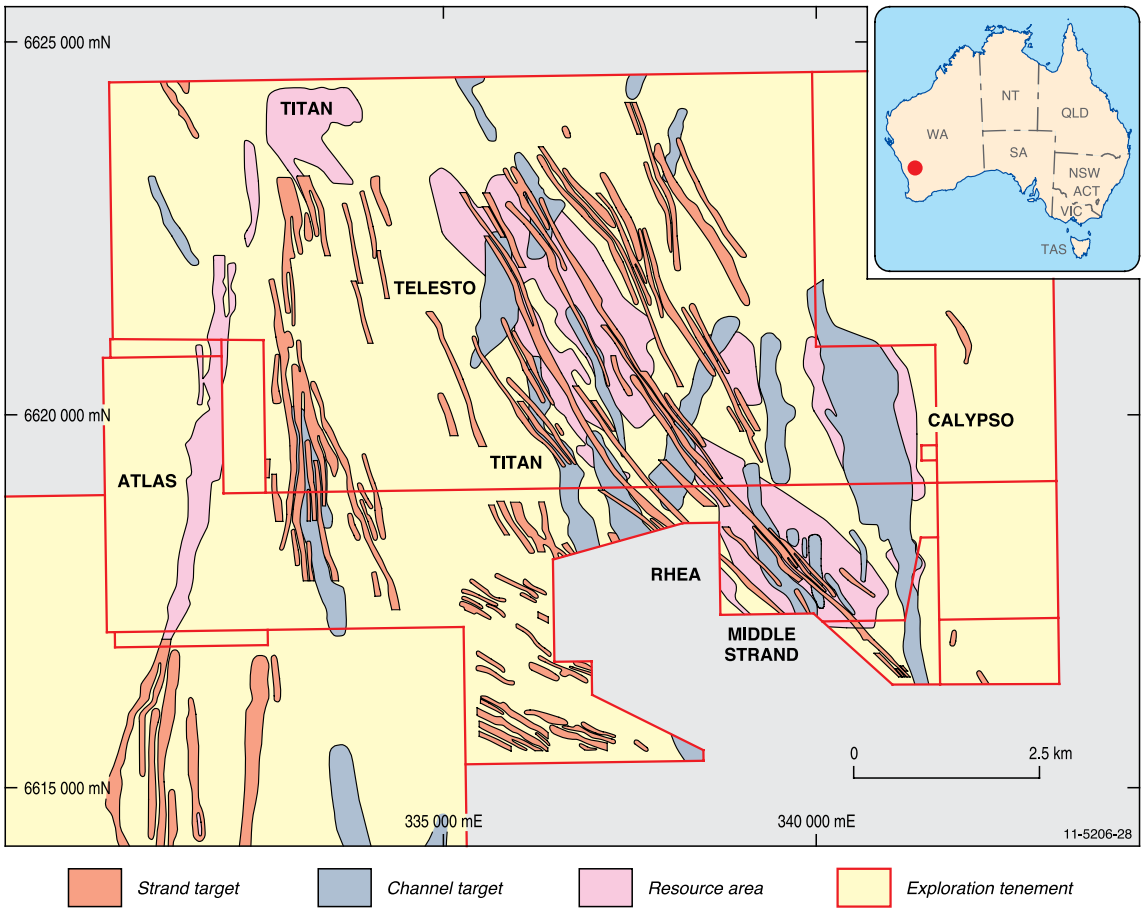

Figure 3.14. Strand and channel heavy-mineral deposits as interpreted from magnetic surveys near Calypso, Western Australia. Modified from Image Resources Limited (2010).

1:250 000 map sheet: Horsham (SJ 54–03)
1:100 000 map sheet: Horsham (7324)

Geological province: Murray Basin in Victoria, New South Wales, and South Australia.

Resources: Current published Indicated and Inferred Resources for WIM 150 stand at 727 million tonnes of sand at about 3.9% HM giving about 28.5 million tonnes of HM. The zircon, rutile, ilmenite, and monazite contents in the HM have not been published, but Williams (1990) reported the HM constituents for the WIM 150 deposit as 13.3% zircon, 8.7% rutile and anatase, 31.6% ilmenite, 11.6% leucoxene, 1.4% monazite, and 0.4% xenotime.

On 27 April 2010, Astron Limited announced a combined Indicated and Inferred Resource for the Donald (WIM 250) and Jackson (WIM 200) deposits of 4.5 billion tonnes of sand grading at 4% HM (Astron, 2010a). On 27 July 2010, Astron also announced areas of higher-grade HM within this resource, which contained 370 million tonnes of Indicated Resources of sand grading 6.1% HM (Astron, 2010b). The HM contained 32% ilmenite, 19.0% leucoxene, 4.5% rutile, and 19% zircon; and 1010 million tonnes of sand grading 5.7% HM containing 33% ilmenite, 16.0% leucoxene, 1% rutile, and 18% zircon.

Current status: Large undeveloped deposit.

Economic significance: In the past the fine grain size of the offshore shallow marine deposits have presented difficulties in processing the heavy-mineral concentrates. Such problems are currently being overcome and government approvals in regard to environmental and mining regulations are currently under way to mine the Donald deposit (previously WIM 250) in Victoria. As noted above, the presence of thorium and uranium in monazite discourages commercial interest in processing monazite for its rare-earth content.

Geological setting: Very fine-grained HM concentrations form as large, tabular deposits thought to be deposited on the lower shoreface/inner shelf under low-energy conditions. Sediment derived from

deeply weathered igneous and metamorphic terranes of sillimanite or higher grade. The origin of these deposits is not well understood.

Host rocks: Fine-grained silt in offshore deposits.

REE mineralisation: The REE is held mainly within the monazite and to a lesser extent within the xenotime content of the HM concentrate, with the REO content in monazite at around 55% to 60% and the thorium content of around 6% Th.

Source of REE: The ultimate source for the REE-bearing monazite in the dune and beach sands is considered to be igneous–high-grade metamorphic rocks but generally monazite was captured with zircon, rutile, and ilmenite in earlier depositional cycles and subsequently eroded.

Age of mineralisation: Age range of Miocene to Holocene, with the WIM-type deposits considered to be part of the Miocene to Pliocene Murray Basin sedimentary sequence.

Genetic model: Margin of craton or intracratonic basin. Crustal stability during deposition and preservation of deposits.

Williams (1990) noted that the major features of the WIM-type deposits (Fig. 3.13) are:

- broad lobate plan geometry;
- lateral continuity of individual heavy-mineral lenses;
- continuity of grades over large areas;
- uniformity of the heavy-mineral assemblage;
- fine-grain size of heavy minerals and host sand; and
- undulating to hummocky cross-stratified heavy-mineral concentrations.

Williams (1990) noted that these features are not shared by heavy-mineral sand deposits formed in coastal beach and dune sand environments and suggested that undulating and hummocky cross-stratification may indicate offshore deposition below the fair weather wave base during storms.

Key references: Williams (1990): regional and local descriptions of WIM 150 deposit.

Deposit Type 3.6: Channel placer heavy-mineral deposits with rare-earth-element-bearing monazite

General description: Heavy-mineral sand concentrations as placers in terrestrial drainage channels rather than in coastal environments.

Australian deposit: Calypso (WA).

Deposits outside Australia: Fluvial deposits of rutile in Sierra Leone and Cameroon; Sao Gancalo do Sapucal (Minas Gerais), Brazil (Jackson and Christiansen, 1993; Orris and Grauch, 2002).

Type example in Australia: Calypso, Western Australia (Fig. 3.14).

Location: Longitude: 115.3423; Latitude: -30.5509
~155 km northeast of Perth, Western Australia
1:250 000 map sheet: Hill River (SH50–09)
1:100 000 map sheet: Wedge Island (1936)

Geological province: Perth Basin, Western Australia.

Resources: The published resources for the Calypso deposit are 51.5 million tonnes of sand grading 1.7% HM at a cut off of 1% HM giving 850 000 tonnes of HM. The HM is reported to contain 598 000 tonnes of ilmenite, 44 000 tonnes of leucoxene/rutile, 90 000 tonnes zircon, 16 000 tonnes monazite, 70 000 tonnes garnet + staurolite and 31 000 tonnes of other heavy minerals (Image Resources NL, 2008).

Current status: Undeveloped deposit, currently under investigation.

Economic significance: Preliminary scoping studies indicate that the deposit could be economic. Under prevailing economic conditions the REE are not extracted from the monazite which would be returned back to the mine site.

Geological setting: According to Image Resources NL (2008), the Calypso mineralisation shown in Figures 3.14 and 3.15 is interpreted to be of fluvial origin. It is hosted in Mesozoic sediments, and appears to be facies controlled. The sediments hosting the mineralisation are typically a very clean fine- to medium-grained sand up to 70 m in depth. They are bounded by clay-rich sediment barren of heavy minerals. The sands are interpreted to be braided streams and the clays thought to represent quiet swamp environs. There are clay intercalations within the sands. The heavy-mineral channel type deposits occur in close association with, and are overlain, by younger fossil beach strandline heavy-mineral deposits (Figs 3.14 to 3.16).

Host rocks: Mesozoic fluvial sands.

REE mineralisation: The REE content in the monazite of this deposit is unknown, but is probably of the order of 45% to 60%.

Source of REE: The ultimate source for the REE-bearing monazite in the dune and beach sands is considered to be igneous–high-grade metamorphic

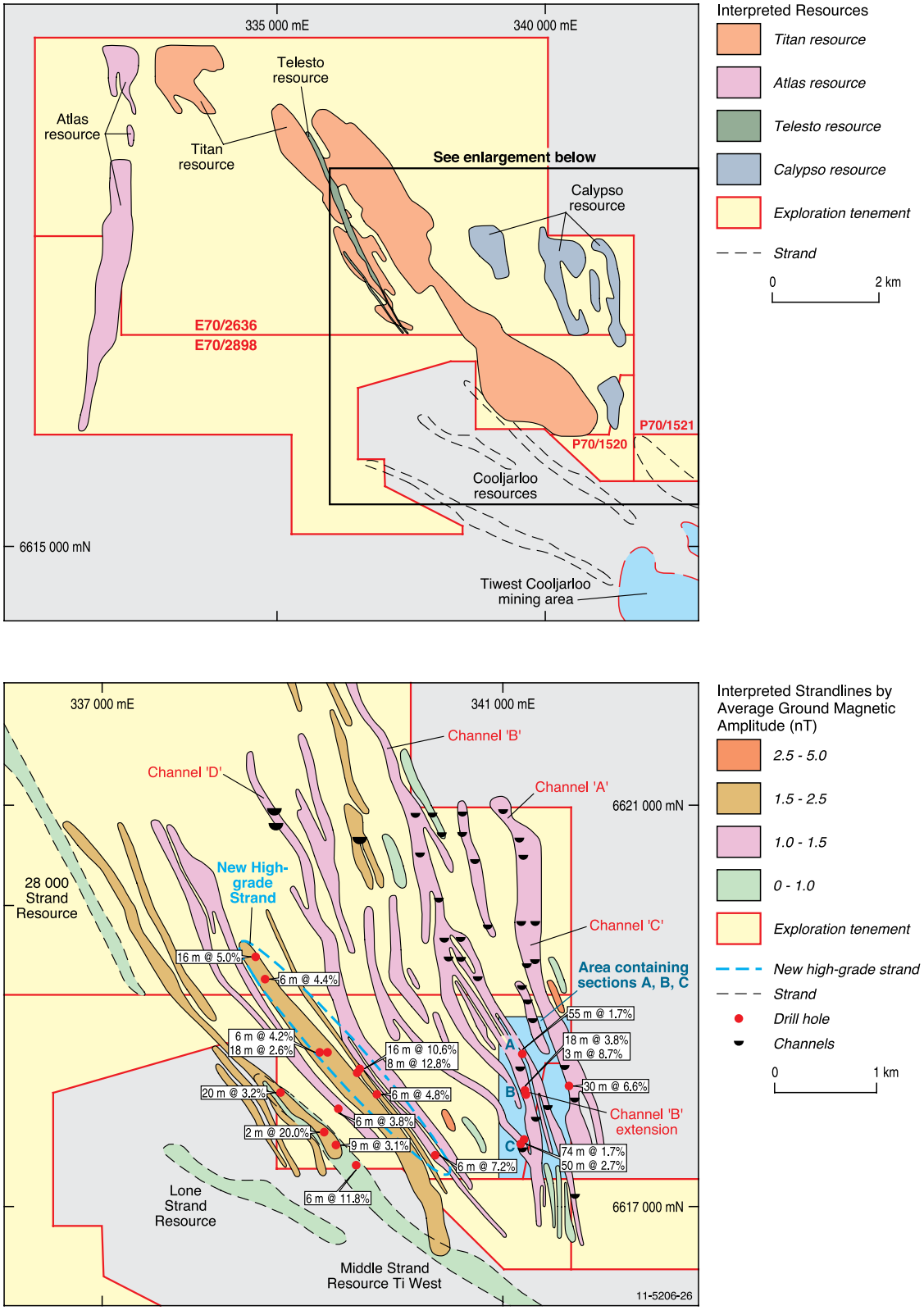

Figure 3.15. Regional and detailed maps of channel-type heavy-mineral deposits near Calypso, Western Australia. Modified from Image Resources Limited (2007a,b; 2008).

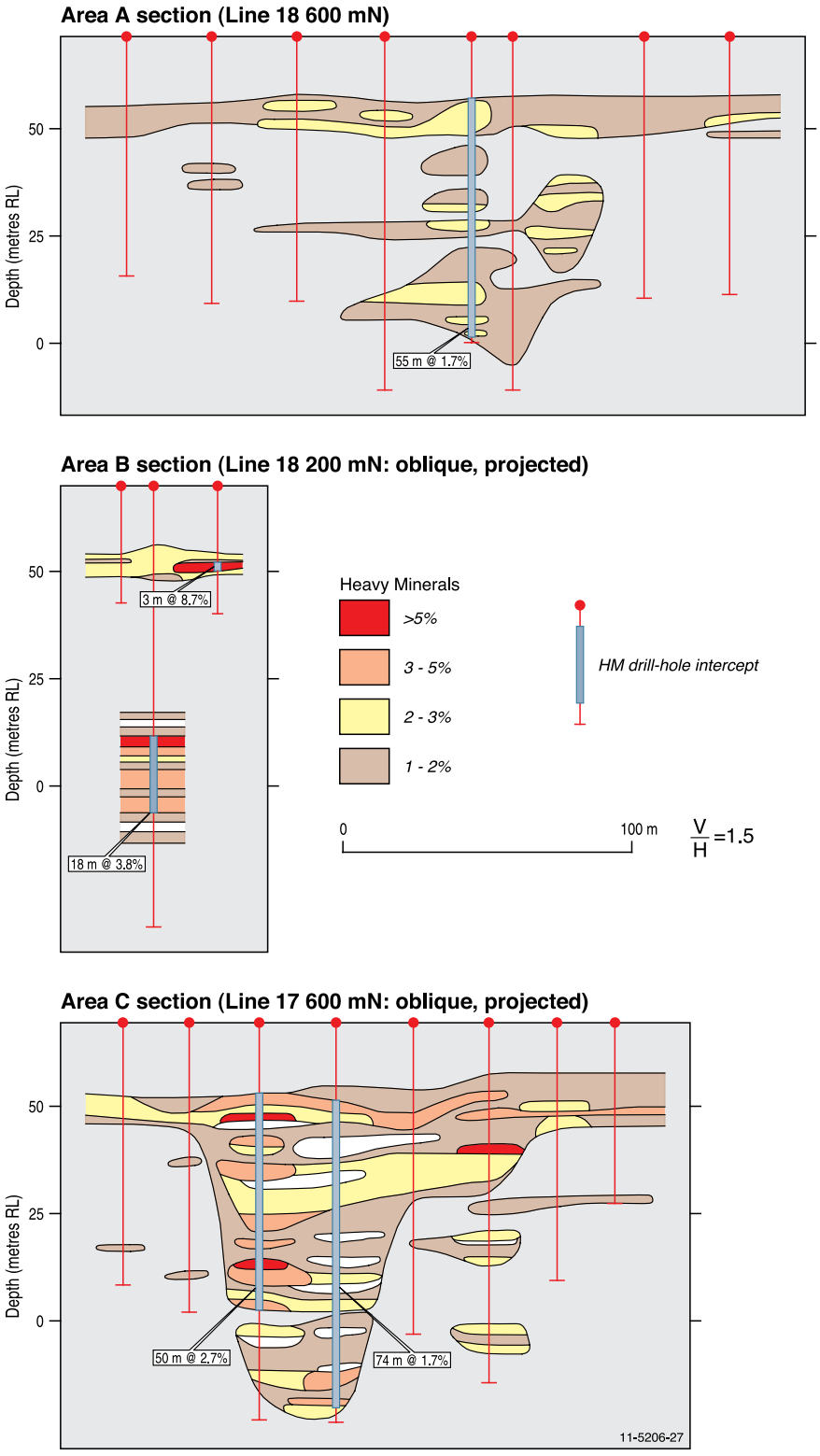

Figure 3.16. Cross-sections showing heavy-mineral concentrations in deposits near Calypso, Western Australia. Modified from Image Resources Limited (2007a,b). Locations of section lines A, B, and C are shown in Figure 3.15.

rocks, but generally monazite was captured with zircon, rutile, and ilmenite in earlier depositional cycles and subsequently eroded.

Age of mineralisation: Mesozoic (?).

Genetic model: Unknown.

Key references: Image Resources NL (2007a,b; 2008): descriptions of channel-type deposits and resources.

Deposit Type 3.7: Rare-earth elements associated with phosphorites

General description: Elevated levels of REE are reported to be associated with deposits of phosphorites in Australia and overseas.

Australian deposits: Korella, Sherrin Creek, D Tree, and Wonnarah (all Georgina Basin, Qld and NT: Fig. 3.17).

Deposits outside Australia: Schevchenko, Kazakhstan (Will et al., 1995); Abu Tartar, Egypt (Hussein and El Sharkawi, 1990); Zhijin, China (Li et al., 2007).

Type example in Australia: Korella, Queensland (Figs 3.17 and 3.18).

Location: Longitude: 139.9667; Latitude: -21.9500
~145 km southeast of Mount Isa, Queensland
1:250 000 map sheet: Duchess (SF 54–06)
1:100 000 map sheet: Dajarra (6854)

Geological province: Georgina Basin, Queensland and Northern Territory.

Resources: Inferred phosphate and REE resources have been published for the Korella phosphate-yttrium deposit as 4.2 Mt @ 746 g/t Y (0.96 kilogram/tonne Y_2O_3) and Nd and Dy are also reported to be present, but their resources have not been estimated (Krucible Metals Limited, 2011). The Korella deposit also has an Inferred Resource 8.3 Mt @ 27.36% P_2O_5 at a cut-off grade of 20% P_2O_5 (Krucible Metals Limited, 2010). The anomalous zone of yttrium enrichment at Korella appears to remain open towards the Duchess deposit to the north. There is little published data in regard to REE resources in phosphorite in Australia. Total phosphate resources in the Georgina Basin are considered to be of the order of 4 billion tonnes (Lottermoser, 1991), but TREE contents in the phosphorites are generally much less than 1000 ppm.

Current status: Korella is an undeveloped phosphate-yttrium deposit (Fig. 3.18).

Economic significance: Korella is a significant phosphate-yttrium deposit being considered for possible development. The economic significance of the elevated values of yttrium in the Sherrin Creek phosphate deposit is unknown. The recovery of europium as a by-product of phosphate mining has been reported for the Schevchenko deposit in Kazakhstan (Orris and Grauch, 2002) and research by Li et al. (2007) have investigated the feasibility of extracting REE as a by-product of phosphate mining from the Zhijin phosphorite deposit in China.

Geological setting: According to Howard (1986), the time and location of major phosphogenesis in Australia was in the Middle Cambrian of the Georgina Basin. About 20 known early Middle Cambrian phosphorite deposits in the Georgina Basin, comprising a major world resource of phosphate, are located along the paleo-periphery of the basin over a distance of 1000 km (Fig. 3.17). The paleogeography and the nature of the contained sediments indicate the Georgina Basin occupies a mild structural downwarp in the pre-Cambrian basement. Three different structural/depositional environments have been postulated for the Georgina Basin phosphorites (Howard, 1986):

- the Duchess phosphorites were deposited across the seaward flanks of the Smokey Anticline structural rise and in the depression of the Burke River Structural Belt;
- the Lady Annie, D Tree, and Sherrin Creek phosphorites were deposited in coastal subtidal, intertidal, and supratidal environments related to a shallow-marine epicontinental basin containing large hypersaline banks surrounded by subtidal channels fringed by embayments, lagoons, and estuaries; and
- the Wonarah and Alroy phosphorites were deposited on the Alexandria-Wonarah Basement High, which was actively rising during sedimentation and the structure was the site of phosphogenesis. The phosphorite beds drape over basement highs which were related to reactivated Paleoproterozoic faults.

Host rocks: Middle Cambrian Phosphorite. The Beetle Creek Formation and the Inca Formation are the main hosts and consist of a sequence of phosphatic siltstone (phosphorite) and chert that overlies limestone, sandstone, and conglomerate.

REE mineralisation: Analyses of phosphorite samples collected by Howard and Hough (1979) show a significant enrichment in yttrium.

- Fourteen samples from the Sherrin Creek deposit exceeding 200 ppm Y and seven of those exceeding 300 ppm reaching a maximum of 624 ppm Y.

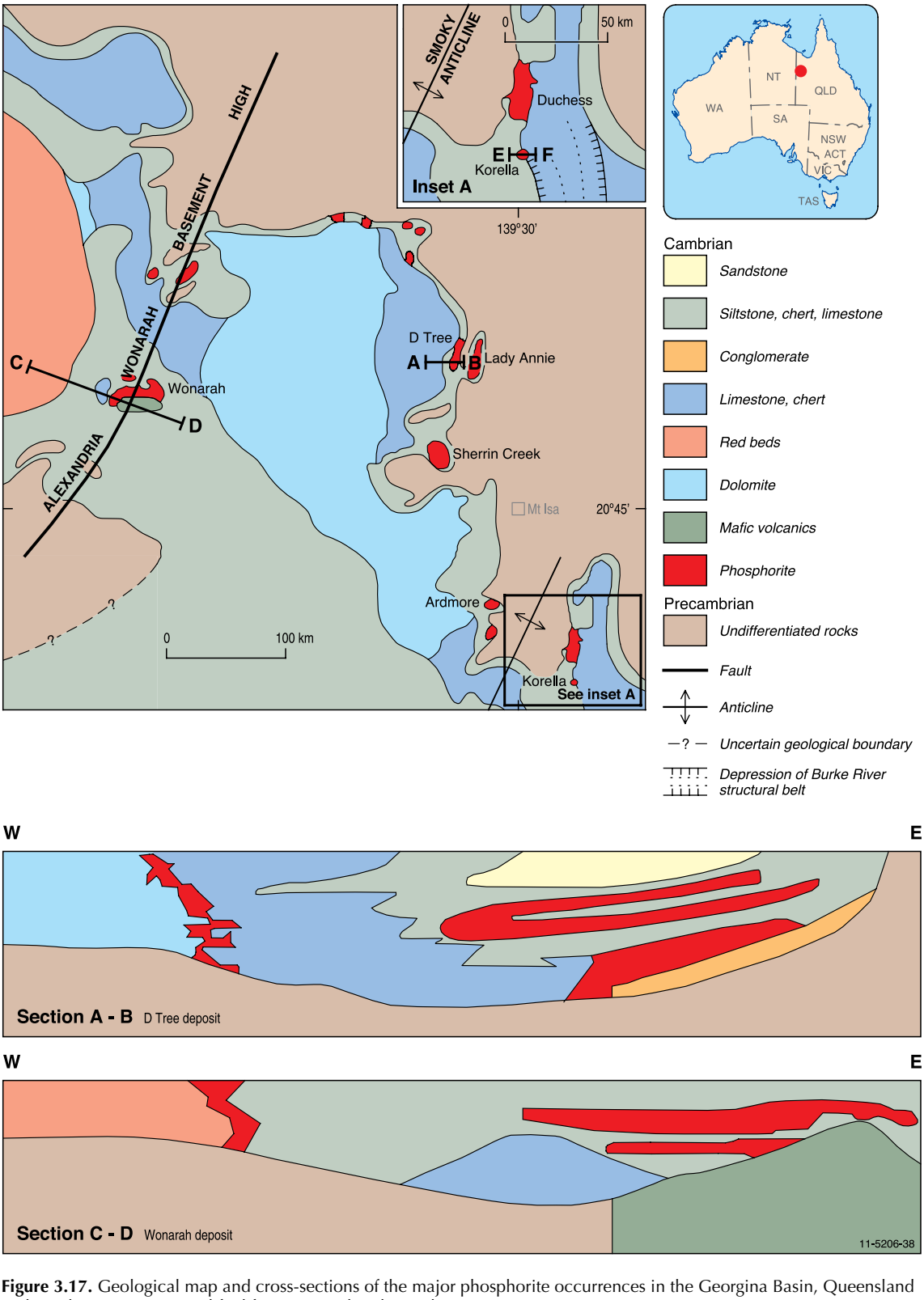

Figure 3.17. Geological map and cross-sections of the major phosphorite occurrences in the Georgina Basin, Queensland and Northern Territory. Modified from Howard and Hough (1979).

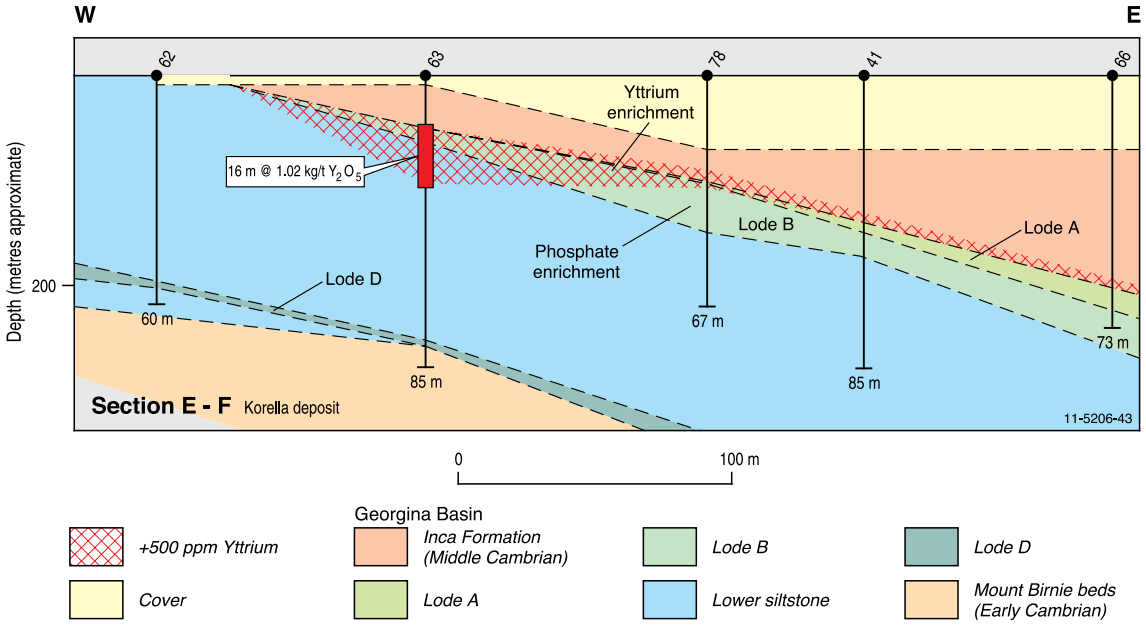

Figure 3.18. Geological cross-section of the Korella phosphorite deposit, Georgina Basin, Queensland. Modified from Krucible Metals Limited (2011).

- The sample with maximum Y value also had a maximum value of 148 ppm La and 214 ppm Ce.
- The plus 300 ppm Y values are usually associated with the higher-grade phosphate samples (>30% P_2O_5).
- Howard and Hough (1979) noted that in unleached Sherrin Creek (and D Tree) phosphorites, yttrium, lanthanum, and cerium correlate with apatite where they substitute for calcium.

- Seven phosphorite samples from the D Tree deposit also exceeded 200 ppm Y, reaching a maximum value of 482 ppm Y, which also had maximum values of 142 ppm La and 214 ppm Ce.
- The Wonarah deposit only had two samples yielding plus 200 ppm Y with a maximum of 336 ppm Y, which also had 41 ppm La and 5 ppm Ce.

Russell and Trueman (1971) noted that the phorphorite in the Dutchess deposit averaged 500 ppm La and 600 ppm Y. Analyses of 17 samples of pelletal phosphorite from the Georgina Basin as published by de Keyser and Cook (1972) indicate higher values of yttrium ranging from 800 to 1500 ppm Y.

Source of REE: Source of REE may be influenced by the nature of the seabed rock. The samples with the highest values of yttrium published in Howard and Hough (1979) are from unleached samples of phosphorite from Sherrin Creek and from unleached and partly leached samples from D Tree. The lowest yttrium values are from Wonarah where all of the samples were leached. However, both Sherrin Creek and D Tree are relatively close to the Mount Isa Inlier, as is the Korella phosphorite deposit, which has the only published resource of yttrium in the Georgina Basin. The close proximity of these deposits to the Mount Isa Inlier may suggest the Precambrian basement as a possible source for yttrium and other REE.

Age of mineralisation: Middle Cambrian age.

Genetic model: Howard and Hough (1979) reviewed the available data on the phosphorite types of the Georgina Basin epicontinental sea and concluded that:

1. phosphate formed in restricted and shallow to very shallow water environments ranging from subtidal to intertidal;
2. contained faunas in different areas of the Georgina Basin are very different in overall composition, and it appears that they developed independently of each other. In this study the geochemical data indicate that there were discernible differences in the chemistry of the waters of these depressions;
3. outside of the restricted areas, phosphogenesis declined rapidly and ceased basinward, even though shallow open-marine conditions persisted. There is a change from a restricted paleodepression containing phosphorites into open basin with a change to phosphatic siltstone and limestone; and
4. phosphogenesis was confined to a specific faunal time zone (Xystridura zone).

The favoured interpretation by Howard and Hough (1979) to account for the characteristic features of the Georgina Basin phosphorites listed above is that there was a set of circumstances which coincided to form a phosphate 'pump'. These were normal sea water saturated in carbonate fluorapatite but supplemented by phosphate from coastal streams in areas of lagoons, estuaries, or more restricted embayments, and a rapid concentrating mechanism which could maintain a high bottom-water concentration. The concentration agent was a prolific phytoplankton population which on death sank and released phosphate in the oxidising environment at the sediment-water interface Howard and Hough (1979).

Key references: Howard (1986), Howard and Hough (1979), and Cook (1972): geological setting and geochemistry;
Krucible Metals Limited (2011): describe first reported REE resource in Georgina Basin.

Deposit Type 3.8: Rare-earth elements associated with lignite in sandstone-hosted polymetallic uranium deposits

General description: Rare-earth elements are associated with lignite in the sandstone-hosted polymetallic uranium deposit at Mulga Rock, in Western Australia.

Australian deposits: Mulga Rock (?Eucla Basin, WA).

Deposits outside Australia: Enrichment of REE occur in germanium-bearing Cretaceous lignite at the Wulantuga deposit, Inner Mongolia, China (Qi et al., 2007), and at the Spetsugli germanium-bearing coal deposit in the Promor'e region, Russia (Seredin, 2005). Gallium-bearing coals at Jungar, Inner Mongolia, are enriched in REE (Dai et al., 2006). Rare earths in acidic waters are being investigated in regard to environmental issues, in pits from a former lignite mine at Lusatia, Germany (Bozau et al., 2008).

Type example in Australia: Mulga Rock, Western Australia (comprises three separate deposits Ambassador, Shogun, and Emperor: Fig. 3.19).

Location: Longitude: 123.5906; Latitude: -29.9057
~220 km northeast of Kalgoorlie, Western Australia
1:250 000 map sheet: Minigwal (SH 51–07)
1:100 000 map sheet: Narnoo (3638)

Geological province: ?Eucla Basin, Western Australia.

Resources: 55.44 million tonnes of Inferred Resources at 0.490 kg/t U_3O_8 (Energy and Minerals Australia Limited, 2010a).

Current status: An undeveloped polymetallic sandstone-hosted uranium deposit currently at a stage of advanced exploration.

Economic significance: A significant polymetallic uranium deposit currently being considered for possible development. Commercial significance of REE undetermined.

The germanium-bearing coal deposits of Wulantuga (referred to as the Wulantuga germanium deposit), Inner Mongolia, and at Spetsugli in Russia are very large. Similarly, the gallium-bearing coal deposit at Jungar (referred to as a superlarge gallium ore deposit), Inner Mongolia is also large. However, the commercial significance of the REE in these overseas deposits is not clear.

Geological setting: The Mulga Rock polymetallic uranium deposit occurs within a buried paleochannel sequence of Phanerozoic age, underlain by predominantly Archean and Proterozoic granites of the Yilgarn Craton and the Albany–Fraser Province. According to Douglas et al. (2011), Pb-Pb data together with a high Th/U ratio suggest that lamproites and carbonatites may be present in the Mulga Rock region of the Yilgarn Craton. The deposit is hosted in lignite and underlying sandstones in the paleochannel which is 5–15 km wide and at least 100 km long. The paleochannel may have received input from drainage systems that extended for over 400 km northwest across the Yilgarn Craton. At Mulga Rock the paleochannel sequence comprises:

- fluviatile sands and interbedded lacustrine sediments (30 m-thick);
- lacustrine to paludal sediments, kaolinitic clays overlying lignite (peat), clay-rich lignite and carbonaceous sands and clays (30 m); and
- basal fluviatile sands and gravels (40 m).

The upper units have been weathered, ferruginised, and silicified. Oxidation, extends to 20–30 m depth with a sharp redox boundary between kaolinitic clay and lignite, usually close to the water table. The oxidation is possibly related to weathering under humid conditions during Oligocene to mid-Miocene followed by later weathering under more arid environment.

Host rocks: At the Ambassador deposit, uranium is hosted in lignite and in the underlying sandstone, but the REE appear to be confined to the mineralised lignite. The abundances of REE in the Emperor and Shogun deposits have not been reported.

REE mineralisation: The uranium mineralisation in the Ambassador deposit is distributed as follows:

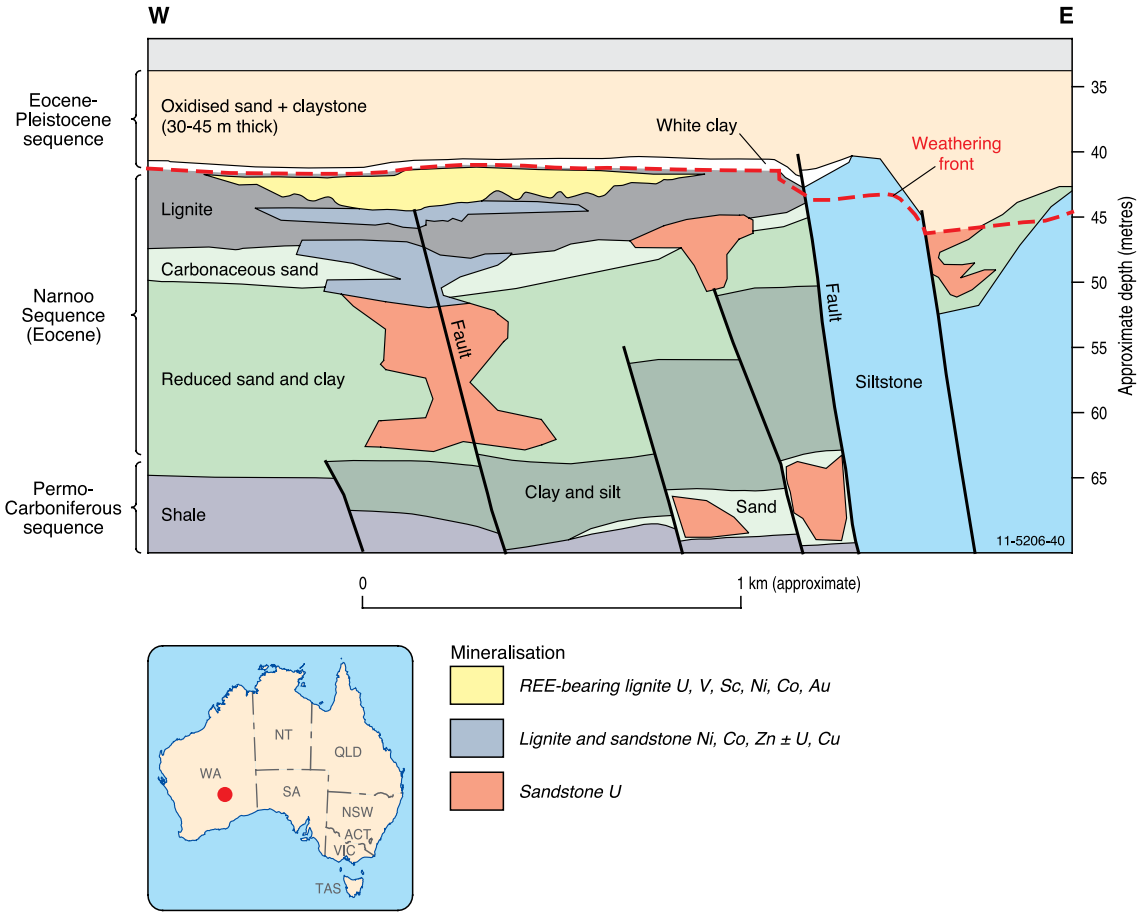

Figure 3.19. Geological cross-section of the Mulga Rock lignite sandstone-hosted uranium deposit, Yilgarn Craton, Western Australia. Modified from Davis (2010).

- Upper lignite—16.7 Mt @ 600 ppm with 10 000 t of contained U_3O_8; main elements are–U, Ni, Co, Cu, Zn, Sc, REE, V, Au, Ag;
- The proportion of REE in upper lignite was reported as 10.8% La, 39.8% Ce, 6.1% Pr, 24.1% Nd, 6.0% Sm, 1.2% Eu, 4.2% Gd, 0.6% Tb, 3.4% Dy, 0.6% Ho, 1.5% Er, 0.2% Tm, 1.2% Yb, and 0.2% Lu: Energy and Minerals Australia Limited (2010c).
- Lower lignite—3.7 Mt @ 320 ppm with 1 200 t of contained U_3O_8; main elements are–U, Ni, Co, Cu, Zn; and
- Sandstone—7.2 Mt @ 240 ppm with 12 900 t of contained U_3O_8; main elements are: U, Ni, Co, Cu, Zn, Au (Energy and Minerals Australia Limited, 2010a).

Some of the best drill-hole intersections in the Ambassador deposit (Energy and Minerals Australia Limited, 2010b) include:

- 5.50 m @ 1900 ppm U_3O_8, 0.24% Ni, 0.09% Co, 153 ppm Sc_2O_3, 390 ppm V_2O_5, and 0.18% Zn;
- 10.0 m @ 2200 ppm U_3O_8. Within this intersection, there is an intersection of 7 m @ 2.2% Zn, 0.14% Ni, 0.06 Co%, and 529 ppm V_2O_5; and
- 5.0 m @ 2200 ppm U_3O_8, 0.27% Ni, 0.11% Co, 192 ppm Sc_2O_3, and 0.30% Zn.

The distribution of the mineralisation at the Emperor and the Shogun deposits has not been published.

Source of REE: Douglas et al. (2011) consider that the Pb-Pb isotopic data suggest a very distinctive lithology, Archean or Proterozoic in age, with a high Th/U ratio is the likely source for the Ambassador mineralisation. In particular, the isotopic composition corresponds to that of Western Australian lamproites and carbonatites. The Mount Weld Carbonatite is adjacent to a paleochannel system, 180 km to the northwest, and other carbonatites are known, or are inferred, to occur in the Mulga Rock area (e.g., Ponton Creek–Cundeelee; Lewis, 1990). Both Sr and Nd isotopic results also support the hypothesis that lamproites or carbonatites could be the source of the mineralisation, however, the Sr and Nd isotopic data are also compatible with a number of granitic lithologies in the Yilgarn

Craton. Douglas et al. (2011) state that lamproites and carbonatites are also geochemically compatible source rocks because they are commonly enriched in a wide range of trace elements, in particular U, Th, and the REE. These rocks could represent a source of mineralisation located either within the basement proximal to the paleochannel, or directly linked via one of the branches of the Minigwal paleochannel system.

In regard to sources of REE in overseas deposits, published information on the REE-enriched germanium-bearing lignite at Wulantuga, the germanium-bearing coal at Spetsugli, and the gallium-bearing coal at Jungar are summarised below:

- Qi et al. (2007) note that the TREE contents of 42 samples from the Wulantuga germanium deposit (WGD) range from 9 ppm to 533 ppm, with a maximum TREE + Y content of 648 ppm.
  - The average REE contents of the WGD samples are slightly higher than those of USA coals and world-wide coals.
  - REE contents of most lignite samples are highly positive correlated with ash yields indicating a mainly detrital source and an association with syngenetic mineral matter.
  - There are no distinct correlations between germanium and any individual REE, or TREE + Y content.
  - The germanium contents of the lignite samples range from 23.3 to 1424 ppm, with an average of 300 ppm.
- According to Seredin (2005) the TREE + Y concentrations of germanium-bearing coals from the Spetsugli deposit range from 86 to 316 ppm.
  - The germanium-bearing coals are strongly enriched in yttrium and HREE as compared with coals located beyond the zone of germanium mineralisation.
  - The REE distribution in the coal seams show no correlation between the REE and germanium contents.
  - Anomalously high REE contents in germanium-bearing coals are of epigenetic origin and accumulated after the formation of germanium mineralisation.
  - The deposits formed from metalliferous REE-enriched and germanium-free or germanium-poor solutions of volcanic origin that circulated during the Pliocene–Early Quaternary period.
- According to Dai et al. (2006):
  - the TREE + Y contents of coal average 255 ppm with a maximum value of 715 ppm;
  - the TREE + Y contents of laboratory ash averages 830 ppm with a maximum value of 2586 ppm;
  - Dai et al. (2006) also state that the average REE + Y concentrations for coal from other regions are as follows:
    - Late Paleozoic coal from North China–111 ppm;
    - most Chinese coal–137.9 ppm;
    - USA coal–62.1 ppm; and
    - most world coal–46.3 ppm.
  - The gallium content of the main minable coal averages 51.9 ppm and 89.2 ppm in laboratory high-temperature ash.
  - The main carrier of the gallium is in the boehmite content of the coal.
    - Boehmite is derived from bauxite in the weathered crust of the underlying Benxi Formation in the north of the basin during peat accumulation.
  - The source of the REE + Y is unknown.

Age of mineralisation: Initially uranium and other metals precipitated syngenetically with organic phases in late Eocene followed by remobilisation during periods of weathering and associated diagenesis with the latest episode in the last 300 000 years (Douglas et al., 2011).

Genetic model: Douglas et al. (2011) favour a chemically syngenetic model where uranium and other trace elements were transported in solution from one or more sources and precipitated in the organic matter as it accumulated, and subsequently mobilised and concentrated during diagenesis/weathering. Solution and mobilisation are postulated to have occurred during a humid weathering event during the late Eocene, based on the palynological dating of the lignite, transported in solution and/or adsorbed to organic colloids in paleorivers. Post-depositional remobilisation and concentration may have occurred at any period since late Eocene, related to changes in water-table during post-Eocene uplift, burial by presumed Miocene sediments and/or related to episodes of more intense weathering.

Key references: Douglas et al. (2011): geology and genesis of Ambassador polymetallic uranium deposit; and
Fulwood and Barwick (1990): exploration history, regional geology, mineralisation, ore genesis.

Deposit Type 3.9: Rare-earth elements associated with alkaline igneous rocks

General description: Significant resources of zirconium-hafnium-niobium-yttrium, and REE occur in highly fractionated sequences comprising A-type alkaline lavas, tuffs, mafic volcanics, and subvolcanic intrusives. Such rare-metal deposits associated with volatile-rich alkaline magmas are typical of intraplate tectonic settings. Mineralisation is the product of early pyroclastic eruption of alkaline trachytic magma enriched in volatiles (in particular, fluorine and water) and incompatible elements (e.g., Zr, Hf, Nb, Ta, Be, Y, REE), that are concentrated in the upper parts of the magma chamber. Late-stage hydrothermal fluids involving fluorine and chlorine associated with the intrusions are important for the enhancement of rare-metal grades in these deposits. The two most important examples of this deposit type in Australia are Brockman (Western Australia) and Toongi (New South Wales). Both these deposits contain significant resources of REE and other rare metals that are currently being assessed.

Australian deposits/prospects: Brockman (Halls Creek Orogen, WA); Toongi–Dubbo Zirconia Project (Lachlan Orogen, NSW).

Deposits outside Australia: Khibini and Lovozero complexes (Kola Peninsula, Russia); Mount Pajarito (New Mexico); Thor Lake (Northwest Territories, Canada: Lake Zone has 64 Mt @ 1.99% REO); Strange Lake/Lac Brisson (Labrador-Quebec, Canada: open-pit mineable reserve of 52 Mt @ 0.54% REE, 0.31% Y_2O_3).

Type example in Australia: Brockman, Western Australia (Fig. 3.20).

Location: Longitude: 127.7820; Latitude: -18.3192
~18 km southeast of Halls Creek, Western Australia
1:250 000 map sheet: Gordon Downs (SE 52–10)
1:100 000 map sheet: Halls Creek (4461)

Geological province: Halls Creek Orogen, Western Australia.

Resources: The Brockman deposit has an estimated JORC-compliant resource (as of September 2010) totalling 22.084 million tonnes grading 0.79% ZrO_2, 0.10% Y_2O_3, 0.31% Nb_2O_5 and 0.023% Ta_2O_5 (http://www.hastingsraremetals.com/?page=88). This resource comprises an Indicated Resource of 8.83 million tonnes grading 0.76% ZrO_2, 0.09% Y_2O_3, 0.31% Nb_2O_5 and 0.022% Ta_2O_5 from surface to 100 m depth, and an Inferred Resource of 13.25 million tonnes grading 0.81% ZrO_2, 0.10% Y_2O_3, 0.32% Nb_2O_5, and 0.024% Ta_2O_5 from 100 m to 250 m depth. The resources are based on a cut-off of 1500 ppm Nb_2O_5.

Current status: Advanced prospect with JORC-compliant resource.

Economic significance: The economic importance of this deposit has traditionally been hindered by the fine-grained (<20 um), hydrous nature of the ore minerals, which requires a specialised chemical leaching process to achieve high degrees of recovery of rare metals (Ramsden et al., 1993; Taylor et al., 1995b). With the advent of more recent, sophisticated metallurgical techniques, these potential complications may be alleviated.

Geological setting: The polymetallic Brockman deposit occurs in the Halls Creek Orogen (HCO), a well-exposed north-northeasterly-trending orogenic belt about 400 km long and at least 120 km wide along the southeastern margin of the Kimberley Basin in northern Western Australia. The HCO is a complex province comprising low- to high-grade metasedimentary and metavolcanic rocks, and voluminous granitic, mafic, and mafic–ultramafic intrusions that collectively range in age from about 1920 Ma to 1800 Ma. Alkaline volcanics and intrusives are a minor component of the igneous stratigraphy. Younger Mesoproterozoic and Neoproterozoic lamprophyric-kimberlitic diatreme intrusions in the Kimberley have significant economic significance (e.g., world-class Argyle diamond deposit: Jaques et al., 1985). Major phases of tectonism occurred along in the HCO during the Paleoproterozoic, Mesoproterozoic, and Neoproterozoic (see references in Chapter 3 of Hoatson and Blake, 2000).

The Brockman deposit occurs in a Paleoproterozoic sequence (>1000-m thick) of alkaline lavas, volcaniclastic sedimentary rocks, felsic volcanics, that is intruded by subvolcanic sheets and interlayered with greywacke, siltstone, and mudstone (Fig. 3.20). Major lithologies include: trachyandesite, trachyte, quartz trachyte, and rhyolitic lavas; pillowed mafic lavas; subvolcanic syenite sheets; volcanic breccias, pyroclastics, and volcaniclastic rocks (including the mineralised 'Niobium Tuff'). Some of the thicker flow may be remnants of lava domes. The lavas are generally amygdaloidal, and they include pillowed and columnar-jointed types. Scoriaceous flow-tops and carbonate-cemented volcanic breccias are preserved locally. Some pillow lavas can be traced into feeder

Figure 3.20 (see opposite). Geological map of the Brockman rare-earth-element deposit area, Halls Creek Orogen, Western Australia. Modified from Sanders (1999).

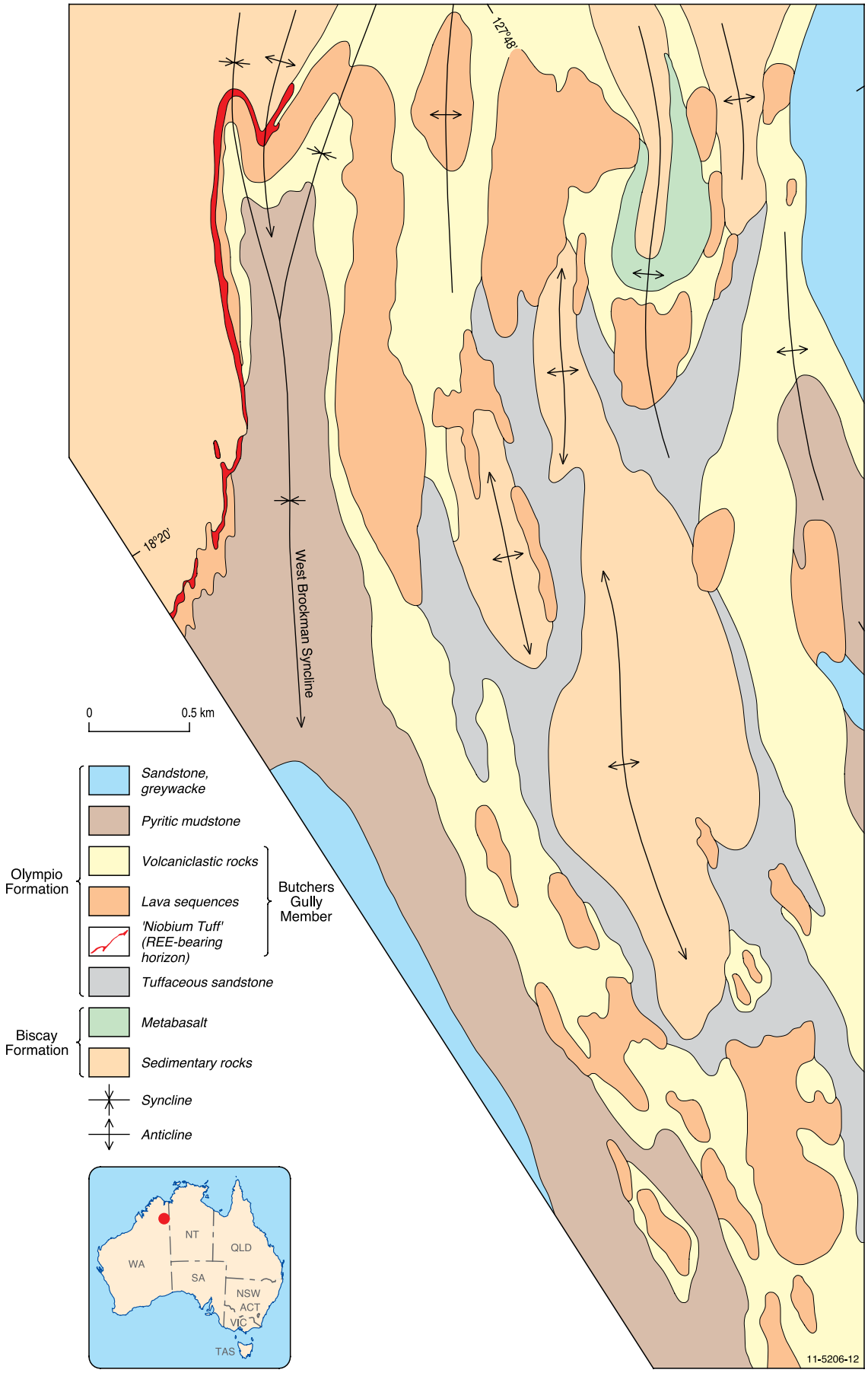
127°48'
18°20'
West Brockman Syncline
0
0.5 km
Sandstone, greywacke
Pyritic mudstone
Volcaniclastic rocks
Lava sequences
'Niobium Tuff' (REE-bearing horizon)
Tuffaceous sandstone
Olympio Formation
Butchers Gully Member
Metabasalt
Sedimentary rocks
Biscay Formation
Syncline
Anticline
NT
QLD
WA
SA
NSW
ACT
VIC
TAS
11-5206-12

dykes and sills (Taylor et al., 1995b). Extensive flows of altered mafic trachyte and sills of altered mafic syenite host gold mineralisation elsewhere (Butchers Creek and Golden Mile mines). The rock types commonly have a penetrative cleavage and are metamorphosed to greenschist facies. Weathering is limited, with oxidation observed down to depths of 30 m below the current surface. The presence of turbidites underlying and overlying the mineralised sequence, and of pillow lavas and pillow breccias within the sequence, indicate that the Butchers Gully alkaline volcanism was dominantly subaqueous.

Chemical analyses show that the alkaline volcanics were derived from quartz normative and metaluminous A-type magmas enriched in Nb, REE, Zr, Y, Ga, and Zn (Taylor et al., 1995a). The common presence of accessory fluorite indicates a significant fluorine content, and gamma-ray spectrometric data show that some of the volcanics have anomalously high thorium contents. The overall chemistry is indicative of intraplate magmatism (Taylor et al., 1995a,b; Blake et al., 1999). The interpreted tectonic setting of the Brockman deposit of intraplate alkaline magmatism in a shallow rift-related marine basin overprinted by orogenic events differs from most Cenozoic to Holocene trachyte volcanic complexes which are largely subaerial, are built on relatively thick continental crust, and show no post-eruptive orogenic activity (Taylor et al., 1995b).

Host rocks: The polymetallic mineralisation is hosted by a fluorite-bearing volcaniclastic unit informally known as the 'Niobium Tuff', which occurs at the base of the Butchers Gully Member of the Olympio Formation (Chalmers, 1990; Ramsden et al., 1993; Taylor et al., 1995a,b). The trachytic ash-flow tuff appears to be composed of two closely spaced units that formed from different eruptive episodes; namely a crystal-rich lower unit with a similar thickness to an overlying pumice-rich unit that collectively cooled as a single unit (Fig. 3.20). Taylor et al. (1995b) describes the 'Niobium Tuff' as a tuffaceous volcaniclastic unit grading into a volcaniclastic sandstone in the distal facies. It varies in thickness from 5 to 35 m and crops out for at least 3.5 km along the western flank and northern closure of a major southwest-plunging syncline, where it has a vertical to steep dips towards the east (Chalmers, 1990). Sub-surface data indicate that the 'Niobium Tuff' unit gradually thickens down-dip to the east where the source volcanic vent is interpreted to be located some 1000 m below the present land surface (Ramsden et al., 1993). The tuff contains strongly foliated microcrystalline quartz and potassium mica, with scattered albite microphenocrysts, lithic fragments, pumice, and possible glass shards set within a devitrified microcrystalline groundmass. Accessory minerals include limonite, carbonate, biotite, chlorite, epidote, and the REE-bearing minerals aeschynite, bastnäsite, parisite, and rhabdophane have been recorded in veins and amygdales. Purple fluorite is common throughout the deposit intimately associated with the ore minerals. It also occurs with coarse-grained biotite, quartz, and muscovite, infilling pumice, and in late-stage discordant carbonate veins at the footwall contact with coarse quartz, carbonate, chlorite, and sphalerite (Ramsden et al., 1993; Taylor et al., 1995b; Blake et al., 1999). The 'Niobium Tuff' contains extreme enrichment in high-field-strength incompatible elements (average 1660 ppm Y, 9700 ppm Zr, 3200 ppm Nb, 175 ppm Yb: Taylor et al., 1995a). Trachytic lavas overlying the 'Niobium Tuff' contain many of the ore minerals, but in trace amounts.

REE mineralisation: The Brockman deposit contains significant quantities of zirconium, yttrium, niobium, tantalum, hafnium, gallium, and HREE, such as terbium and dysprosium. Chalmers (1990) provides the following summary of the mineralogy of the REE. Electron microprobe studies by CSIRO have shown that the ore minerals are extremely fine grained with few species greater than 20 µm and most less than 10 µm in diameter. They are dispersed throughout the quartz, potassium mica, and albite host, usually occurring in layers and on grain boundaries. Major ore minerals include zircon and gel-zircon (unusual hydrous Y-Th-Nb-bearing variety of zircon: Ramsden et al., 1993), columbite, and Y-bearing rare-earth niobates. The hydrous gel-zircon contains about 5000 ppm Dy, 5000 ppm Er, 6000 ppm Yb, 1400 ppm Gd, 600 ppm Sm, in addition to anomalous Y, Th, and Nb. The REE minerals bastnäsite, calcian-bastnäsite, parisite, and synchysite, have been documented with chalcopyrite, galena, pyrite, sphalerite, thorite, gel-thorite, and ilmenite. Gel-zircon is the principal host of the HREE, and disseminated bastnäsite (± parisite and synchysite) carries the LREE. Bertrandite ($Be_4Si_2O_7(OH)_2$), in late-stage calcite veins, is the main host for Be, and Ga is enriched in potassium mica (300 ppm Ga) in the groundmass (Ramsden et al., 1993). The textures of the ore minerals are in part controlled by the fabric of the host tuff unit, and there is much evidence for remobilisation and redistribution associated with fluoritisation. However, there is not a typical texture and the ore minerals are generally disseminated throughout the 'Niobium Tuff'.

Source of REE: Taylor et al. (1995a) state that the large degrees of crystallisation required to derive the more differentiated rocks of the Brockman deposit are

best explained by a process of 'liquid fractionation' resulting in internal compositional stratification of the magma chamber with extreme differentiates such as the 'Niobium Tuff' forming a volatile-enriched 'cap' in the magma chamber-roof zone. The REE and other rare metals were derived from fertile (i.e., REE-bearing) quartz-oversaturated, metaluminous alkaline magmas which underwent a widespread and protracted fractionation process, and progressive contamination with upper crustal granitic-metasedimentary rocks. This very efficient mineralising system was overprinted by late-stage fluorine-rich fluids. The fine-grained rare-metals mineralisation is the result of alteration and remobilisation of magmatic columbite and zircon. Chondrite-normalised REE distributions for the 'Niobium Tuff' show strong enrichment in HREE, which is in marked contrast to the LREE-enriched overlying trachytic lavas (Ramsden et al., 1993).

Age of mineralisation: A trachytic pillow lava belonging to the Butcher's Gully Member has a SHRIMP U-Pb zircon age of 1848 ± 3 Ma (Blake et al., 1999). The pillow lava, from a sequence of trachytic to rhyolitic volcanics overlying the 'Niobium Tuff', provides the most reliable age for the timing of the alkaline magmatic event. Older zircons dated at 1870 ± 4 Ma (Taylor et al., 1995b) and 1868 ± 3 Ma (Blake et al., 1999) from the mineralised 'Niobium Tuff' at the base of the Butcher's Gully Member are interpreted to be volcanic detritus in the host rock.

Genetic model: Brockman-style rare-metal deposits are characterised by preservation of subaqueous volcanics beneath a thick sedimentary sequence, eruption of early incompatible-element-enriched products followed by less differentiated magmas, widespread activity of volatile-rich fluids (particularly fluorine and water), and fine-grained mineralogy influenced by alteration processes (Taylor et al., 1995a,b). Taylor et al. (1995b) interpreted the geological setting of the mineralised 'Niobium Tuff' in the Brockman deposit as either a pyroclastic-flow deposit, or as a subaqueously-deposited mass-flow that incorporated pyroclastic debris. An initial pyroclastics ash-flow eruption of crystal-rich magma enriched in incompatible elements and F formed the lower part of the 'Niobium Tuff' unit, followed by pyroclastic eruption of pumice-rich material also enriched in incompatible elements formed the upper part. The REE mineralisation is believed to have formed from extreme enrichment of the tuff unit during deuteric alteration of an unusual suite of highly fractionated, A-type felsic lavas, tuffs, and subvolcanic intrusives. The mineralisation is believed to be essentially syngenetic, with fluorine-rich fluids moving through the cooling and consolidating tuff units soon after deposition (Chalmers, 1990). These volatile-rich fluids reacted with precursor magmatic minerals, such as zircon and columbite, and transported the REE, Be, and Ga as stable fluoride complexes. The fluorine-rich fluids played an important role in enhancing rare-metal abundances by increasing the efficiency of crystal-liquid separation and decreasing mineral-melt K_d's (Taylor et al., 1995a). Ramsden et al. (1993) and Taylor et al. (1995a) provide comprehensive interpretations for the petrogenesis of the Brockman polymetallic deposit.

Key references: Chalmers (1990): regional and local geological setting, mineralisation;
Ramsden et al. (1993): mineralogy and geochemistry, mineralisation; and
Taylor et al. (1995a,b): geochemistry, geochronology, petrogenesis.

Deposit Type 3.10: Rare-earth-element-bearing carbonatite

General description: Carbonatites (rocks with more than 50% modal carbonate) occur both as intrusive and volcanic rocks and are invariably associated with a wide range of alkalic rocks (see Chapter 4 for a description of important mineral system features of mineralised carbonatite). They are generally surrounded by a zone of sodic and/or potassic metasomatic rocks called fenites. The REE mineralisation can be both magmatic and metasomatic (formed from fluids released from a carbonatitic melt). Mineralisation can be found in lava flows and tuff, plugs, cone sheets, dykes, and rarely sills. Generally, large homogenous plutons of carbonatites are rarely mineralised. REE-mineralisation shows strong enrichment in light REE. In many carbonatites, economic mineralisation is associated with supergene processes (see Deposit Type 3.1).

Australian deposits/prospects: Yangibana (Capricorn Orogen, WA); Ponton Creek (Yilgarn Craton, WA); Yungul dykes (Halls Creek Orogen, WA); Cummins Range (Cummins Range (junction of Halls Creek and King Leopold orogens, WA). Mud Tank (Arunta Region, NT). Carbonatites and/or related veins are also reported at Mordor Igneous Complex (Arunta Region, NT) and Walloway (Gawler Craton, SA).

Deposits outside Australia: Mountain Pass (USA); Phalaborwa (South Africa); Kangakunde Hill (Malawi); Gallinas Mountain (USA); Saima (China); Bayan Obo (China), Mato Preto (Brazil); Qaqarssuk (Greenland), Sarfartoq (Greenland), Aley (Canada); Argor (Canada); Oka (Canada).

Type example in Australia: Yangibana, Western Australia (Fig. 3.21).

Location: Yangibana: 116.197215,
Latitude -23.890331
~300 km northeast of Carnarvon, Western Australia
1:250 000 map sheet: Edmund (SF 50–14)
1:100 000 map sheet: Edmund (2150)

Geological province: Gascoyne Complex, Capricorn Orogen, Western Australia.

Resources: The Yangibana 'ironstones' prospect has a recorded resource of 3.5 Mt @ 1.7% REO. The REE are in coarse-grained monazite and carbonatite containing up to 20% Nd_2O_5 and 1600 ppm Eu_2O_3. Flint and Abeysinghe (2000; cited in Sheppard et al., 2010) estimated a similar total resource of about 2.77 Mt @ 1.52% REO.

Current status: Prospect.

Economic significance: Unknown.

Geological setting: The REE-bearing ~1.25 Ga Yangibana 'ironstones' are part of the ~1.68 Ga Gifford Creek alkaline complex in the Capricorn Orogen (Pearson, 1995; Pearson and Taylor, 1996; Pearson et al., 1996). The alkaline complex intrudes Paleoproterozoic migmatite and granite and is spatially bound by two major west-northwest-trending lineaments (Fig. 3.21). The Yangibana and nearby Fraser prospects are also spatially close to a regional northeast-trending lineament delineated by O'Driscoll (1990). The REE-bearing ferrocarbonate-magnetite-hematite dykes occur as lenses and pods.

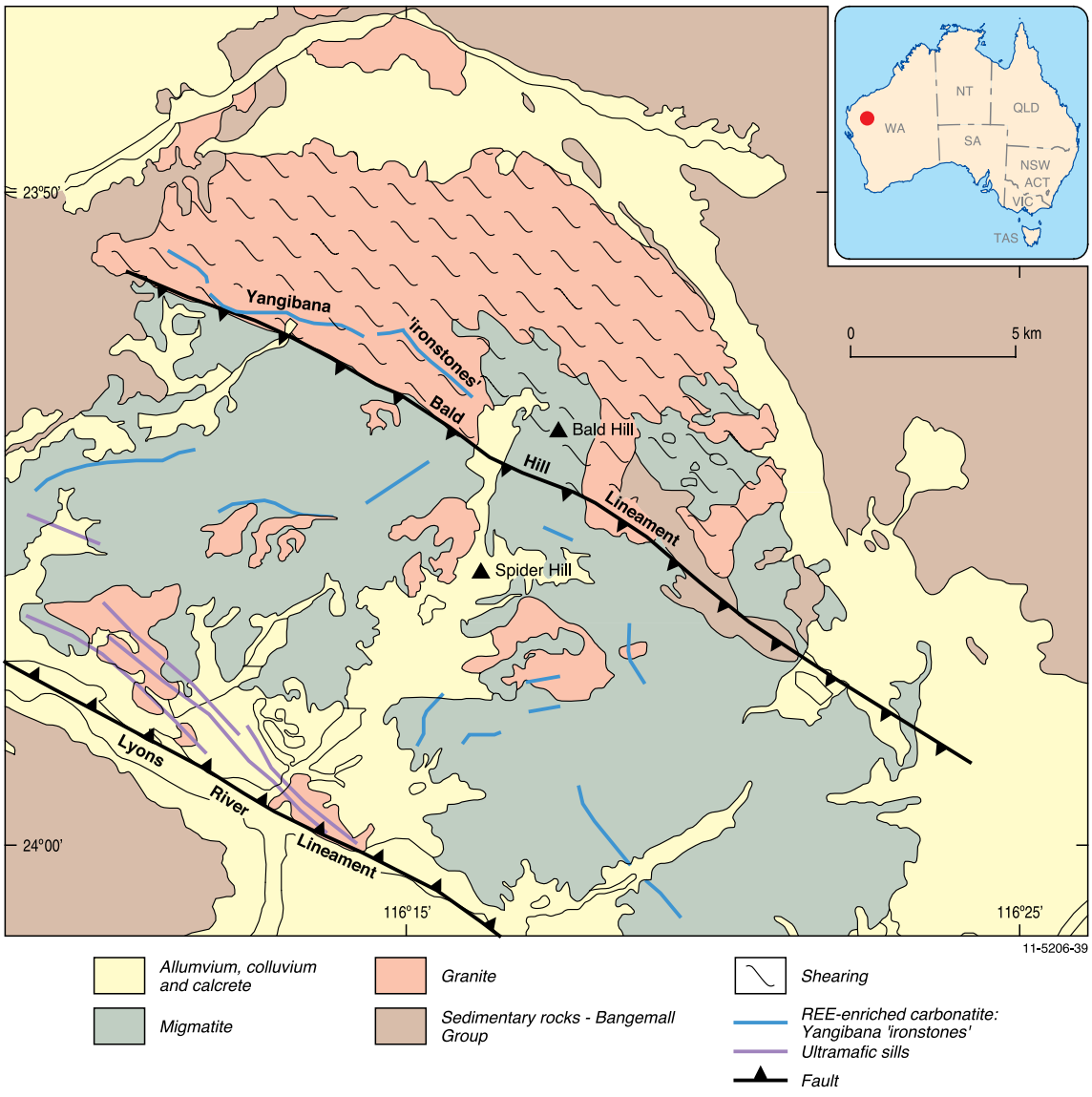

Figure 3.21. Simplified geological map of the Gifford Creek Complex and Yangibana 'ironstones'. Modified from Pearson and Taylor (1996).

Other components of Gifford Creek alkaline complex include carbonate-rich ~1.68 Ga ultramafic sills (Lyons River sills), pyrochlore-bearing sills (Spider Hill sill), limonitic weathered intrusions (Bald Hill intrusion), and fluidisation breccias (Pearson, 1995; Cassidy et al., 1997; Jaques, 2008).

Host rocks: Pearson et al. (1996) subdivided the alkaline rocks into five groups: alkali-amphibole and/or sodic pyroxene-rich ultramafic sills; magnetite- and hematite-rich pods (the Yangibana 'ironstones') and ferrocarbonatite dykes; aegirine-phlogopite-magnetite-apatite-pyrochlore-bearing sills and dykes; limonitic and weathered intrusions with basal layers of the Bangemall Group sedimentary rocks; and fluidisation breccias. The Yangibana dykes are generally 2 to 25 m in width and extend for up to 25 km along strike over an area of 500 square kilometres. The dykes have narrow zones of K-feldspar-magnetite alteration and are subconformable to metamorphic and shear foliations. Drilling has intersected carbonate-rich (ferrocarbonatite) rocks underneath the dykes.

REE mineralisation: The REE- and uranium-thorium mineralisation is hosted by ferrocarbonatite dykes and is enriched in LREE. The main minerals in the mineralised zones comprise dolomite, siderite, fluorite, magnetite, phlogopite, ilmenite, allanite, apatite, pyrite, sodic amphibole, and aegerine. The zones contain traces of sphalerite, galena, and molybdenite. Weathering has leached carbonates to form strongly cemented ironstones (Lottermoser, 1991). The ironstones contain up to 40% REO, with bastnäsite and monazite the major REE-bearing minerals. Significant zirconium (3.2%), niobium (1.8%), hafnium (0.3%), and scandium (110 ppm) are probably related to pyrochlore (Nb), zircon, and baddeleyite (Zr, Hf: Lottermoser, 1991).

Source of REE: Mineralised ferrocarbonatites represent the final stage of fractionation of a carbonatitic melt intimately associated with the emplacement of the Gifford Creek ultramafic-alkaline complex (Pearson et al., 1996). Hence the REE could have been sourced from the ultramafic-alkaline melt. The REE-enrichment observed in the ironstones could have been caused by supergene processes affecting ferrocarbonatites and associated fenites. Scandium was most probably sourced from ultramafic sills (Table 2 of Pearson et al., 1996).

Age of mineralisation: A SHRIMP U-Pb zircon age of 1679 ± 6 Ma obtained from a xenolith of metasomatised granite within an ultramafic sill (Lyons River sills) gives the age of the intrusion of the sills and of metasomatism. This age is similar to the SHRIMP U-Pb zircon age of 1674 ± 6 Ma from the alkaline feldspar granite with trachytic texture (Dingo Granite), which provides the age of emplacement for the Gifford Creek Alkaline Complex (Pearson et al., 1996). Pearson and Taylor (1996) suggest that the emplacement of the Gifford Creek Complex occurred as two episodes: first episode comprising ~1.68 Ma ultramafic sills, which also generated extensive fenitic alteration; and a second episode involved the emplacement of carbonatitic rocks at ~1.25 Ma. The first episode occurred prior to the sedimentation of the Bangemall Group rocks, whereas the second episode occurred after the initial phase of sedimentation (Pearson et al., 1996). The primary REE mineralisation was partially remobilised during weathering.

Genetic model: According to Pearson et al. (1996) the early phase of the Gifford Creek Complex may be related to the initial stage of rifting and opening of the Bangemall Basin at ~1.68 Ma. This was followed by the emplacement of carbonatitic magma after sedimentation in the basin had begun and was related to the continuing extension in the basin. Remobilisation of the ultramafic sill in the second phase was caused possibly due to reactivation of faults. REE mineralisation hosted by ferrocarbonatites was formed in the second phase and could have been magmatic and/or hydrothermal. It is possible that this involved remobilisation of magmatic and/or metasomatic REE-mineralisation formed during the first stage. Primary REE-mineralisation was also remobilised during weathering of ultramafic, fenitic, and ferrocarbonatitic rocks.

Key references: Pearson et al. (1996): geology, petrography, geochemistry; and
Pearson and Taylor (1996): mineral chemistry, whole-rock chemistry, stable isotopes, genesis.

Deposit Type 3.11: Rare-earth-element-bearing pegmatite

General description: REE-bearing pegmatites are formed from peraluminous, metaluminous, and peralkaline felsic melts (Fig. 3.22; Table 3.9; Long et al., 2010). Most pegmatites show an overprinting by magmatic-hydrothermal fluids. According to Cerny (1991a), REE-bearing pegmatites belong to NYF (Niobium-Yttrium-Flourine) and mixed families of rare-element pegmatites (Table 3.10). Pegmatites often form structurally controlled lenticular and tabular bodies within or in proximity to felsic intrusions and are characterised by homogenous, zoned and layered internal structures (Cerny, 1991a). In the NYF pegmatites, the late (hydrothermal) units show

a dramatic increase in the concentration of REE. The main REE minerals in pegmatites are gadolinite, fergusonite, euxenite, and monazite (Cerny, 1991a). The pegmatites are generally formed at temperatures between ~750°C and 150°C, with temperatures decreasing from the margins to the internal zones and secondary (hydrothermal) units.

Australian deposits/prospects: Cooglegong and Pinga Creek Tin fields (Abydos), (Pilbara Craton, WA); Waddouring Rock Pegmatite Group (Yilgarn Craton, WA); Wodgina Pegmatite districts (Pilbara Craton, WA).

Deposits outside Australia: Khibina Massif, Aldan (Russia); Motzfeldt, Greenland; Shatford Lake Field, Bancroft-Renfrew Field, Five Mile (Canada); Spruce Pine, South Plate, Topsham, Mount Antero, Wasau Complex (USA); Ytterby (Sweden).

Type example in Australia: Cooglegong–Pinga Creek, Western Australia (Fig. 3.23)

Location: Cooglegong: 119.4167, Latitude -21.5834; Pinga Creek (Abydos): Longitude 119.00, Latitude -21.75
~150 km southeast of Port Hedland, Western Australia
1:250 000 map sheet: EDMOND (SF5014)
1:100 000 map sheet: EDMOND (2150)

Geological province: Pilbara Craton, Western Australia.

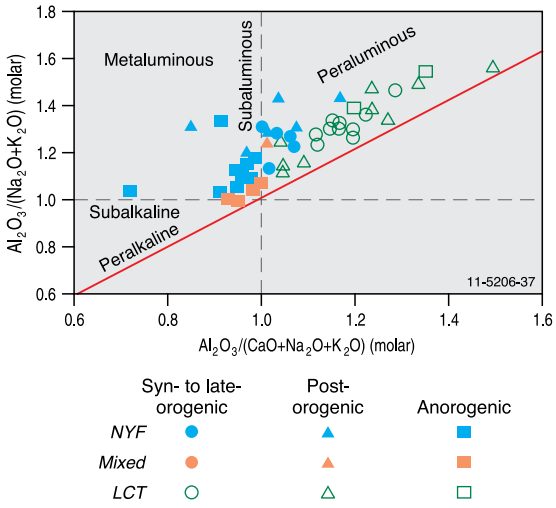

Figure 3.22. Fertile granites and associated pegmatite types coded by tectonic affiliation. Three major groups of pegmatites are shown, namely: NYF: Niobium–Yttrium–Fluorine; LCT: Lithium–Cesium–Tantalum; and Mixed. REE-bearing NYF-type pegmatites are associated predominantly with metaluminous and peraluminous granites (see Table 3.1 for definitions of granite types). Modified from Cerny (1991b).

Resources: The pegmatites and associated alluvial placers were mined for tin. It is not clear if REE were extracted with the tin.

Current status: Old mine. Prospect.

Economic significance: Unknown. The pegmatites in the region need more work to assess the potential of REE mineralisation.

Geological setting: The Cooglegong and Pinga Creek pegmatite fields (Figs 3.23 and 3.24) are associated with the 2890 Ma to 2830 Ma granite suites emplaced in the Eastern Pilbara tectonic zones (Sweetapple and Collins, 2002). The NYF family and mixed Lithium–Cesium–Tantalum pegmatite (LCT)–NYF-family pegmatites are predominantly located in domains 3 and 2 of the Eastern Pilbara Craton as defined by Krapez and Eisenlohr (1998). Some pegmatites constitute part of a 120-km-long north-northeast-trending linear array (Wodgina-Strelley belt). More than 55% of the pegmatites in the Pilbara Craton are interpreted to be spatially related to major faults. Pegmatites were emplaced into brittle and ductile deformation regime and their shapes appear to be determined by the nature of the host rocks. The pegmatite veins and swarms often use narrow tension gashes, dilational jog-type, and horse-trail brittle structures in granite-gneiss (Sweetapple and Collins, 2002).

Host rocks: The mineralisation is hosted by NYF and mixed LCT–NYF-family pegmatites which are emplaced in Archean gneissic granites, migmatites, and monzogranites (Table 3.11). The Cooglegong pegmatites are associated with the Cooglegong and Spear Hill monzogranties of the Shaw Granitoid complex whereas the Pinga Creek pegmatites are associated with the Numbana Monzogranite of the Yule Granitoid complex (Figs 3.23 and 3.24). The internal structure of the pegmatites is layered and simple. Some pegmatites in the Pinga Creek field are aplitic (Table 3.11).

REE mineralisation: The primary REE mineralisation in the pegmatites is poorly described. The presence of REE mineralisation is interpreted from REE-bearing minerals in the alluvial concentrates derived from them. The main REE-bearing minerals include tanteuxenite, gadolinite, yttrotantalite, fergusonite, monazite, and samarskite (Sweetapple, 2000). The alluvial concentrates also contain cassiterite and tantalite-columbite.

Source of REE: The peraluminous nature of granites and a high initial $^{87}Sr/^{86}Sr$ ratio of the Cooglegong Granite suggest that the NYF-type pegmatites were

most likely derived from partial melting, or reworking of older felsic material that also generated the granites (Sweetapple, 2000). Like most other pegmatites of this type the REE were most probably derived from a fluid-rich pegmatitic melt.

Age of mineralisation: SHRIMP $^{206}Pb/^{207}Pb$ analyses of cassiterite from the Cooglegong pegmatites yielded an age of 2839 ± 16 Ma. This is slightly younger than the age obtained from cassiterite by secondary ion mass spectrometry (2901 ± 16 Ma). Geochronological data from rare-metal pegmatites in the region indicates that emplacement of associated granites (post-dating peak metamorphism at 2950 Ma and 2900 Ma) occurred between 2800 Ma and 2900 Ma. The pegmatites are interpreted to have been emplaced during two periods: an early phase at 2890 to 2880 Ma and a later phase between 2840 Ma and 2830 Ma (Sweetapple and Collins, 2002).

Genetic model: The REE mineralisation was most probably formed during crystallisation of a fluid-rich pegmatitic melt. In the pegmatites of the Wodgina Pegmatite Group, tantalum mineralisation is interpreted to have formed in the early stages of crystallisation from the melt. Some tantalum was remobilised later and dispersed within secondary (hydrothermal) albite and lepidolite. It is possible that similar process occurred for the NYF-type pegmatites in the Cooglegong and Pinga Creek fields, however, more detailed information on the mineralogy and paragenesis is required to indicate an evolutionary model for the REE-bearing pegmatites.

Key references: Cerny (1991a,b): regional to global environments, petrogenesis, evolution;
Sweetapple and Collins (2002): classification, petrogenesis, metallogeny; and
Sweetapple (2000): age, classification, exploration methods.

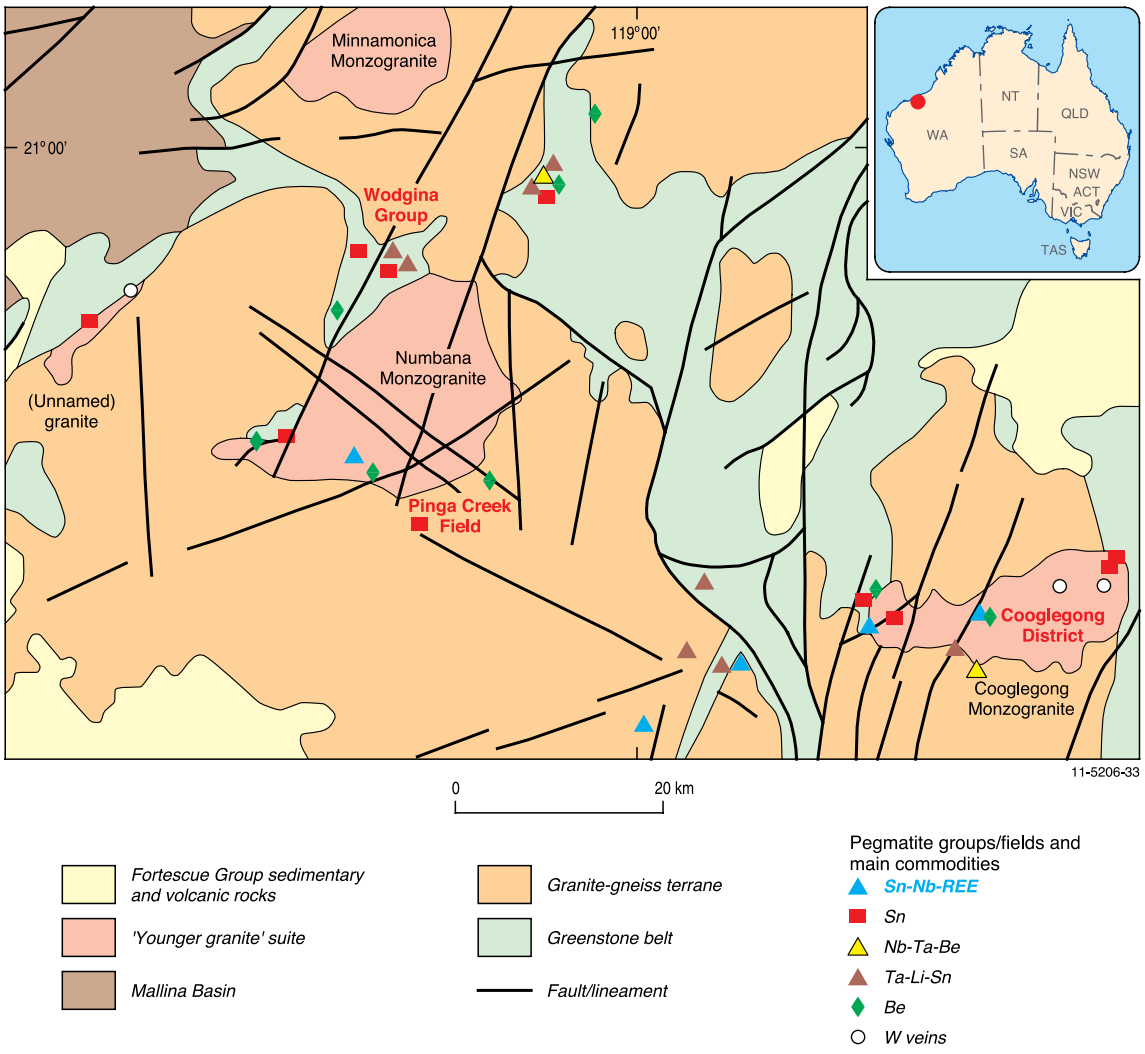

Figure 3.23. Regional geological map of the major mineralised pegmatite fields in the east Pilbara Craton, Western Australia. Modified from Sweetapple and Collins (2002).

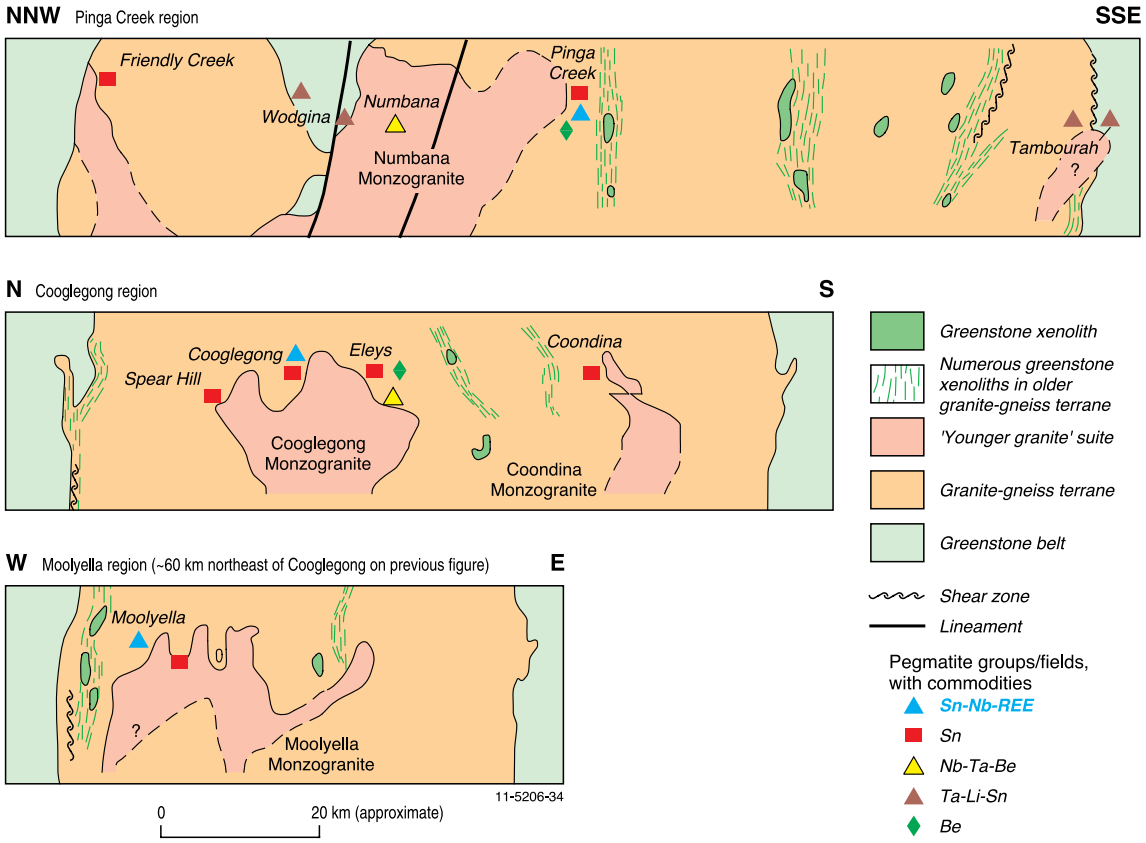

Figure 3.24. Schematic cross-sections through the Yule, Shaw, and Mount Edgar granitic complexes showing general location of rare metal and rare-earth-element-bearing pegmatites. Modified from Sweetapple and Collins (2002).

Table 3.9. Three petrogenetic families of rare-earth-element-bearing pegmatites (Cerny, 1991a).

Family	Pegmatite types	Geochemical signature	Pegmatite bulk composition	Associated granites	Source lithologies	Examples
LCT	Beryl, complex albite-spodumene, albite	**Li**, Rb, **Cs**, Be, Sn, Ga, **Ta** > Nb (B, P ,F)	Peraluminous	Syn- to late-orogenic; Peraluminous S, I or mixed types	Undepleted upper- to middle- crust supracrustals and basement gneisses	Biktia field, Zimbabwe; Uto-Mysingen field, Sweden,; White Picacho field, New Mexico; Wodgina, Pilbara (WA)
NYF	Rare earth	**Nb** > Ta, Li, **Y**, Sc, REE, Zr, U, Th, **F**	Subaluminous, metaluminous (subalkaline)	Mostly anorogenic; peraluminous to metaluminous (rarely peralkaline) A and I types	Depleted middle to lower crustal granulites, or undepleted juvenile granites	Shatford Lake group, Canada; Stockholm area, Sweden; Cooglegong and Abydos, Pilbara (WA)
Mixed	'Cross-bred' LCT and NYF	Mixed	Metaluminous to moderately peraluminous	Post-orogenic to anorogneic; subaluminous to slightly peraluminous; mixed geochemical signature	Mixed protolith; or assimilation of supracrustals by NYF granites	Tordal district, Norway; Kimito, Finland; Moolyella, Pilbara (WA)

LCT = Lithium–Cesium–Tantalum pegmatite; NYF: Niobium–Yttrium–Fluorine pegmatite. Peraluminous = (A/CNK) >1; subaluminous = (A/CNK) ~1; metaluminous = (A/CNK) <1 at (A/NK) >1; subalkaline = (A/NK) ~1; peralkaline = (A/NK) <1. A = molecular Al_2O_3; CNK = CaO + Na_2O + K_2O; and NK = Na_2O + K_2O.

Table 3.10. Four classes of granitic pegmatites (modified from Cerny, 1991a).

Class	Family	Typical minor elements	Metamorphic environment	Relation to granites	Structural features
Abyssal		U, Th, Zr, Nb, Ti, **Y**, **REE**, Mo; poor to moderate mineralisation	Upper amphibolite to low- to high-P granulite facies	None (anatectic segregations)	Conformable to mobilised cross-cutting veins
Muscovite		Li , Be, **Y**, **REE**, Ti, U, Th, Nb > Ta; poor to moderate mineralisation; ceramic minerals	High P, Barrovian amphibolite facies (kyanite– sillimanite)	None (anatectic segregations) to marginal and exterior	Quasi-conformable to cross-cutting
Rare-element	LCT	Li, Rb, Cs, Be, Ga, Sn, Hf, Nb > or < Ta, B, P, F; poor to abundant mineralisation; gemstock, industrial minerals	Low P, Abukama amphibolite to upper greenschist facies (andalusite–sillimanite)	(Interior to marginal to) exterior	Quasi-conformable to cross-cutting
	NYF	**Y**, **REE**, Ti, U, Th, Zr, Nb > Ta, F; poor to abundant mineralisation; ceramic minerals	Variable	Interior to marginal	Interior pods, conformable to cross-cutting
Miarolitic	NYF	Be, **Y**, **REE**, Ti, U, Th, Zr, Nb > Ta, F; gemstock; poor mineralisation	Shallow to sub-volcanic	Interior to marginal	Interior pods, conformable to cross-cutting dykes

LCT = Lithium–Cesium–Tantalum pegmatite; NYF: Niobium–Yttrium–Fluorine pegmatite.

Table 3.11. Rare-earth-element-bearing pegmatites in the Pilbara Craton, Weatern Australia (modified from Sweetapple and Collins, 2002).

Pegmatite field/district/ group	Associated granite complexes	Host rock	Morphology	Internal structure	REE minerals	Pegmatite class/ and type/subtype
Pinga Creek	Numbana Monzogranite; Yule Granitoid complex	Gneissic granite, migmatite, greenstone xenoliths	Unknown	Layered aplite-pegmatites	Gadolinite	Rare element/rare earth/gadolinite
Cooglegong	Cooglegong Monzogranite; Spear Hill Monzogranite; Shaw Granitoid Complex	Granite gneiss, migmatite, monzogranite	Swarms of shallow-dipping sheets	Layered and simple pegmatites	Tanteuxenite, yttrotantalite	Rare element
White Springs	Unknown	Granite gneiss, migmatite	Dyke	Simple unzoned pegmatites	Gadolinite, monazite, tanteuxenite	Rare element/rare earth/gadolinite
Abydos	Unknown	Granite gneiss, migmatite	Sheets and dykes	Simple to complex zoned pegmatites	Gadolinite, monazite	Rare element/rare earth/gadolinite
Wodgina	Numbana Monzogranite	Mafic-ultramafic metavolcanics	Veins	Layered and massive pegmatites		Rare element
Moolyella	Moolyella Monzogranite	Gneissic granite	Veins	Layered aplite-pegmatites and simple pegmatites	Monazite	Rare element

Deposit Type 3.12: Rare-earth-element-bearing skarn

General description: Skarn is a rock dominated by calcium and magnesium silicates typically formed from the alteration of carbonate rocks as a result of metasomatic replacement by fluids derived from felsic melts. Some skarns can be formed from thermal and regional metamorphism. In skarns, often the initial thermal-metamorphic hornfels are overprinted by anhydrous and hydrous silicates of calcium, iron and magnesium. Economic-grade concentrations of ore minerals are generally formed in the later stages of cooling of the fluids (Eckstrand et al., 1995; Meinert, 1993). REE mineralisation in skarn is hosted by calc-silicate rocks formed from fluids derived from predominantly felsic magmatic melts, which also form granites intruding calcareous rocks. Some REE-bearing skarns are also derived from fluids sourced from carbonatites (e.g., Saima in China; Long et al., 2010). In some REE-bearing skarns, the mineralisation involves two stages—in the first stage skarns with REE-bearing minerals are formed, which are remobilised by metamorphic fluids generated from regional metamorphism at the second stage.

Australian deposits/prospects: Mary Kathleen (Mount Isa Orogen, Qld).

Deposits outside Australia: Saima (China); Skye (Scotland).

Type example in Australia: Mary Kathleen, Queensland (Fig. 3.25).

Location: Longitude 140.013, Latitude -20.746
~50 km east of Mount Isa, Queensland
1:250 000 map sheet: Cloncurry (SF 54–02)
1:100 000 map sheet: Marraba (6956)

Geological province: Mount Isa Orogen, Queensland

Resources: Significant REE mineralisation has been intersected at the Mount Dorothy and Elaine Dorothy prospects. An inferred Resource of 83 000 tonnes at 280 ppm U_3O_8 and 3 200 ppm TREO was reported in March 2010.

Current status: Mined out. The deposit was mined for uranium, but the REE were left in the tailings dumps.

Economic significance: Unknown, but high for other prospects in the area.

Geological setting: The Mary Kathleen deposit is located within the Mary Kathleen Belt (10 to 30 km wide and >200 km long) of metasedimentary rocks metamorphosed to amphibolite facies (Bierlein et al., 2008). An ENE–WSW-directed extension created a rift basin (Leichhardt Superbasin), which was filled (between ~1800 Ma to ~1750 Ma) with a thick pile of mafic rocks and fluvial to lacustrine siliciclastic and lesser carbonate-bearing sedimentary rocks (Jackson et al., 2000; Gibson et al., 2008). The metasediments of the Corella Formation hosting the Mary Kathleen deposits were deposited during this event. Felsic magmatism related to the Wonga Extension Event occurred in the belt between 1760 Ma and 1720 Ma during which the Wonga and the Burstall Suites were emplaced (Neumann, 2007). This Phase 1 was overprinted by a Phase 2 comprising regional metamorphism and deformation between 1550 Ma and 1500 Ma (Oliver et al., 1999).

Host rocks: The REE and uranium mineralisation is hosted by hornfelsed calc-silicate rocks, skarns, quartzite, and marble. The precursor rocks of the skarns comprised calcareous pebble conglomerate, an ophitic-textured 'monzonitic' intrusion and minor banded calcareous sediments (Fig. 3.25). Stratigraphically these rocks belong to the upper parts of the Corella Formation (Derrick, 1977; Oliver et al., 1999). The mineralisation is structurally controlled by Phase 1 and Phase 2 skarns occupying the axial zone and the western limb of the Mary Kathleen Syncline (Fig. 3.25). Paragenetic studies show two episodes of skarn-formation (Oliver et al., 1999).

REE mineralisation: The high-grade uranium, thorium, and REE mineralisation forms infilling- and replacement-style veins. A later phase of REE mineralisation is represented by anastomosing array of veins and 'metasomatic' breccia (Oliver et al., 1999). The main REE-ore minerals are allanite and stillwellite [$(Ce,La,Ca)BSiO_5$] associated with uraninite, garnet, pyroxene, and apatite. Apatite, garnet, and titanite also contain REE. The REE mineralisation overprints skarns. In the marginal zone fractured skarn is cut by a network of allanite veins. In the main ore zone, coarse bladed allanite is accompanied by second-generation garnet, apatite, and uraninite sheathed with silica. A late generation of allanite forms alteration patches and infills post-ore fractures. The post-ore assemblage also contains calcite, prehnite, albite, and variable amounts of epidote, garnet, chalcopyrite, and hematite (Oliver et al., 1999). The mineralisation is cross-cut by late calcite veins with accessory chalcopyrite, garnet, and rare clinopyroxene. The late veins are interpreted to be related to a ~1500 Ma deformation event (Oliver et al., 1999). The REE content of the deposit is around 4% (Scott and Scott, 1985), with the REE

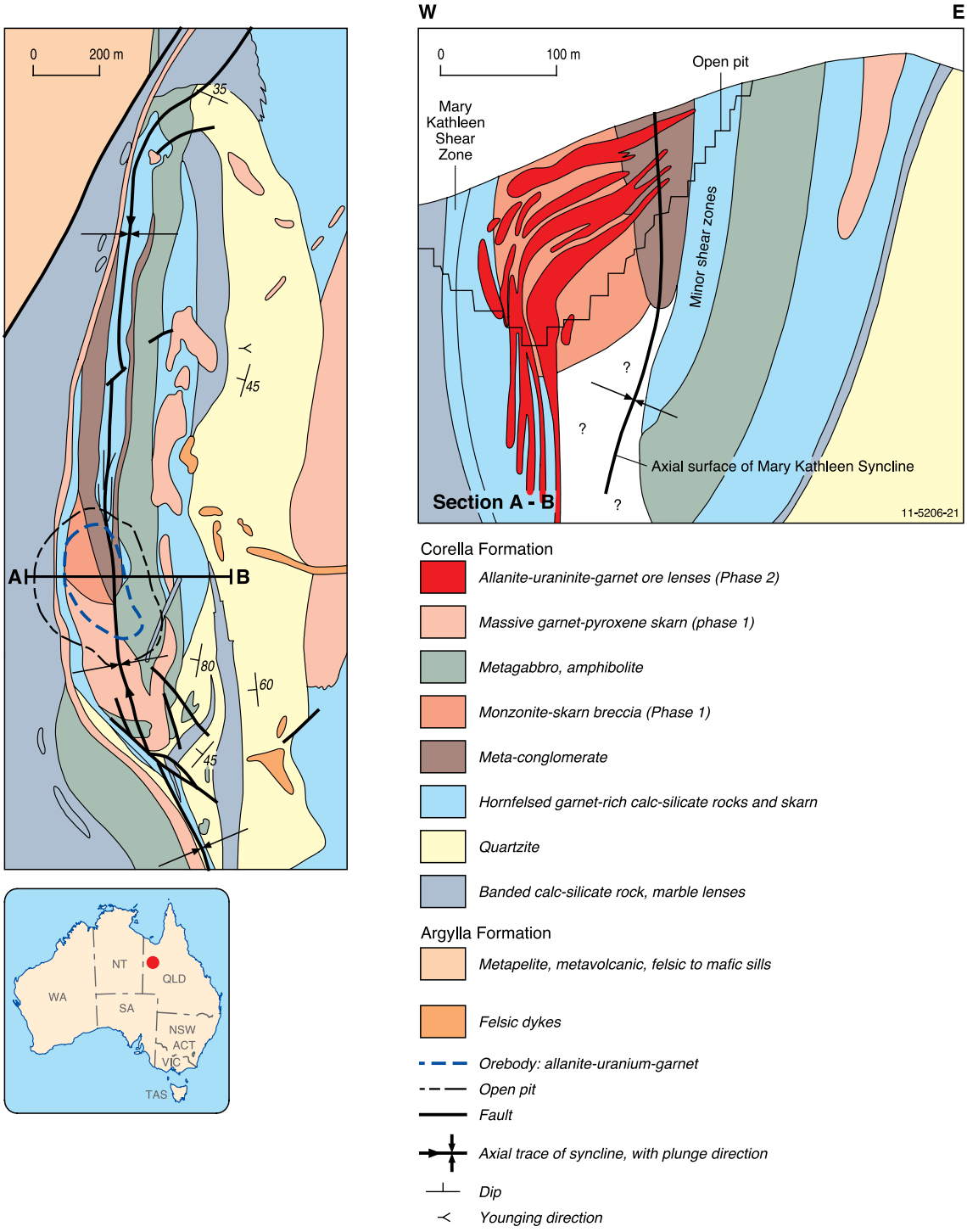

Figure 3.25. Geological map and cross-section of the Mary Kathleen uranium-rare-earth-element deposit, Queensland. Modified from Oliver et al. (1999).

content of individual ore samples ranging from 14 to 16 wt% (Table 3.12). The ore samples show extreme enrichment in LREE (Tables 3.12 and 3.13). Amongst the skarns, paragenetically early banded skarns are more enriched in REE than massive skarns. Recent drilling at the Mount Dorothy project located near Mary Kathleen shows intervals containing up to ~5000 ppm TREE, with HREE + yttrium accounting for more than 50% of the TREE (ASX/media announcement by China Yunnan Copper Australia Limited, 6th January 2011). This hole intersected a strongly weathered/oxidised zone rich in iron-oxides and clay.

Source of REE: Available data do not permit clear identification of the source of REE. The REE distributions and initial $^{143}Nd/^{144}Nd$ ratios in the ores suggest that magmatic fluids associated with the Burstall Granite could have leached REE from the Corella Formation to form a REE-rich skarn protore (Maas et al., 1987). Oliver et al. (1999) proposed a more complex model in which REE are derived from two (or more) sources which include extremely light REE-enriched old (>2300 Ma) rocks and rocks within the Mary Kathleen Syncline (skarns and the Burstall Granite).

Age of mineralisation: The age of mineralisation is contentious. U-Pb dating of uraninite from an apatite-allanite assemblage gave an age of 1550 ± 15 Ma (Page, 1983). This age is close to the age of D_3 deformation and peak metamorphism in the belt (Oliver et al., 1999). The Burstall Suite granites, which are interpreted to be related to the formation of skarns, yield a U-Pb TIMS age of ~1740 Ma (Page, 1983). More recent SHRIMP U-Pb ages confirm a magmatic age of 1740–1735 Ma (Neumann, 2007). Mineral separates from the garnet ± pyroxene skarn assemblage yield a Sm–Nd isochron age of 1766 ± 80 Ma (Maas et al., 1987) which overlaps the age of the Burstall Suite granites.

Genetic model: The mineralisation is interpreted to have formed in two stages (Maas et al., 1987; Oliver et al., 1999). The first stage resulted in the formation of skarns from predominantly magmatic fluids associated with the Burstall Suite granites. In the second-stage metamorphic fluids generated during peak metamorphism recrystallised and upgraded REE and uranium mineralisation. The second-stage fluid-flow was structurally controlled.

Key references: Page (1983): U-Pb geochronology, lead isotopes;
Maas et al. (1987): Sm-Nd isotopes, REE abundances, geochronology; and
Oliver et al. (1999): mineral chemistry, petrography, structure, geochronology, ore genesis.

Table 3.12. Concentration (in ppm) of rare-earth elements in ore and granite, Mary Kathleen deposit (Maas et al., 1987).

Element	Ore (MK 68)	Ore (MK 69)	Ore (MK 70)	Fresh Burstall Granite (237 G)	Fresh Burstall Granite (241 A)	Altered Burstall Granite (240 A)	Altered Burstall Granite (240 E)
La	54 675	60 845	46 922	51	79.3	4.1	3.3
Ce	77 113	87 015	80 692	93.6	160.1	13.9	31.7
Pr	7648	7503	5325				
Nd	16 252	15 680	10 584	45.5	59.4	6.5	3
Sm	1002	638	487	8.4	9.6	2.2	0.83
Eu	35	34	33	0.25	0.81	0.37	0.13
Gd				13.6	6.9	4.4	3.8
Tb				1.56	1.27	1.59	1.58
Dy	28	46	33				
Ho				2.02	1.75	1.08	0.88
Yb		2	1	4.16	4.56	3.31	2.61
Lu				0.59	0.7	0.41	0.36
LREE	156 725	171 715	144 043	199	309	27	39
HREE	28	48	34	22	15	11	9
LREE/ HREE	5597	3615	4224	9	20	3	4
Total REE	156 753	171 763	144 077	221	324	38	48

Note: The number in brackets indicates the sample number.

Table 3.13. Concentration (in ppm) of rare-earth elements in skarns, Mary Kathleen deposit (Maas et al., 1987).

Element	Banded Skarn (1262D1)	Banded Skarn (1262D5)	Banded Skarn (5013A1)	Banded Skarn (5013A3)	Massive Skarn (0832A2)	Massive Skarn (0822C1)	Massive Skarn (0822C2)
La	17.3	23.3	183	40.2	3.6	10.7	13
Ce	39.7	37.8	205	58.9	12.9	34.3	38.6
Pr							
Nd	19.3	21	62.6	34	21.9	23.8	23.7
Sm	3.5	4	6.8	7.7	7.4	4.9	4.4
Eu	0.45	0.58	0.89	1.25	2.3	1.9	1.68
Gd	2.36	3.98	6.6	6.6	5.2	4.6	4.3
Tb	0.39	0.66	0.39	1.08	0.65	0.76	0.66
Dy							
Ho	0.54	1.02	0.41	1.44	0.77	1.26	1.04
Yb	1.37	2.92	1.65	3.65	2.02	3.79	3.11
Lu	0.19	0.44	0.15	0.55	0.31	0.58	0.49
LREE	80	87	458	142	48	76	81
HREE	5	9	9	13	9	11	10
LREE/HREE	17	10	50	11	5	7	8
Total REE	85.1	95.7	467.49	155.37	57.05	86.59	90.98

Note: The number in brackets indicates the sample number.

Deposit Type 3.13: Apatite and/or fluorite veins

General description: The vein deposits include REE-enriched veins of apatite and/or fluorite. In some deposits mineralisation is hosted in quartz veins. The veins are formed from hydrothermal fluids predominantly derived from alkaline and/or carbonatite melts. In many regions the veins may be distal to alkaline and carbonatite complexes. In some deposits the veins may have formed from non-magmatic fluids or fluids related to later magmatic melts.

Australian deposits/prospects: Nolans Bore (Arunta Region, NT); ?John Galt (Halls Creek Orogen, WA).

Deposits outside Australia: Lehmi Pass, Idaho (USA); Gallinas Mountains, New Mexico (USA); Kangakunde Hill (Malawi).

Type example in Australia: Nolans Bore, Northern Territory (Figs 3.26 and 3.27).

Location: Longitude 133.238557, Latitude -22.59385
~135 km north-northwest of Alice Springs
1:250 000 map sheet: Napperby (SF 53–09)
1:100 000 map sheet: Aileron (5552)

Geological province: Arunta Region, Northern Territory.

Resources: Measured, Indicated and Inferred Resources totalling 30.3 million tonnes to a depth of 130 m which grades at 2.8% REO, 12.9% P_2O_5, 0.44 pounds per tonne U_3O_8, and 0.27% Th. According to Arafura, the distribution of the LREE currently being considered for extraction, (La, Ce, Pr, and Nd) amount to 95%, whereas the HREE (Sm, Eu, Gd, Tb, Dy) amount to 4.23% (Miezitis, 2010).

Current status: Deposit–advanced project (Fig. 3.28).

Economic significance: High.

Geological setting: The Nolans Bore deposit is spatially close to several tin and tantalum pegmatites, and REE-bearing carbonatite/alkaline complexes (Mud Tank and Mordor Igneous Complex). This mineral field of carbonatites, pegmatites, and other REE occurrences is in a region transacted by three major lineaments delineated by O'Driscoll (1985), which include the north–northwest-trending G2-gravity lineament that is considered to be spatially related to the Olympic Dam deposit and northwest-trending G3-gravity

and R16 lineaments (Fig. 3.26). At a more local scale both the Mud Tank Carbonatite and Mordor Igneous Complex are located near the Woolanga Lineament, a deep-seated NW-trending crustal structure which may have controlled the emplacement of alkaline rocks in the Aileron Province (Jaques, 2008; Hoatson et al., 2005). The mineral field traverses the northern Willowra Gravity Ridge high (Fig. 3.26) that forms the boundary between the Aileron Province in the south and the Tanami Orogen in the north and which is interpreted to be a suture zone where the thickness of the crust (in the Aileron Province) increases to ~60 km (Goleby et al., 2009). Thus like many other alkaline and carbonatite provinces, the Nolans Bore deposit and other pegmatites and carbonatites in the area can be spatially related to a zone of thickened crust (lithospheric?) crosscut by deep crustal structures.

Host rocks: The mineralised fluorapatite veins at the Nolans Bore deposit are hosted predominantly by granite (metamorphosed to gneiss) which intruded the Lander Rock beds consisting of schist, phyllite, hornfels, granofels and tourmaline-bearing quartzite (Fig. 3.27; Huston et al., in press). The granites are correlated with the Boothby Gneiss (dated at 1806 ± 4 Ma) and the Napperby Gneiss (1778 ± 8 Ma; cited in Huston et al., in press).

REE mineralisation: The mineralisation at the Nolans Bore deposit (Fig. 3.29) is hosted in a series of east-northeast-trending, and steeply dipping to the northwest, fluorapatite veins and breccia zones (Fig. 3.27). The granite-gneiss host has been strongly kaolinised due to weathering. The weathering zone shows secondary enrichment with REE. Huston et al. (in press) describe four styles of mineralisation: (1) massive fluorapatite veins that typically contain 4–6% REE oxides and constitute most of the defined resource; (2) very high-grade (7%–10% REE oxide) zones found in cheralite-bearing, apatite-poor kaolinitic zones outside of the veins; (3) apatite-allanite-epidote zones hosted by calc-silicates; and (4) low-grade stockwork zones in gneiss and kaolinitised rock adjacent to the veins and mylonite zones. The main ore minerals are cheralite, thorite, allanite, bastnäsite, monazite, and

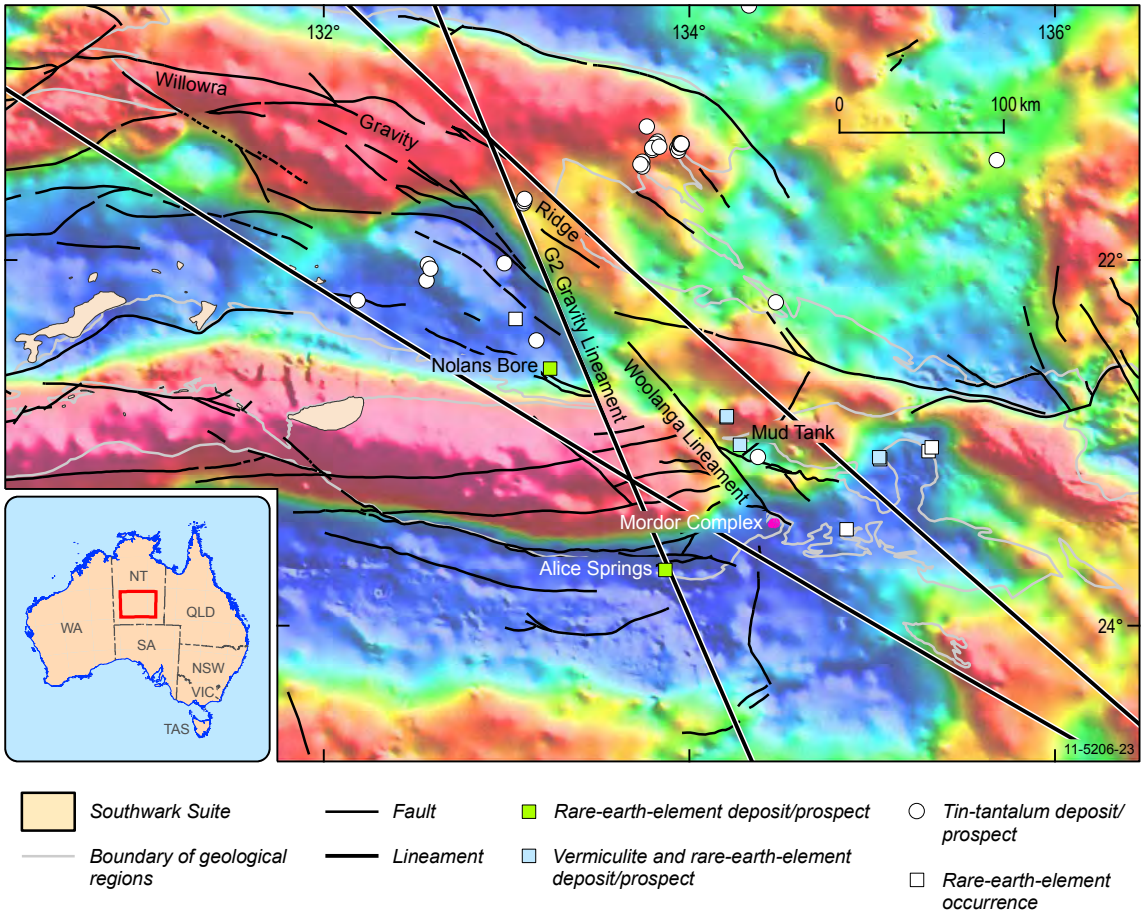

Figure 3.26. Locations of Nolans Bore and other rare-earth-element-bearing prospects and deposits in central Australia. The major structural and gravity lineaments are shown on a background gravity image. Locations of deposits and prospects are from Geoscience Australia's OZMIN database.

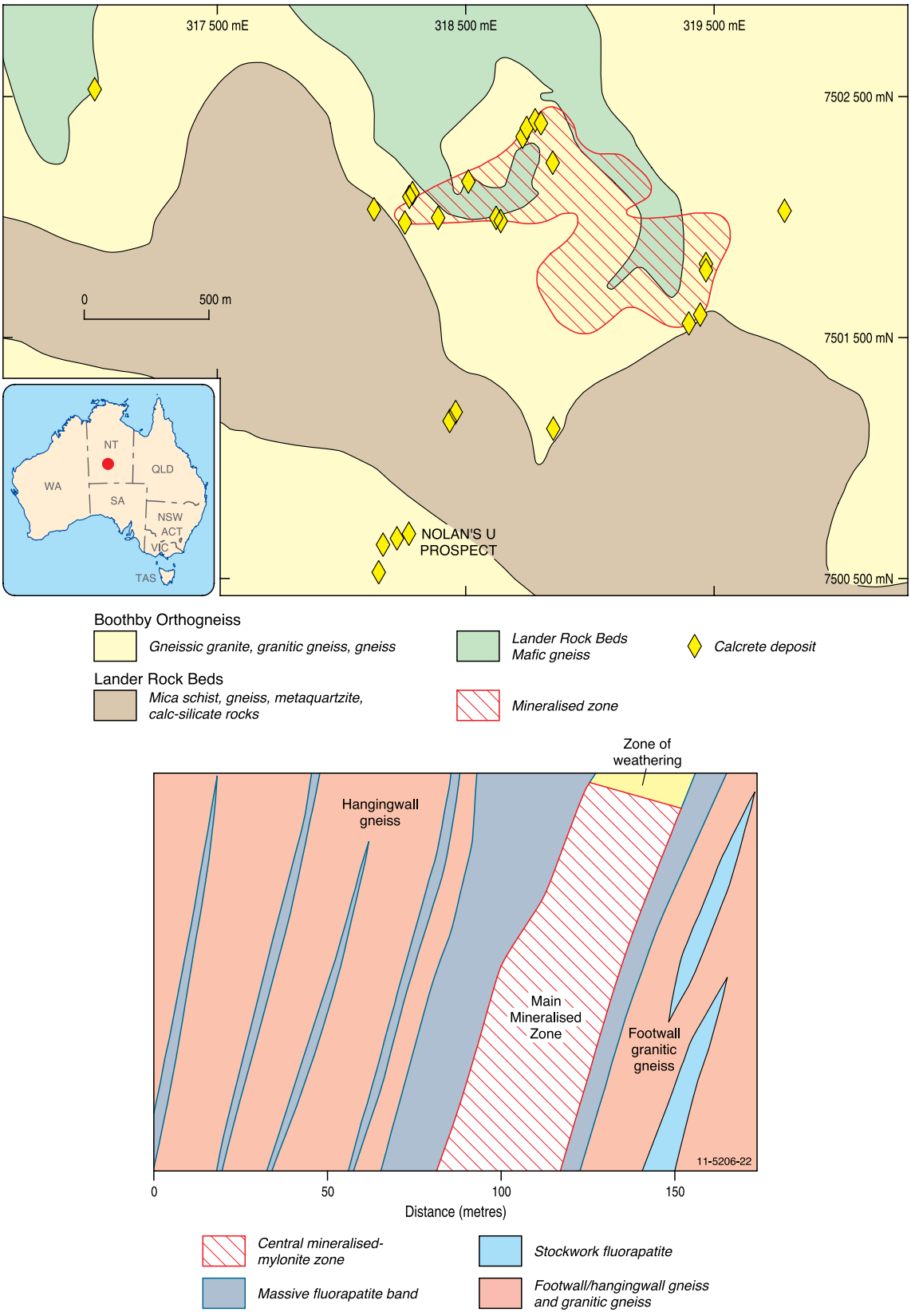

Figure 3.27. Geological map and cross-section of the Nolans Bore rare-earth-element deposit. The section is from the northwestern part of the deposit. Modified from Lockyer and Brescianini (2007).

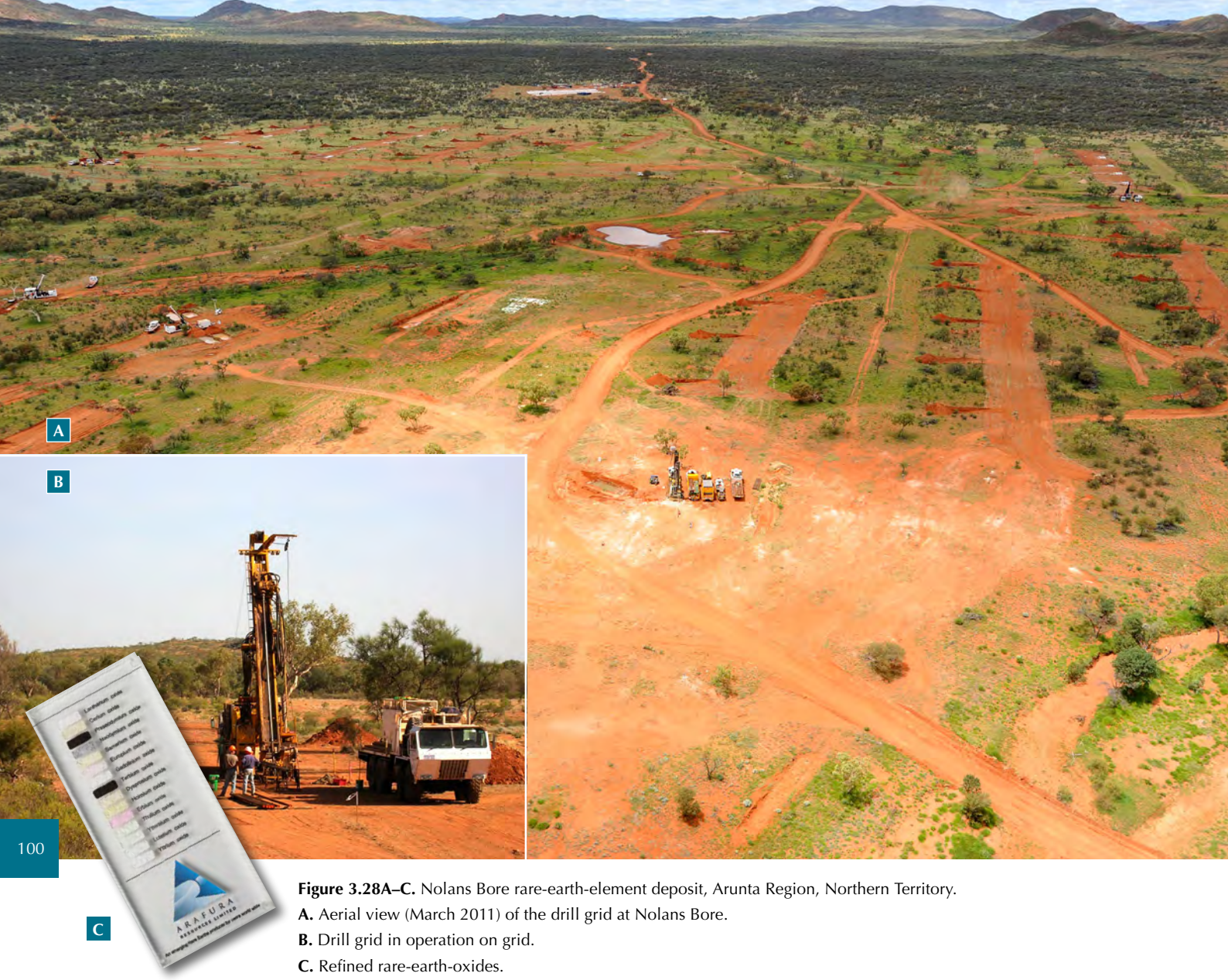

Figure 3.28A–C. Nolans Bore rare-earth-element deposit, Arunta Region, Northern Territory.
A. Aerial view (March 2011) of the drill grid at Nolans Bore.
B. Drill grid in operation on grid.
C. Refined rare-earth-oxides.
Richard Brescianini (Arafura Resources Limited: http://www.arafuraresources.com.au/) provided the photographs.

several REE-bearing fluorocarbonates (Lockyer and Brescianini, 2007; Huston et al., in press). Often brecciated apatite is infilled and replaced with Ce- and La-bearing cheralite monazite and bastnäsite (Lockyer and Brescianini, 2007).

Source of REE: The Nolans Bore deposit is located in a zone that also contains the Mud Tank Carbonatite, Mordor Igneous Complex, and several tin- and tantalum-bearing pegmatites. It is possible that REE in the deposit were derived from alkaline and/or carbonatite melts or from felsic melts which formed tin-tantalum pegmatites. On the basis of high thorium content of the Nolans Bore fluorapatite, Hussey (2003) suggests that it was unlikely to be related to a carbonatite or carbonatite-derived fluid, but is more likely to be sourced from a NYF-type (Niobium-Yttrium-Fluorine type, Cerny, 1991a) pegmatite melt. The REE patterns for fluorapatite, however, are similar to that of apatite from both peralkaline and carbonatitic melts (Hussey, 2003). Juvenile initial $^{87}Sr/^{86}Sr$ (0.705-0.707) and evolved Nd isotopes (Nd 1250 = -12 to -4) suggest an enriched mantle source of REE (Korsch et al., 2009).

Age of mineralisation: The mineralised veins and breccias are hosted by granite gneisses interpreted to be emplaced at ~1880 Ma to 1780 Ma (see above). This provides a maximum age for mineralisation. Preliminary U-Pb dating of apatite from the veins yields an age of 1244 ± 10 Ma (Korsch et al., 2009). If this age is correct the mineralisation is neither related to the Mordor Igneous Complex (with a SHRIMP U-Pb crystallisation age of 1133 ± 5 Ma, Hoatson et al., 2005), nor with the Mud Tank Carbonatite, which has a much is younger emplacement age of 732 ± 5 Ma (Black and Gulson, 1978). Although the ~1244 Ma age is thought to broadly coincide with the age of the Mudginberri phonolite dykes (Rb-Sr isochron age of 1316 ± 40 Ma, Page et al., 1980) in the Pine Creek

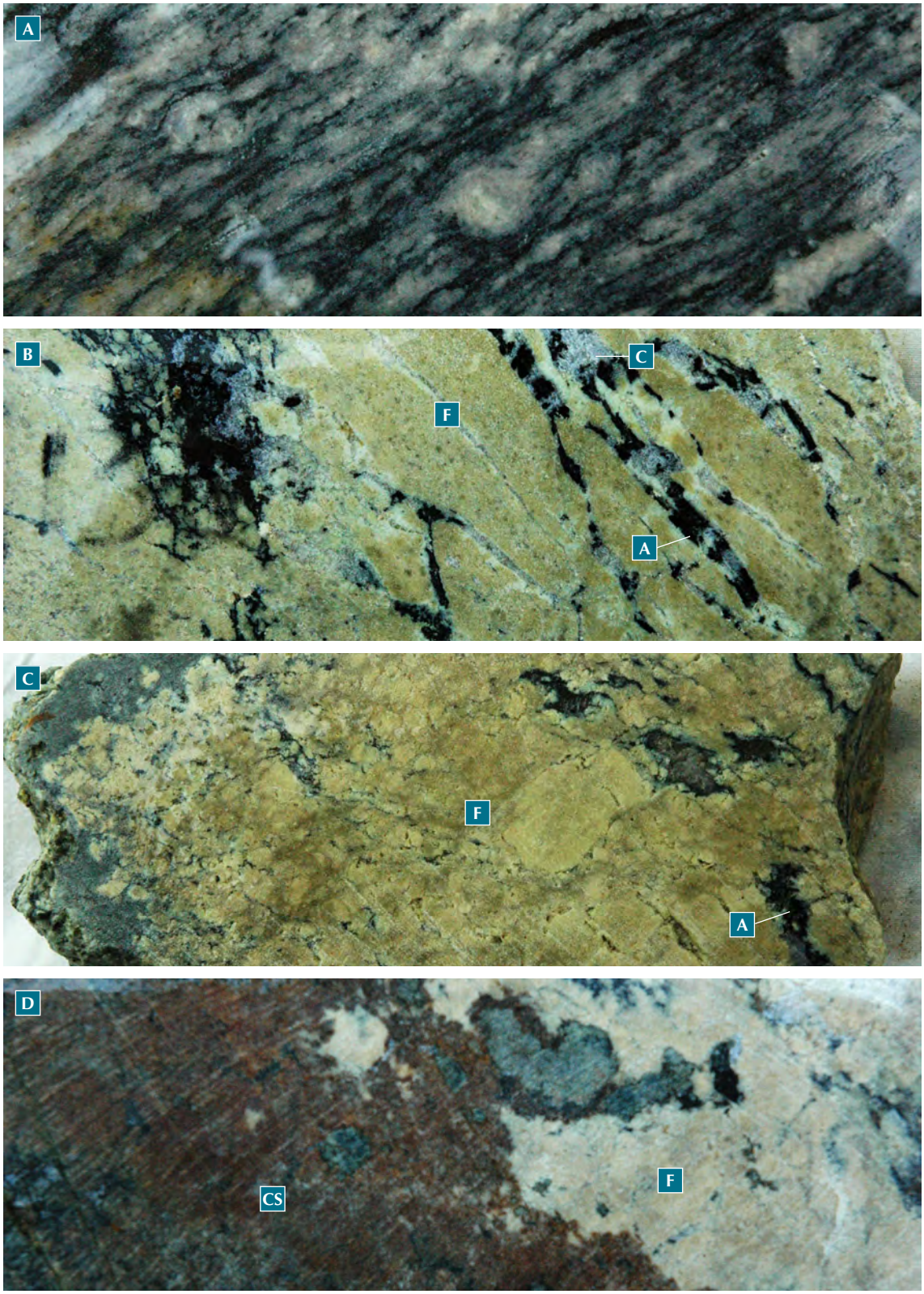

Figure 3.29A–D. Major rock types from the Nolans Bore rare-earth-element deposit, Northern Territory.

A. Gneissic granite country rock (Boothby Orthogneiss).

B. REE-bearing fluorapatite (F) cut by calcite (C) and REE-bearing allanite (A) veins.

C. Moderately to slightly weathered, brecciated fluorapatite (F) with irregular allanite (A) veins.

D. Irregular contact between massive fluorapatite and calc-silicate assemblage (CS). Field of view (short dimension) of drill core is ~5 cm. Reproduced with permission from Arafura Resources Limited (http://www.arafuraresources.com.au/).

David Huston (GA) and Kelvin Hussey (Arafura Resources Limited) provided the photographs.

Orogen and a global carbonatitic and alkalic magmatic event between 1300 and 1130 Ma (Pidgeon, 1989) it could also be related to the tin and tantalum pegmatites in the area, the age of which is unknown. Korsch et al (2009) suggest that the mineralisation was emplaced during a widespread Mesoproterozoic thermal event which included syn- to post-tectonic felsic magmatism (ranging between 1235 Ma and 1195 Ma) in the Musgrave Province.

Genetic model: The close spatial association between the mineralisation at the Nolans Bore deposit and other carbonatite, alkaline, and tin- and tantalum-bearing pegmatites suggests that it could have formed from magmatic fluids released from any of the above mentioned melts. The ~1244 Ma age of mineralisation however indicates that it could represent a distal hydrothermal event (Hussey et al., 2008) related from an intensive Mesoproterozoic thermal event (between 1235 Ma and 1195 Ma) during which REE were remobilised. The REE mineralisation also shows a thermal overprint during the Alice Springs Orogeny (Hussey, 2003). REE in the zone of secondary enrichment indicate that primary REE mineralisation was remobilised during weathering and/or calcrete formation in the area.

Key references: Hussey (2003): regional geology, deposit types, mineralisation;
Korsch et al. (2009): U-Pb, K-Ar, Rb-Sr geochronology, regional geology, stratigraphy; and
Huston et al. (in press): geology, mineralisation, genesis.

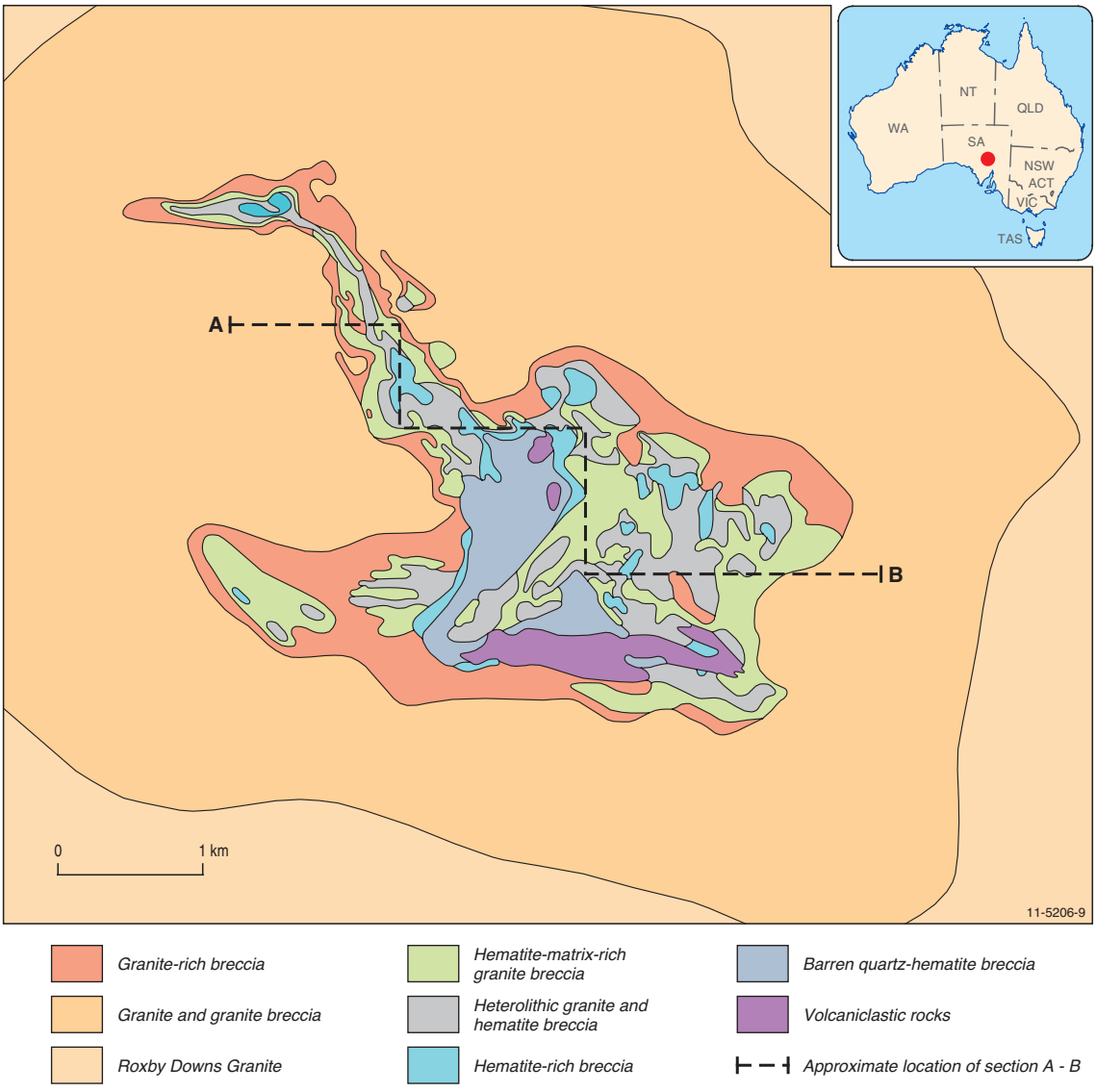

Figure 3.30. Schematic geological map of the Olympic Dam Cu-Au-U deposit, South Australia. Modified from Reynolds (2001).

Deposit Type 3.14: Iron-oxide breccia complex (or iron-oxide copper, gold, uranium deposits) with rare-earth elements

General description: Iron-oxide copper-gold-uranium (IOCG) deposits generally form in extensional environments and range in age from the present at least back into the Late Archean. Many deposits of this type are enriched in a distinctive, geochemically diverse suite of minor elements, including F, P, Co, Ni, As, Mo, Ag, Ba, LREE, Th, and U. These deposits contain mineable resources of more than one commodity, such as copper, gold, uranium, and iron. Although some of these deposits are enriched in REE, these elements are not currently extracted.

Australian deposits/prospects: Olympic Dam, Prominent Hill, Carrapateena (all Gawler Craton, SA); Mount Gee (Mount Painter Inlier, SA); Ernest Henry (Mount Isa Orogen, Qld).

Deposits outside Australia: Salobo, Cristallino, Sossego, Alemão (Carajás, Brazil), and Candeleria-Punta del Cobre and Manto Verde (Chile). (Williams et al., 2005).

Type example in Australia: Olympic Dam, South Australia (Figs 3.30 and 3.31).

Location: Longitude: 122.547515;
Latitude: -28.862596
~560 km north-northwest of Adelaide
1:250 000 map sheet: Andamooka (SH 53–12)
1:100 000 map sheet: Mattaweara (6237)

Geological province: Gawler Craton, South Australia.

Resources: Submarginal and Inferred Resources of REO of ~53 million tonnes (predominantly 0.2% La and 0.3% Ce). Currently not economic (Miezitis, 2010).

Current status: Operating mine, but REE are currently not extracted.

Economic significance: Unknown (REE).

Geological setting: According to Williams et al. (2005) these deposits occur in crustal settings with very extensive and pervasive alkali metasomatism. Skirrow et al. (2007) highlight the importance of pre-deposit continental margin setting for the Olympic Dam deposit and the Olympic Dam IOCG province in the Gawler Craton that produced during orogenesis over-thickened crust and mantle lithosphere. This setting was conducive in generating large volumes of high-temperature crustal melts emplaced during compression. The deposit lies at the intersection of major north–northwest-trending and west–northwest-trending gravity lineaments (O'Driscoll, 1985). Regional geophysical datasets indicate that the deposit is located at one of numerous coincident, but slightly displaced magnetic and gravity anomalies caused by hematite alteration of the host rocks.

Host rocks: The Olympic Dam deposit is hosted within a large body of hydrothermal breccia (Figs 3.30 and 3.31) occurring entirely within the Roxby Downs Granite (Reynolds, 2001). The funnel-shaped breccia complex primarily comprises a barren, hematite-quartz breccia core surrounded by variably mineralised and zoned hematite-granite breccia bodies. The breccia complex is interpreted to have formed from polycyclic events of alteration and brecciation. Heterolithic breccias contain a wide variety of altered clasts of granite, porphyritic volcanics, ultramafic to felsic intrusives, vein fragments of copper sulphides, fluorite, barite, siderite, and fine-grained laminated arkosic sedimentary rocks. The breccia complex is intruded by a variety of ultramafic, mafic, and felsic dykes. The breccias are interpreted to have formed in a phreato-magmatic diatreme structure located in the central part of the breccia complex (Reeve et al., 1990).

REE mineralisation: Hematite is the main iron-oxide which replaces magnetite, preserved now only at depth and within less evolved breccia at the peripheries of the breccia complex. Hematite is more abundant and intense towards the centre of the deposit (locally >95% of the rock) and replaces minerals and also forms veins and fills vugs. Ore zones form only a small fraction of breccia complex but weak mineralisation at background level is widespread within it. There is a general spatial correlation between higher grade copper-uranium mineralisation and more hematite-altered rocks, although the central hematite-quartz breccia zone is essentially barren of copper-uranium mineralisation. Low-grade economic gold mineralisation occurs in the copper-uranium ore zones, but higher grade gold mineralisation also occurs in small zones locally separate from or adjacent to copper-uranium zone (Reeve et al., 1990).

Most lithologies of the breccia complex are strongly enriched in REE, especially the LREE. REE mineralisation averaging 3000–5000 ppm combined lanthanum and cerium occurs throughout the breccia zones, including the central hematite-quartz core, where concentrations are generally higher (Reynolds, 2001). Typically there is about 0.59% TREO in the orebody (Roberts and Hudson, 1983). As granite breccia with hematite matrix and hematitised granite contain

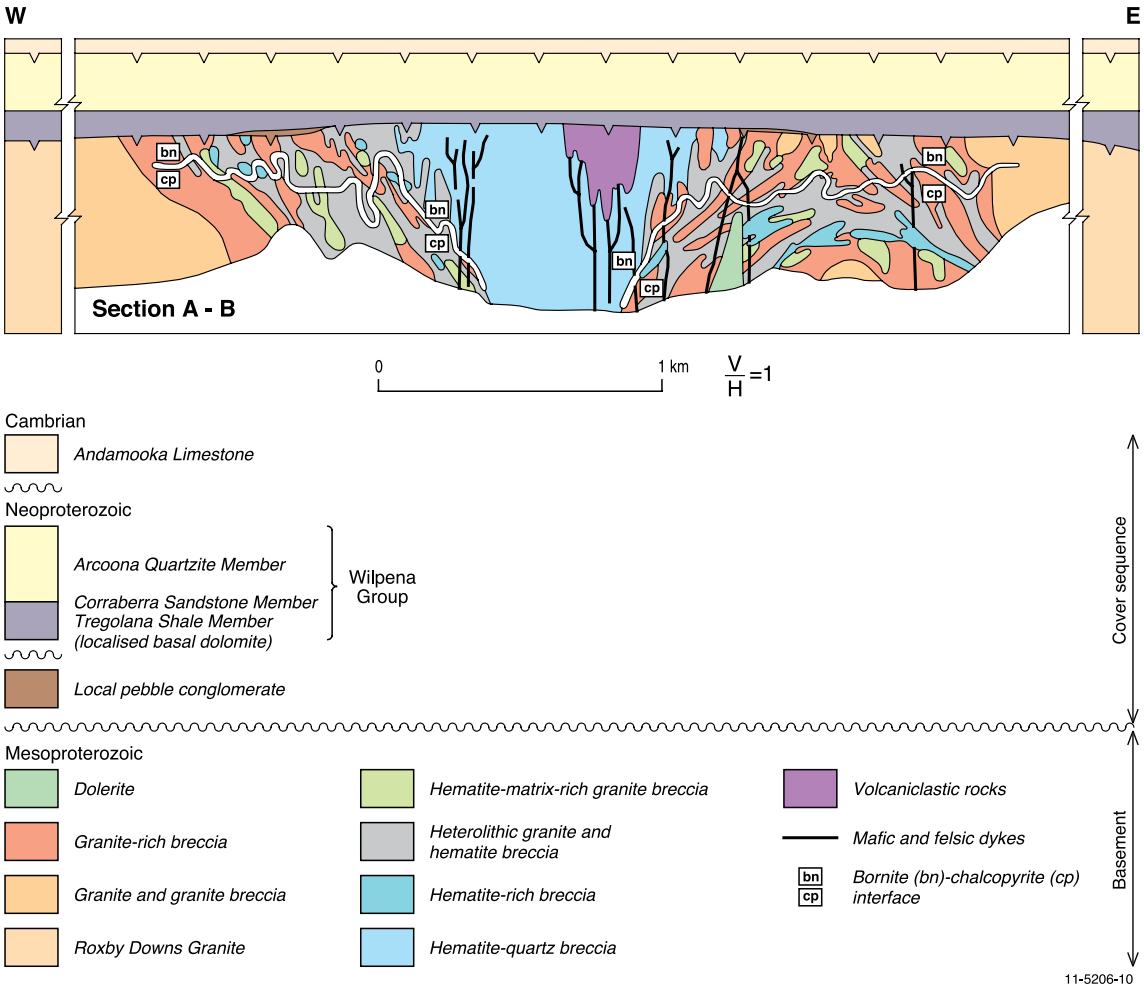

Figure 3.31. Schematic cross-section of the Olympic Dam Cu-Au-U deposit, South Australia. The approximate location of the stepped cross-section A–B is indicated on Figure 3.30. Modified from Reynolds (2001).

similar relative and absolute abundances of REE, the distribution of REE is not controlled by the mode (replacement or infilling) of hematite introduction (Oreskes and Einaudi, 1992). The absolute abundance of REE increases with increasing hematite content of the breccia. REE are also enriched in quartz-sericite veins and laminated barite fragments. According to Oreskes and Einaudi (1992), the REE were introduced into the altered rocks during breccia formation. LREE were mobile during all stages of alteration whereas the mobility of HREE was restricted to the most extreme stages of iron metasomatism.

Four major minerals of REE have been identified in the breccias: bastnäsite [(Ce, La)CO_3(F.OH)], florencite [(Ce,Al_3(PO_4)$_2$(OH)$_6$], monazite, and xenotime. In addition a U-Y-Si-P phase (probably a britholite series mineral) is also present. Oreskes and Einaudi (1992) did not report the presence of REE in zircons. However, LA–ICPMS analysis of zircons from an altered dyke show enrichment in HREE (Jagodzinski, 2005).

Mineral paragenetic studies indicate that REE minerals were deposited during much of the hydrothermal history of the deposit.

Source of REE: The high concentration of REE in the Olympic Dam deposit is in agreement with a general REE-enrichment of magmatic rocks of the Hiltaba Suite. According to Agangi et al. (2010), rhyolites of the Gawler Range Volcanics are enriched in REE, Y, and fluorine. The whole-rock geochemistry of these rocks suggests that because of high-fluorine concentration in the melt the REE behaved incompatibly during magmatic crystallisation and were enriched in a volatile-rich late-stage magmatic fluid, which deposited REE-rich minerals in vesicles, micromiaroles, and interstices between major mineral phases of rhyolites. On the basis of the differences in Nd isotopic values of the hematitic ores and of less mineralised granite host rock Johnson and McCulloch, (1995) suggested that the REE were derived in part from a source more primitive (possibly mantle) than that of the granitic host. They also noted

a correlation between Nd isotope value (εNd) and copper concentration in highly altered breccia and argued that copper and REE had a common source. These conclusions were supported by a later province-scale study (Skirrow et al., 2007) that also established the difference in Nd values of the hematitic ores in the Olympic Dam deposit (higher εNd values and hence a primitive source of REE) and of all other prospects in the Olympic Dam province, such as Titan and Emmie Bluff (lower εNd values hence crustal or evolved source of REE). Thus REE in the supergiant Olympic Dam deposits and other smaller prospects were probably derived form different sources.

Age of mineralisation: The SHRIMP U-Pb zircon age of 1588 ± 4 Ma age (Creaser and Cooper, 1993) of the Roxby Downs Granite constrains the maximum age of brecciation at the deposit. SHRIMP U-Pb analysis from three felsic dykes within the breccia complex yield an age of ~1590 Ma. These ages are confirmed by more recent data (Jagodzinskii, 2005). On the basis of textural relationships between sulphides and iron-rich breccias and the crosscutting relationship between the igneous units and the mineralised breccia it has been argued that brecciation, mineralisation, and magmatic activity were broadly contemporaneous and occurred at ~1590 Ma (Johnson and Cross, 1995). Based on Ar/Ar age of alteration muscovite, and SHRIMP U-Pb ages of titanite and zircon in the Olympic Dam district, Skirrow et al (2007) postulated another younger hydrothermal magnetite alteration event followed by hematitic alteration in the district at ~1575 Ma.

Genetic model: The current consensus among researchers is that mineralisation at the deposit was formed form an evolving hydrothermal system in which most of the metals and hydrothermal fluids were derived from a magmatic source. The hydrothermal system was driven by high-level felsic Hiltaba Suite plutons coeval with Gawler Range Volcanics. The fluid inclusion and silicate geothermometry data suggest the involvement of at least two fluids (Oreskes and Einuadi, 1992) one of which was hot (~ 400°C) and saline (up to ~ 42 wt% eq. NaCl), and the other relatively cooler (160°C to 250°C) and of moderate salinity. It is argued that early magnetite was formed from the first fluid, whilst hematite was deposited from the second fluid (Oreskes and Einuadi, 1992). The fluid inclusions associated with the magnetite-stage alteration and mineralisation in the Olympic Dam province are enriched in copper (from 300 to 600 ppm to 2 to 4 wt%, Bastrakov et al., 2007). These fluids were thus capable of transporting large quantities of copper and iron (Reeve et al., 1990). The low- to moderately-high-temperature fluids were relatively enriched in fluorine and relatively more oxidised and hence capable of transporting uranium, REE, and possibly copper (Reeve et al., 1990). Haynes et al. (1995) proposed a fluid-mixing model in which the two above-mentioned fluids mixed in a shallow phreato-magmatic setting. Bastrakov et al. (2007) suggest a similar two-stage model in which the early magnetite-bearing stage of alteration and mineralisation was overprinted by a hematitic stage during which copper, gold, and uranium were remobilised.

Key references: Reynolds (2001): regional geology, geology of deposit, mineralisation, structure, U-Pb zircon geochronology, genesis; and
Reeve et al. (1990): regional geology, alteration, igneous intrusions, mineralisation, ore genesis.

3.3.2. Additional geological information on rare-earth-element-bearing deposits not included in Section 3.3.1.

Heavy-mineral sands: The most common REE-deposit type in Australia is associated with heavy-mineral sands which are formed by enrichment of heavy minerals in marine and aeolian sands (generally of low grade). These placer deposits are concentrated along Cenozoic and older shorelines on both the southwest and east coasts of Australia. Beach, high dune, and offshore shallow marine deposits of Eocene to Holocene age occur mainly along coastal strips in southwestern Western Australia and they also extend for about 1300 km from near Gosford in New South Wales to just north of Rockhampton in Queensland. Shallow-marine-tidal deposits of similar age occur inland in the Murray Basin near the junction of South Australia, Victoria, and New South Wales. Older channel heavy-mineral deposits extend back into the Mesozoic with the Calypso deposit north of Perth being the type example. The heavy-mineral placers contain varying concentrations of monazite, xenotime, zircon, and titanium-bearing oxides, such as ilmenite, rutile, and leucoxene.

The importance of heavy-mineral deposits as a source of REE depends upon the content of monazite, and to a lesser degree xenotime, in the heavy-mineral concentrate. Up to 1995, Australia exported significant quantities of monazite, as a by-product from heavy-mineral-sand mining, for the extraction of REE and thorium overseas. Monazite was separated from heavy-mineral concentrates containing as little as 0.1% to 0.3% monazite. The bulk of Australia's monazite production was derived from the Eneabba and Cooljarloo regions in the Phanerozoic Perth Basin, north of Perth. Heavy-mineral concentrates for deposits

in these two regions contain 0.5 to 1.0% monazite, and from the Capel area, again in the Perth Basin, south of Perth, the heavy-mineral concentrates contain around 0.4% monazite (Cassidy et al., 1997). The heavy-mineral sand mines on the east coast of New South Wales and Queensland generally accounted for less than 10% of the monazite production, where the monazite contents in the heavy-mineral concentrates were generally 0.1 to 0.3%. The fine-grained fossil shallow marine deposits of the WIM 150-type in the Murray Basin, western Victoria, have reported monazite and xenotime contents of ~1.4% and ~0.4%, respectively (Williams, 1990).

Detailed descriptions of individual heavy-mineral deposits can be found in Shepherd (1990), Wallis and Oakes (1990), Williams (1990), Towner et al. (1996), Cassidy et al. (1997), Roy (1999), and Roy and Whitehouse (1999). The heavy-mineral sand deposits are described in detail in Section 3.3.1.

Carbonatite: Most carbonatite complexes in the world are localised within stable continental tectonic units. Within these large regional structures, the carbonatites are generally confined to alkaline magmatic provinces controlled by intracontinental rift and fault systems (Berger et al., 2009). Carbonatite and alkaline igneous magmatism produces several types of significant REE deposits. Some deposits are closely related to the cooling and crystallisation of magma, whereas others are formed from hydrothermal fluids released by magmatic melts, or from supergene-enrichment processes operating in the weathered zone of the carbonatite body.

Jaques (2008) divided Australia's major carbonatite occurrences into two major groups: (1) those associated with kimberlites and/or ultramafic lamprophyres; and (2) those occurring in alkaline complexes or discrete bodies. Examples of the first group include Mount Weld, Ponton Creek (Cundeelee), veins at Granny Smith and Wallaby gold mines (all Yilgarn Craton, WA), Yungul (Halls Creek Orogen, WA), and Walloway (Gawler Craton, SA). Occurrences with alkaline affinities in the second group include Cummins Range and Copperhead (Halls Creek Orogen), Yangibana 'ironstones' of the Gifford Creek alkaline complex (Capricorn Orogen, WA: see Section 3.3.1), and the Mud Tank and Mordor igneous complexes (Arunta Region, NT). The geological features and mineral resources of these carbonatite-associated deposits are summarised in Table 3.14. REE mineralisation is associated with both groups of carbonatites, with the most significant deposits hosted by large carbonatite bodies at Mount Weld and Cummins Range (Duncan and Willett, 1990; Andrew, 1990). Although rare-earth minerals can be formed during crystallisation of carbonatite melt and also from later hydrothermal fluids, most of the known resources are concentrated in the regolith cover over the main intrusive carbonatite complex. The base of the regolith is commonly defined by a karst-like interface with the underlying carbonatite. Leaching of soluble minerals such as carbonates and silicate produces a residual zone enriched in rare restite minerals, such as primary and secondary monazite, apatite, zircon, pyrochlore, cerianite, churchite, and crandallite. Enrichment of REE in the residual zones can attain up to 10 times their original concentration. The Ponton Creek and Yangibana (see Deposit Type 3.10) are rare examples in Australia where the REE are hosted in the unweathered primary zone of the carbonatite body.

The ~2025 Ma (Re-Os isochron) Ponton Creek carbonatite (previously called Cundeelee) is located at the southeastern margin of the Archean Yilgarn Craton near the intersection of a shear system associated with the Fraser Complex to the southeast and the southern extensions of the Laverton Tectonic Zone. The emplacement of the Ponton Creek complex may have been facilitated by the intersection of these two regional structural corridors. The main basement lithologies comprise granitic gneiss, migmatite, and intrusives overprinted by the northeast-trending tectonic fabrics of the Proterozoic Albany–Fraser Orogen. The complex is overlain by 350 to 500 m of Permian tillite. The 10 km-wide central core of alkaline ultramafic cumulates is cut by veins of primary apatite-rich rauhaugite (hypabyssal dolomitic carbonatite), secondary calcite-magnetite-bearing rocks, and pods and veins of pegmatitic aegirine syenite. The best drill intersections in the primary zone are 16 m @ 14.48% TREO + Y, and 28 m @ 10.50% REO. There is no paleo-regolith profile due to the action of Permian glaciation (Lewis, 1990).

The Cummins Range Carbonatite (Fig. 3.32) in the Halls Creek Orogen of Western Australia consists of a central carbonatite plug with a weathered capping of silicified, limonitic collapse breccia that is enclosed by an envelope of carbonated, mica-rich pyroxenite that is largely altered to amphibolite (see Appendix 7). Calcite (sövite)- and dolomite (rauhaugite)-dominant carbonatites contain apatite, phlogopite, magnetite, and clinopyroxene (Lewis, 1990). Steeply dipping carbonatite veins, up to 60-m wide, traverse the weathered zone (Andrew, 1990). Isotopic dating (1012 ± 12 Ma U-Pb zircon and 905 ± 2 Ma Rb-Sr) indicates that the carbonatite pre-dates the ~800 Ma kimberlites

of the Kimberley region, but it may be coeval with Bow Hill lamprophyres further to the north (Jaques et al., 1985; Jaques, 2008). Weathering and leaching of the oxidised zone above the carbonatite has enriched (by up to 10 times) LREE, Y, U, Nb, V, and P mineralisation with associated high levels of Ta, Zr, Nb, Sc, Sr, Ti, and Th, in such minerals as monazite, apatite, zircon, pyrochlore, and magnetite. As of September 2009, the Cummins Range deposit has an Inferred Resource of 4.17 Mt @ 1.72% TREO, 11.0% P_2O_5, and 187 ppm U_3O_8.

The Yungul carbonatite dykes and the associated Speewah fluorite deposit occur on a north-trending splay from the northeast-trending Greenvale Fault which defines the western margin of the Halls Creek Orogen, Western Australia (Rogers, 1998; Alvin et al., 2004). The carbonatite is spatially associated with Neoproterozoic (~800 Ma) kimberlites and lamprophyres (e.g., Bow Hill lamprophyre dyke), but its intrusion age is unknown (Jaques, 2008). The dykes in the Speewah Dome are up to 15-m wide and are concentrated in a 150 m-wide zone along a fault splay of the regional northeast-trending Greenvale Fault. The dykes are massive calcite carbonatites that host very coarse, pegmatitic veins and pods of calcite (Gwalani et al., 2010). They have carbonatised and fenitised the ~1790 Ma Hart Dolerite country rocks.

The Mordor Complex (Langworthy and Black, 1978; Barnes et al., 2008) in the eastern Arunta Region is a composite plug-like alkaline-ultramafic body that has been explored for REE, PGEs, Ni, Cu, Cr, diamonds, vermiculite-phlogopite, and U. The complex crops out over 6 by 6 km and can be broadly subdivided into a western zone of homogeneous syenite and an eastern zone comprising a highly fractionated comagmatic suite of alkaline felsic and mafic rocks (syenite, monzonite, melamonzonite, shonkinite) spatially associated with phlogopite-bearing ultramafic cumulate rocks (wehrlite, olivine clinopyroxenite, lherzolite, dunite, pyroxenite). The ultramafic rocks make up less than 5% of the intrusion. Pegmatites and carbonate-rich dykes and veins cut the intrusion. Previous investigators have interpreted these dykes and veins to be carbonatites with associated fenitic alteration. Geochemical data show that the Mordor Complex forms a differentiated ultrapotassic suite of uniform silica content (43–53%) enriched in K, Al, Rb, Ba, Sr, and La (Appendix 7). Plagioclase pyroxenite from the northeastern corner of the intrusion has a U-Pb zircon crystallisation age of 1133 ± 5 Ma (Claoué-Long and Hoatson, 2005), which is consistent with the mineral Rb–Sr isochron ages of 1128 ± 20 Ma and 1118 ± 17 Ma (Langworthy and Black, 1978). The alkaline felsic rocks and discordant carbonate-bearing dykes have been a focus for REE exploration, however, drilling programs have generally returned disappointing results. Stratabound PGE mineralisation (8 m @ 0.67 ppm Pt+Pd+Au) hosted by cyclic sequences of ultramafic rocks (Barnes et al., 2008), and base-precious mineralisation (1 m @ 1.4% Cu, 0.3% Ni, 0.4 ppm Pt+Pd, and 0.1 ppm Au) at the Braveheart ironstone on the southeast margin of the intrusion highlight the polymetallic character of the complex.

The Mud Tank Carbonatite (Knutson and Currie, 1990; Currie et al., 1992), located 52 km north-northwest of the Mordor Complex, was the first

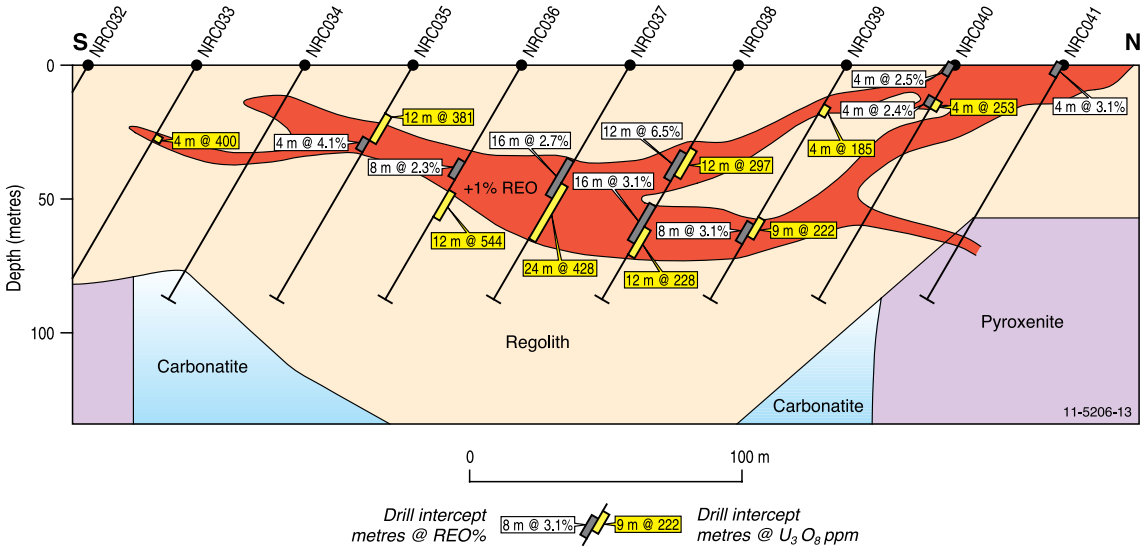

Figure 3.32. Geological cross-section of the Cummins Range Carbonatite rare-earth-element deposit, Halls Creek Orogen, Western Australia. Modified from Navigator Resources Limited (2010).

Table 3.14. Major carbonatite occurrences in Australia.

Carbonatite	Geological setting	Size	Resources	Reference(s)
Mount Weld, Yilgarn Craton, WA	Paleoproterozoic (~2025 Ma) carbonatite intrusive with thick mineralised laterite[2] profile	4 km[1]	17.49 Mt @ 8.1% TREO; significant resources of P_2O_5	Duncan and Willett (1990); Lottermoser (1990); Graham et al. (2003, 2004)
Ponton Creek, Yilgarn Craton, WA	Large Paleoproterozoic (~2025 Ma) carbonatite stock covered by 500 m of Permian tillite	10 km[1]	28 m @ 10.5% REO and 16 m @ 14.48% REO; no resource defined	Jaques (2008)
Copperhead, Halls Creek Orogen, WA	Small Paleoproterozoic (1821 Ma) carbonatite plug-like body	110 m by 80 m	Low anomalous REE concentrations: <76 ppm Y; <600 ppm Ce; <86 ppm La	Rugless and Pirajno (1996); Jaques (2008)
Yangibana 'ironstones', Capricorn Orogen, WA	Mesoproterozoic (~1250 Ma) ferrocarbonate-magnetite-hematite dykes	10-m wide, up to 25 km long	3.53 Mt @ 1.64% REO	Pearson and Taylor (1996); Jaques (2008)
Mordor, Arunta Region, NT	Mesoproterozoic (1133 Ma) alkaline ultramafic plug cut by carbonate-rich dykes and veins	6 by 6 km (plug)	Anomalous REE, PGEs, Ni, Cu, U, Au	Barnes et al. (2008); Hoatson et al. (2005;) Langworthy and Black (1978)
Cummins Range, Halls Creek Orogen, WA	Mesoproterozoic (~1012 Ma) carbonatite intrusive stock with mineralised laterite profile	1.8 km[1]	4.17 Mt @ 1.72% TREO, 11.0% P_2O_5 , 187 ppm U_3O_8	Andrew (1990); Jaques (2008)
Mud Tank, Arunta Region, NT	Neoproterozoic (732 Ma) carbonate-rich lenses in granite, schist, and mafic granulite	Four separate lenses crop out over 4 km by 700 m	Vermiculite; gem-quality zircon	Currie et al. (1992); Knutson and Currie (1990); Black and Gulson (1978)
Yungul, Halls Creek Orogen, WA	Phanerozoic (not dated: probably post-Early Cambrian) carbonatite dykes	Less than 15-m wide	Low REE abundances (174 to 493 ppm TREE); fluorite resources	Alvin et al. (2004); Gwalani et al. (2010)
Walloway, Gawler Craton, SA	Jurassic (~170 Ma) carbonate-rich lamprophyric plugs and dykes	Small	NA	Tucker and Collerson (1972); Ferguson and Sheraton (1979)
Granny Smith and Wallaby gold mines, Yilgarn Craton, WA	Carbonatite veins (not dated) associated with ~2.66 Ma monzodiorite-syenite stocks, dykes, and carbonate-rich rocks	Less than 2-m thick	NA	Jaques (2008); Mueller et al. (2008)

[1] Maximum diameter dimension of plug- and stock-like bodies.
[2] Age of mineralised laterite ranges from approximately Late Mesozoic to Early Cenozioc.
NA = Not Available.
Locations for the carbonatites listed in this table are shown in Figure 5.4.

carbonatite recognised in Australia (Gellatly, 1969). The carbonatite consists of four separate carbonate-rich lenses within a north–northeasterly-trending zone some 4 km long. It was emplaced into granitic and mafic granulite rocks at mid-crustal levels and was subsequently remobilised to higher-crustal levels (Currie et al., 1992). Most of the carbonatite is altered and ferruginised at the surface, and was originally found by the large detrital concentrations of coarse apatite, magnetite, and zircon. Three major types of carbonatite have been recognised (Black and Gulson, 1978): (1) an abundant foliated micaceous carbonatite containing phlogopite, carbonate, soda-amphibole, apatite, and magnetite that grade into; (2) a calcite- and dolomite-bearing carbonatite with apatite, magnetite, phlogopite, chlorite, soda-amphibole, zircon, and pyrite; and (3) feldspathic carbonates with andesine, carbonate, aegirine, soda-amphibole, hastingsite, biotite, apatite, and Fe-oxides. Currie et al. (1992) report maximum REE concentrations of 335 ppm La, 595 ppm Ce, 264 ppm Nd, 68 ppm Pr, 67 ppm Sc, and 70 ppm Y from the carbonatite lithologies. The Mud Tank Carbonatites have significantly higher Cu, Ni, and Cr contents, and lower Sr, Zr, Nb, Mo, La, and Ce contents than the average carbonatite (Currie et al., 1992). The Mud Tank Carbonatite and Mordor Complex occur near the northwest-trending Woolanga Lineament—a deep-seated crustal dislocation that may have facilitated the emplacement of these unusual plug-like bodies. The younger emplacement of the Mud Tank Carbonatite (U-Pb zircon age of 732 ± 5 Ma: Black and Gulson, 1978) relative to the Mordor Complex may indicate reactivation along this regional lineament or associated fault structures.

Unconformity-related: The Killi Killi Hills uranium-REE prospects, located about 150 km southeast of Halls Creek, in the Proterozoic Birrindudu Basin near the Western Australian–Northern Territory border represent an interesting style of mineralisation where the main ore mineral xenotime is thought to have formed from fluids released during diagenesis of the Mesoproterozoic Gardiner Sandstone (Vallini et al., 2007). The presence of xenotime and florencite highlights the potential for

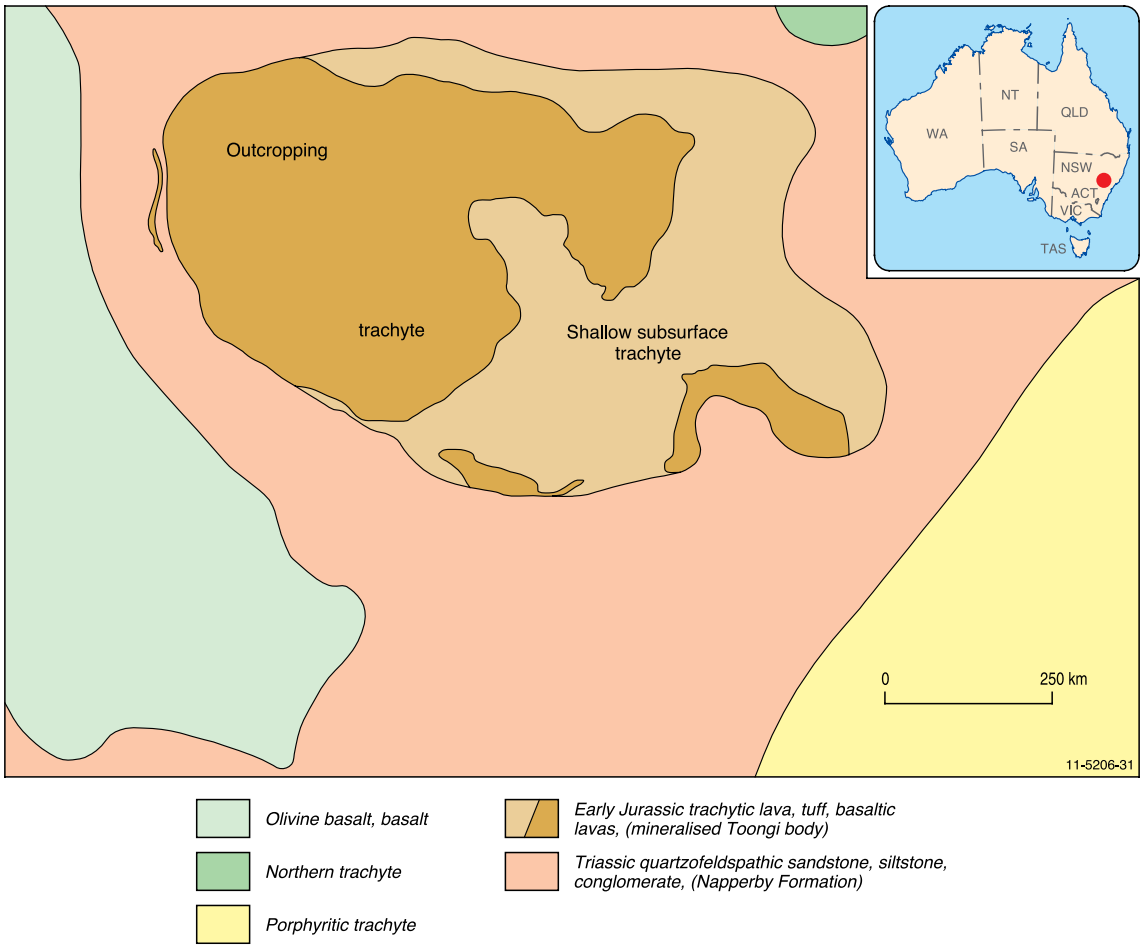

Figure 3.33. Geological map of the Toongi polymetallic deposit, Lachlan Orogen, New South Wales. Modified from Alkane Resources Limited (2011).

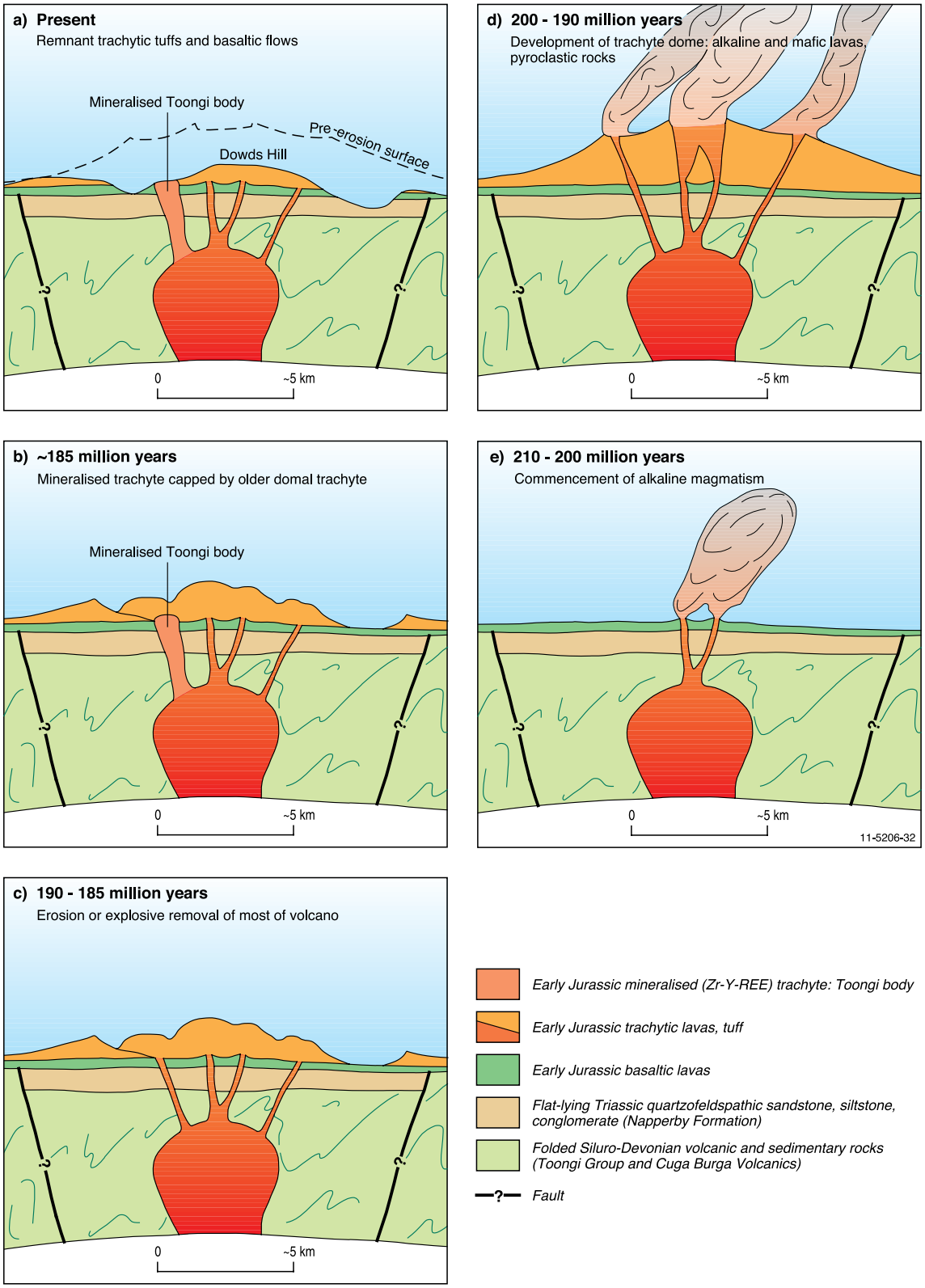

Figure 3.34. Time-event evolution of the Toongi deposit, New South Wales. Modified from Alkane Resources Limited (2007).

HREE and uranium. Xenotime from the Gardiner Sandstone has high concentrations of yttrium and phosphorous, with an average of 48% yttrium oxide and 16–20% phosphorous oxide. The mineralisation is confined to conglomerates at the base of the Gardiner Sandstone, which unconformably overlies steeply dipping, Paleoproterozoic shale and greywacke of the Killi Killi Formation (Blake et al., 1979). Similar diagenetic-fluid processes occur in other sedimentary basins, which unconformably overlie carbonaceous-rich rock and host world-class unconformity-related uranium deposits in the Pine Creek Orogen of the Northern Territory. Ores and altered host rocks in unconformity-related uranium deposits show elevated concentrations of REE (Jefferson et al., 2007; Fisher and Cleverley, 2010) indicating that some of these deposits may have economic resources of REE (see Caramel in Appendix 7).

Alkaline igneous rocks: The Dubbo–Mudgee region of New South Wales contains a number of Mesozoic alkaline complexes that range in age from about 225 million years to 165 million years (Warren et al., 1999). The complexes comprise stocks, sills, dykes, and flows that appear to be structurally controlled and aligned along regional lineaments. They range in composition from basalt, alkali diorite, trachyte, syenite, to quartz monzonite, with the trachytic variants having the greatest potential for REE. The Dubbo Zirconia Project (Toongi: Figs 3.33 and 3.34), located 25 km south of Dubbo, contains one of the world's largest in-ground resources of zirconium, hafnium, niobium, tantalum, yttrium, and REE. It was discovered in 1988, although serious investigations did not commence until 1999. The Toongi deposit has a Measured Resource of 35.7 million tonnes grading 1.96% ZrO_2, 0.04% HfO_2, 0.46% Nb_2O_5, 0.03% Ta_2O_5, 0.14% Y_2O_3, 0.75% TREO, 0.014% U_3O_8, and 0.0478% Th, and an Inferred Resource of 37.5 million tonnes of similar grades (http://www.dpi.nsw.gov.au/__data/assets/pdf_file/0003/316839/Rare_Earth_Elements.pdf). The mineralisation is hosted in a hydrothermally altered pipe-like body that outcrops over an area of about 400 m by 600 m, with shallow subsurface extensions of alkaline rocks indicating the overall dimensions of the body are approximately 900 m east-west by 600 m north-south (Fig. 3.33). Trachytic lavas, tuffs, and olivine basaltic lavas are interpreted to represent the volcanic phase of an alkaline magmatic event that occurred during the late Triassic to early Jurassic. The pipe-like body cuts folded Siluro-Devonian volcanic and sedimentary rocks (Toongi Group and Cuga Burga Volcanics) and a flat-lying Triassic sequence of quartzofeldspathic sandstone and minor siltstone and conglomerate (Napperby Formation). Narrow (up to 3 m) basaltic dykes intrude the body. Figure 3.34 shows a schematic time sequence of the major geological events Chalmers (1999) describes the Toongi body as a remarkably uniform, very fine-grained (<0.5 mm) massive alkali trachyte comprising K-feldspar (partly sericitised), albite, and aegerine pyroxene microphenocrysts, with minor carbonate, quartz, and 'ore' minerals. The intrusive contact is defined by a 2 to 10 m-wide zone of silicified trachyte with chalcedonic veining and a possible preserved vesicular cap to the body. Hydrothermal alteration involving significant carbonate, chloritic, potassic, and argillic alteration has modified the Toongi prospect (Christie et al., 1998). Weathering persists for up to 15 m below the surface, but its effect on the host trachyte and ore minerals is limited, causing only minor variations in the mineral species. The trachyte body exhibits uniformly elevated abundances of Zr, Hf, Nb, Ta, Y, and REE laterally and vertically. The orebody also contains low levels of uranium and thorium, but it is not classified as a radioactive ore. Scanning electron mineralogical studies indicate that the ore minerals are very fine-grained, being less than 100 µm in size (most less than 20 µm) and generally having unusual compositions. Un-named calcium- and REE-bearing zirconium silicates (similar to eudialyte and armstrongite: $ZrSiO_4$ ± Ca, Y, REE, H_2O, ?U) are the dominant ore minerals of zirconium and yttrium, while natroniobite ($NaNbO_3$) and calcian bastnäsite ($Ca(REE)CO_3F$) are the major sources of niobium and REE, respectively (Chalmers, 1999).

Elevated levels of zirconium, thorium, and REE are associated with deeply weathered and fresh peralkaline granite at the Narraburra deposit, 12 km northeast of Temora in central New South Wales (Wormald et al., 2004). A Late Devonian total-rock Rb-Sr isochron age of 365 ± 4 Ma for the emplacement of the granite has been implied by Wormald et at. (2004). This deposit contains an inferred resource of 55 Mt @ 60 ppm Y_2O_3, 300 ppm REO with up to 50 ppm thorium.

Pegmatite: Pegmatites in the Wodgina–Mount Francisco area (see Section 1.6 and Appendix 7) of the Pilbara Craton, Western Australia, are known to contain REE (Witt, 1990). The albite pegmatites and associated tourmaline lodes have been mined for tin, tantalum, and lithium (Ferguson and Ruddock, 2001).

Fluorite veins: The high-grade John Galt hard-rock resource and adjacent Corkwood Yard alluvial REE deposit are located near the western end of the Osmond Range, in the East Kimberley. REE mineralisation at John Galt consists of disseminations of xenotime in lithic quartz sandstone and conglomerate of

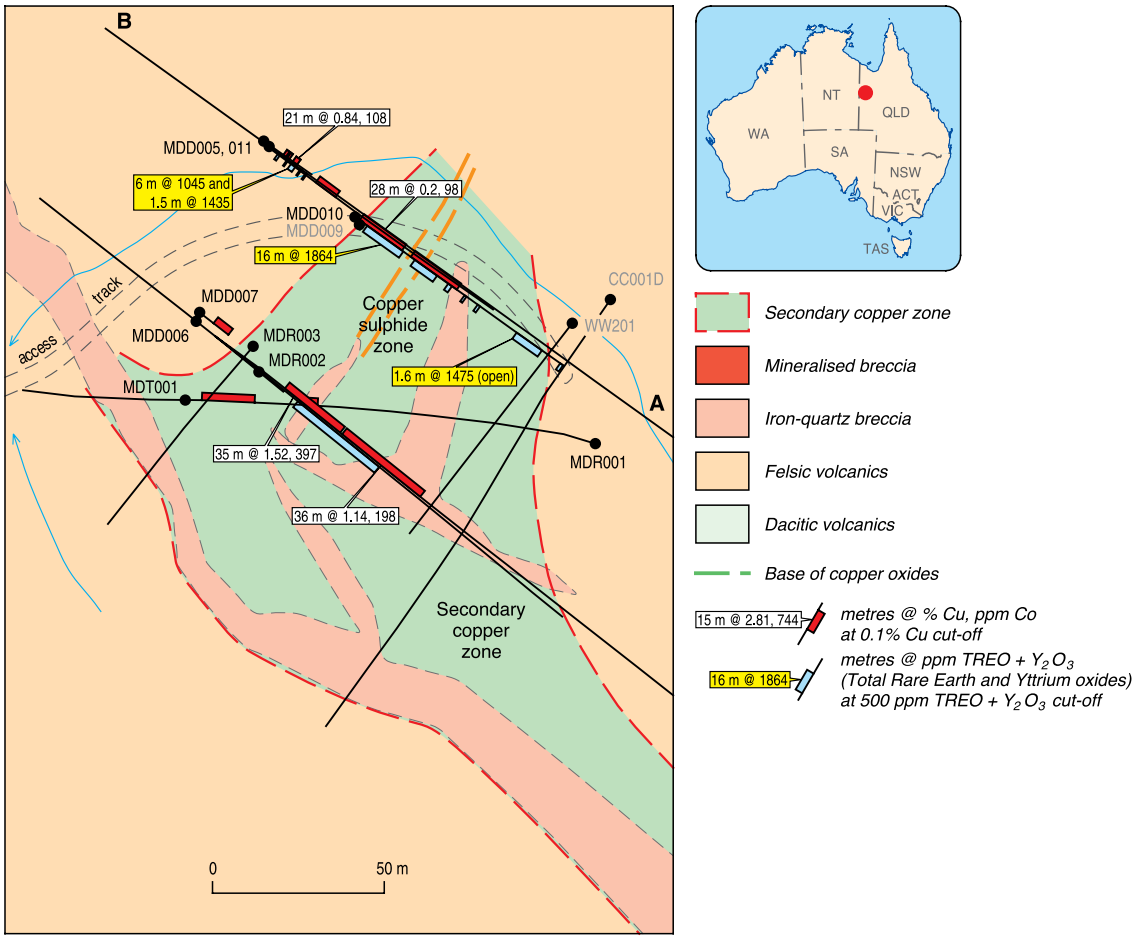
B
A
21 m @ 0.84, 108
MDD005, 011
6 m @ 1045 and
1.5 m @ 1435
28 m @ 0.2, 98
MDD010
MDD009
16 m @ 1864
CC001D
WW201
track
MDD007
MDD006
MDR003
MDR002
access
Copper
sulphide
zone
1.6 m @ 1475 (open)
MDT001
35 m @ 1.52, 397
MDR001
36 m @ 1.14, 198
Secondary
copper
zone
0
50 m
NT
QLD
WA
SA
NSW
ACT
VIC
TAS
Secondary copper zone
Mineralised breccia
Iron-quartz breccia
Felsic volcanics
Dacitic volcanics
Base of copper oxides
15 m @ 2.81, 744
metres @ % Cu, ppm Co
at 0.1% Cu cut-off
16 m @ 1864
metres @ ppm TREO + Y2O3
(Total Rare Earth and Yttrium oxides)
at 500 ppm TREO + Y2O3 cut-off

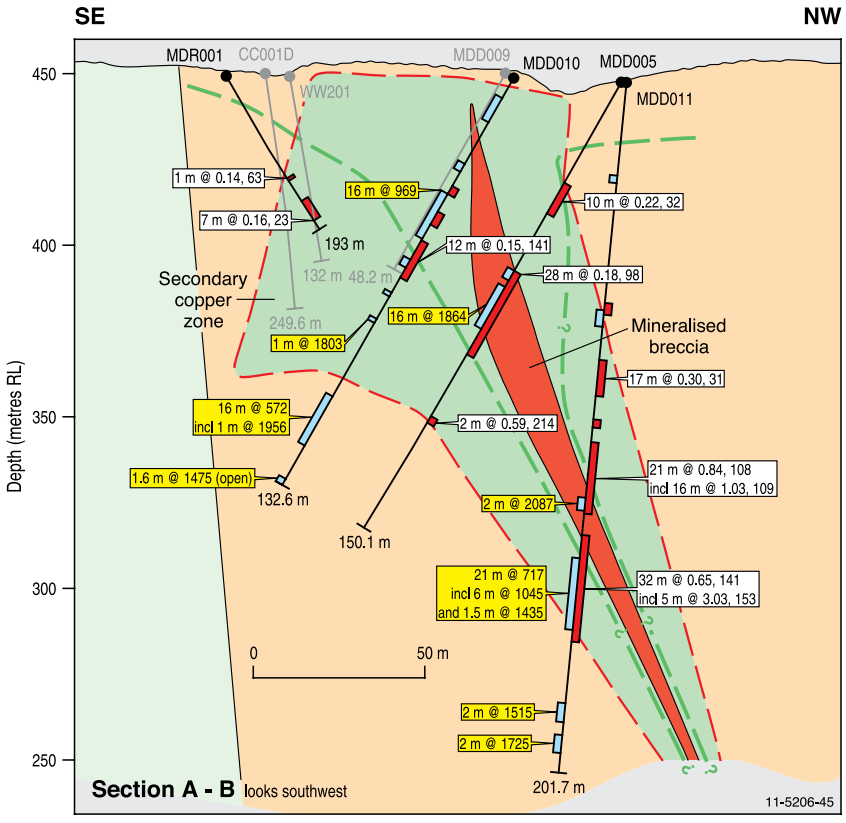
SE
NW
MDR001
CC001D
MDD009
MDD010
MDD005
WW201
MDD011
1 m @ 0.14, 63
7 m @ 0.16, 23
193 m
16 m @ 969
10 m @ 0.22, 32
12 m @ 0.15, 141
132 m
48.2 m
28 m @ 0.18, 98
Secondary
copper
zone
249.6 m
16 m @ 1864
1 m @ 1803
Mineralised
breccia
17 m @ 0.30, 31
16 m @ 572
incl 1 m @ 1956
2 m @ 0.59, 214
1.6 m @ 1475 (open)
132.6 m
21 m @ 0.84, 108
incl 16 m @ 1.03, 109
2 m @ 2087
150.1 m
21 m @ 717
incl 6 m @ 1045
and 1.5 m @ 1435
32 m @ 0.65, 141
incl 5 m @ 3.03, 153
0
50 m
2 m @ 1515
2 m @ 1725
201.7 m
Depth (metres RL)
450
400
350
300
250
Section A - B looks southwest
11-5206-45

the Proterozoic Red Rock Formation, as well as in joint- and fault-controlled veins up to 30 cm wide (Fetherston, 2008). The epithermal quartz veins are hosted by a brittle variant of the sedimentary rocks about 1 km east of the regional Halls Creek Fault. The veins form a cliff up to 30-m wide and 10 m high, and have been investigated over a distance of 4.5 km (Lottermoser, 1991). The mineralisation appears to be structurally controlled and possibly related to fluids from deeper level, alkaline source rocks (Sanders, 1999). Noble Resources (1992) determined inferred resources of 0.051 Mt @ 0.35% REO. Similarities in deformational style and vein morphology, and a possible association with late-tectonic alkaline source rocks, indicate comparisons with very late-stage epithermal mineralisation (Yungul carbonatite, fluorite) in the Speewah Dome.

Iron-oxide breccia complex: In addition to the world-class Olympic Dam copper, gold, uranium deposit, several large breccia complexes are also developed in the Mount Painter and Mount Babbage inliers of the Curnamona Province of South Australia. The Inliers consist of Proterozoic granites, metasedimentary rocks, and volcanic rocks that have been intruded by Paleozoic granites (Cassidy et al., 1997). Large bodies of breccia (e.g., Radium Hill breccia) occur in the Mount Painter Complex and the Paleozoic granites. The Radium Hill hematitic breccia contains base-metal sulphides, uraninite, monazite, chlorite, carbonate, fluorite, quartz, and magnetite (Drexel and Major, 1990). They are enriched in REE with reported concentrations of 1% TREO. The hematitic breccia and sinter at Mount Gee contain elevated concentrations of uranium, copper, and cerium (average concentrations of up to 6100 ppm; Drexel and Major, 1990). Many investigators have made comparisons between the hematitic breccias at Mount Painter with those at Olympic Dam (Cassidy et al., 1997).

The Radium Hill uranium deposit in the Olary district of South Australia is located within shears of Precambrian feldspathic gneiss, aplitic gneiss, and schist, which are intruded by mafic and felsic bodies (Cassidy et al., 1997). The main uraniferous-REE ore mineral mined was davidite. Approximately 136 kg of high-purity scandium was produced as a by-product of the uranium (Towner et al., 1987).

Skarn: The Mary Kathleen-Mount Isa region of northwestern Queensland may represent a new REE province with a number of significant discoveries in the last few years. Previous exploration in the region largely targeted uranium with little exposure devoted to REE. The Mount Dorothy (Fig. 3.35) and Elaine Dorothy REE ± Cu ± Co prospects have similar broad magmatic-metamorphic signatures to the previously mined Mary Kathleen uranium-REE breccia-skarn deposit (see Table 3.13). China Yunnan Copper Australia Limited announced the discovery of the Mount Dorothy HREE prospect in January 2011, with a broad zone of yttrium and HREE mineralisation in drill-hole MDD005, e.g., 16 m @ 1249 ppm (1.24 kg/tonne) total HREE-Y from 71 m. A northeast-trending, steeply plunging mineralised breccia occurs in a native copper-bearing zone hosted in felsic volcanics. High-grades of HREE and yttrium are spatially associated with secondary copper-cobalt mineralisation and the breccia (http://www.cycal.com.au/IRM/Company/ShowPage.aspx?CPID=1428&EID=49766522&PageName).

Figure 3.35 (see opposite). Geological map and cross-section of the Mount Dorothy rare-earth-element-copper-cobalt deposit, Queensland. Modified from Chinalco–China Yunnan Copper Australia Limited (2011).